Proceedings of the

International Symposium on Vibrations of Continuous Systems

The Stanley Hotel
Estes Park, Colorado, U.S.A.
11-15 August 1997

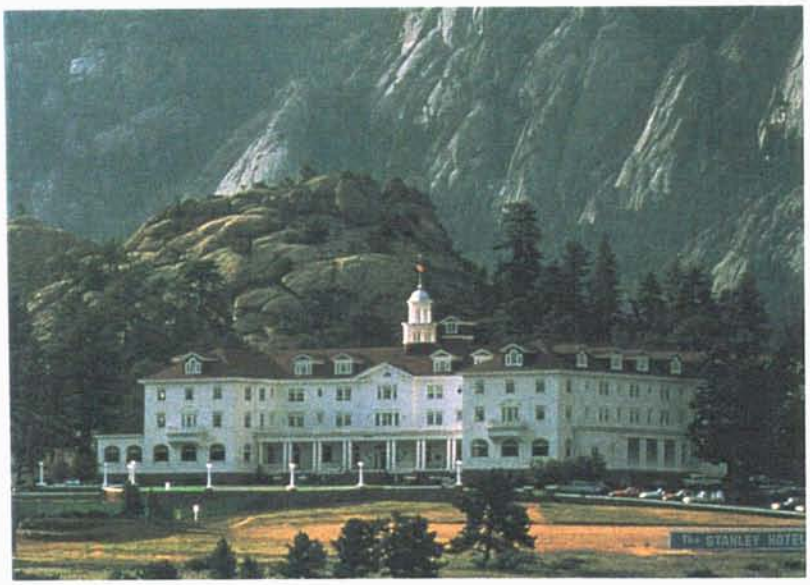

Preface

The International Symposium on Vibrations of Continuous Systems is a forum for leading researchers from across the globe to meet with their colleagues and present both old and new ideas on the field. Each participant has been encouraged to either present results of recent research or to reflect on some aspect of the vibration of continuous systems ***which is particularly interesting, unexpected or unusual****. This type of presentation-- of which there are several--was proposed to encourage participants to draw on understanding obtained through--in many cases--decades of research.*

The location chosen for the Symposium is one of the most beautiful towns in the United States--Estes Park, Colorado. With nearby Rocky Mountain National Park, this area gives a backdrop of unsurpassed natural beauty. Because of this location, mornings of the symposium have been kept free to permit hiking, sightseeing and mountain climbing, in order to avoid the thunderstorms which come often in the early afternoons. As such, a hike has been planned for each morning of the Symposium.

This Proceedings contains short summaries of the presentations to be made at the Symposium. An accompanying addendum is a collection of short biographical sketches submitted by many of the participants.

Mark S. Ewing
General Chairman

Art Leissa
Honorary Chairman

Mohamad Qatu
Editorial Chairman

Contents

Contents

Contents

EFFECT OF LAYUP ON THE BEHAVIOR OF COMPOSITE STRUCTURES

Serge Abrate
Department of Technology
Southern Illinois University
Carbondale, IL 62901-6603

Laminated composite materials can be tailored for each application by properly selecting the layup. The total number of plies, the thickness of each ply and the fiber orientation for each ply are variables affecting the behavior of the laminate. A maximum of 12 nondimensional lamination parameters describe the effect of lamination for the most general layups regardless of the number of plies. For symmetric laminates in bending, only four such parameters are needed and in most practical cases the effect of two of those parameters is negligible. Therefore, all symmetric laminates can be considered for optimization purposes by studying the effect of only two parameters. A review of the literature on optimum design of composite structures[1] shows that the stiffness invariant formulation is seldom used and that many studies do not consider all possible layups in the optimization in order to reduce the number of design variables. Another limitation of previous studies was the limited nature of the results presented. Typically, results were given for a given geometry, on set of boundary conditions, and for one material system. Studies of the optimum design of rectangular[2-5] and triangular[6,7] symmetrically laminated plates using the stiffness invariant formulation and a variational approximation method allowed to obtain results for a large number of cases with various boundary conditions. This work was extended to optimize the buckling load[8] and minimize the thermal deflections[9] of composite plates. This presentation will give an overview of the results obtained and suggestions for future work.

For symmetrically laminated plates, the transverse and in-plane motions are uncoupled and the motion is governed by the equation

$$M_{x,xx} + 2M_{xy,xy} + M_{y,yy} + p = 0$$

where p is the applied pressure for static problems or the inertia load $-m\frac{\partial^2 w}{\partial t^2}$ for free vibration problems. The moment resultants $M = [M_x, M_y, M_{xy}]^T$ are related to the curvatures $\kappa = [-w_{,xx}, -w_{,yy}, -2w_{,xy}]^T$ by $M = D\kappa$ and the elements of the bending rigidity matrix can be written as

$$\begin{Bmatrix} D_{11} \\ D_{22} \\ D_{12} \\ D_{66} \\ D_{16} \\ D_{26} \end{Bmatrix} = \frac{h^3}{12} \begin{bmatrix} 1 & \zeta_9 & \zeta_{10} & 0 & 0 \\ 1 & -\zeta_9 & \zeta_{10} & 0 & 0 \\ 0 & 0 & -\zeta_{10} & 1 & 0 \\ 0 & 0 & -\zeta_{10} & 0 & 1 \\ 0 & +\zeta_{11}/2 & \zeta_{12} & 0 & 0 \\ 0 & +\zeta_{11}/2 & -\zeta_{12} & 0 & 0 \end{bmatrix} \begin{Bmatrix} U_1 \\ U_2 \\ U_3 \\ U_4 \\ U_5 \end{Bmatrix}$$

in terms of the laminate thickness h, the stiffness invariants U_i which depend on the elastic properties E_1, E_2, G_{12} and ν_{12}, and the lamination parameters defined as

$$\zeta_9 = \frac{12}{h^3} \int_{-h/2}^{+h/2} z^2 \cos 2\theta \, dz, \qquad \zeta_{10} = \frac{12}{h^2} \int_{-h/2}^{+h/2} z^2 \cos^2 2\theta \, dz,$$

$$\zeta_{11} = \frac{12}{h^3} \int_{-h/2}^{+h/2} z^2 \sin 2\theta \, dz, \qquad \zeta_{12} = \frac{12}{h^3} \int_{-h/2}^{+h/2} z^2 \sin 2\theta \cos 2\theta \, dz$$

The effects of ply orientation and ply thickness distributions through the thickness of the laminate are included in these four parameters which for all symmetric laminates regardless of the number of plies. As the number of plies becomes larger than 8, the last two lamination parameters become small and their effect on the behavior of the structure becomes negligible[9]. Then, only two parameter need to be considered when studying the effect of layup and determining the optimum design for a given application.

For simple geometries, the solution to the structural problem is found most efficiently using a variational approximation method. Here, the Rayleigh-Ritz method with polynomial approximation function was used to model rectangular or triangular plates with arbitrary support conditions along the edges and internal line supports. For example, for rectangular plates extending from 0 to a in the x-direction and from 0 to b in the y-direction, with a line support along x=c, clamped along x=0 and x=a, simply supported along y=0 and free along y=b, the displacements can be approximated by

$$w = \sum_{I=1}^{N} c_I \phi_I(x,y)$$

The approximation functions are taken as

$$\phi_I(x,y) = x^{i+2} y^j (x-a)^2 (x-c)$$

where i and j vary from 1 to p and 1 to q respectively, and p.q = N. Rectangular and triangular plates with arbitrary aspect ratio, support conditions along the edges and intermediate line supports can be analyzed. Point supports are introduced using the method of Lagrange multipliers.

This approach is used to determine the best fiber orientations for maximizing the fundamental natural frequency of laminated plates with various shapes, aspect ratios and boundary conditions. Results indicate that truly optimum layups can be selected with this approach by considering all possible symmetric laminates. The optimal layup is not necessarily an angle-ply laminate or a cross-ply laminate and depends strongly on the support conditions and the aspect ratio of the plate. In most cases, the effect of material properties on the optimal layup is small for most of the material systems currently available. Therefore, a layup that is optimum with one material system will be nearly optimum for other material systems. The same approach was used to determine optimal fiber orientations to maximize buckling loads and to minimize thermal effects.

REFERENCES

1- Abrate S., 1994. Optimum Design of Laminated Plates and Shells. *Composite Structures* 29(3): 269-286.

2- Abrate S., and Foster, E. 1995. Vibrations of Composite Plates with Intermediate Line Supports. *J. Sound and Vibration* 179(5): 793-815.

3- Abrate S., 1994. Vibration of Composite Plates with Internal Supports. *Int. J. Mechanical Sciences* 36(11): 1027-1043.

4- Abrate S., 1995. Design of Multispan Composite Plates to Maximize the Fundamental Natural Frequency. *Composites* 26(10): 691-697.

5- Abrate S., 1995. Free Vibration of Point Supported Rectangular Composite Plates. *Composites Science and Technology* 53: 325-332.

6- Abrate S., 1996. Maximizing the Fundamental Natural Frequency of Triangular Composite Plates. *J. Vibration and Acoustics* 118: 141-146.

7- Abrate S., 1995. Free Vibration of Point Supported Triangular plates. *Computers and Structures* 58(2): 327-336.

8- Abrate S., 1995. Stability and Optimal Design of Laminated Plates with Internal Support. *Int. J. Solids and Structures* 32(10): 1331-1347.

9- Abrate S., 1993. On Minimizing Thermal Deflections of Laminated Plates", ASME Publ. DE-Vol.55, pp 1-8

Pure Shear Modes of Free Vibration of Rectangular Parallelepipeds

Moinuddin Malik and **Charles W. Bert**
School of Aerospace and Mechanical Engineering
The University of Oklahoma, Norman, OK 73019-0601

Using three-dimensional displacement-equilibrium equations of the theory of elasticity, exact expressions for the natural frequencies of pure shear vibrational modes of rectangular parallelepipeds simply supported on four vertical sides were first given by Srinivas et al. (1970). In the present work, rectangular parallelepipeds having two opposite vertical sides simply supported and general boundary conditions on the two other opposite vertical sides are considered. Exact closed-form expressions for frequencies of various types of pure shear modes for vibration of five other types of boundary conditions are given.

Consider an isotropic-material parallelepiped bounded by the vertical planes $x = 0, a$ and $y = 0, b$, and the top and bottom planes $z = 0, h$. The governing elasticity equations of the parallelepiped undergoing simple harmonic oscillations in a principal vibratory mode are written in a nondimensional form as (Srinivas et al., 1970)

$$\nabla^2(U,V,W) + [1/(1-2\nu)](\partial_x, \lambda\partial_y, \alpha\partial_z)\Theta = -\Omega^2(U,V,W) \tag{1}$$

where $(U,V,W) = (u,v,w)/h$ are the dimensionless displacement components in the x, y, and z directions, respectively; $(X,Y,Z) = (x/a, y/b, z/h)$ are the normalized coordinates;

$$\nabla^2 = \partial_{xx} + \lambda^2\partial_{yy} + \alpha^2\partial_{zz}$$

is the Laplacian operator;

$$\Theta = \partial_x U + \lambda\partial_y V + \alpha\partial_z W$$

is the volume dilatation; ∂ indicates partial derivatives with respect to the X, Y, and Z coordinates as indicated by its subscripts, e.g.,

$$\partial_x = \partial/\partial x, \quad \partial_{xx} = \partial^2/\partial x^2;$$

$\alpha = a/h$ is the lateral aspect ratio; $\lambda = a/b$ is the in-plane aspect ratio; ν is the Poisson's ratio; and Ω is the dimensionless frequency

$$\Omega^2 = (\rho a^2/G)\omega^2$$

in which ω is the circular frequency (rad/s); and G and ρ are, respectively, the shear modulus and density of the material.

Let the parallelepiped be simply supported on the sides $x = 0, a$, i.e., $X = 0, 1$; the boundary conditions on these sides are prescribed by the normal traction and the tangential displacements being equal to zero so that

$$\partial_x U = 0, \quad V = 0, \quad W = 0 \text{ at } X = 0, 1 \tag{2}$$

The displacement components satisfying the boundary conditions on the x-sides, eqn (2), may be expressed as

$$U = \bar{U}(Y,Z)\cos\bar{m}X, \quad V = \bar{V}(Y,Z)\sin\bar{m}X, \quad W = \bar{W}(Y,Z)\sin\bar{m}X \tag{3}$$

where $\bar{m} = m\pi$ and m is an integer.

The sides $y = 0,\ b$ may be either simply supported, clamped, or free. At a simply supported y-side, with zero normal traction and zero tangential displacements, the boundary conditions in terms of reduced displacement variables become

$$\bar{U} = 0, \quad \partial_y \bar{V} = 0, \quad \bar{W} = 0 \text{ at } Y = 0 \text{ and/or } 1 \tag{4}$$

At a clamped y-side, $u = 0$, $v = 0$, and $w = 0$ so that

$$\bar{U} = 0, \quad \bar{V} = 0, \quad \bar{W} = 0 \text{ at } Y = 0 \text{ and/or } 1 \tag{5}$$

At a free y-side, the conditions of components of traction equal to zero may be written as

$$\lambda \partial_y U + \partial_x V = 0, \quad \partial_x U + \lambda[(1-\nu)/\nu]\partial_y V + \alpha \partial_z W = 0,$$

$$\alpha \partial_z V + \lambda \partial_y W = 0 \text{ at } Y = 0 \text{ and/or } 1$$

and using eqns (3), these conditions become

$$\lambda \partial_y \bar{U} + \bar{m}\bar{V} = 0, \quad \bar{m}\bar{U} - \lambda[(1-\nu)/\nu]\partial_y \bar{V} + \alpha \partial_z \bar{W} = 0,$$

$$\alpha \partial_z \bar{V} + \lambda \partial_y \bar{W} = 0 \text{ at } Y = 0 \text{ and/or } 1 \tag{6}$$

The lateral surfaces of the parallelepiped are assumed to be free so that the traction components are zero on $z = 0,\ h$. These conditions may be written as

$$\alpha \partial_z U + \partial_x W = 0, \quad \alpha \partial_z V + \lambda \partial_y W = 0,$$

$$\partial_x U + \lambda \partial_y V + \alpha[(1-\nu)/\nu]\partial_z W = 0 \text{ at } Z = 0 \text{ and/or } 1$$

which, on using eqns (3), become

$$\alpha \partial_z \bar{U} + \bar{m}\bar{W} = 0, \quad \alpha \partial_z \bar{V} + \lambda \partial_y \bar{W} = 0, \quad \bar{m}\bar{U} - \lambda \partial_y \bar{V} - \alpha[(1-\nu)/\nu]\partial_z \bar{W} = 0 \text{ at } Z = 0 \text{ and } 1 \tag{7}$$

In case of the pure shear modes of vibration, the volume dilatation equals zero, i.e.,

$$\Theta = \partial_x U + \lambda \partial_y V + \alpha \partial_z W = 0 \tag{8}$$

and consequently, eqns (1) are reduced to the following equations

$$\nabla^2 (U, V, W) = -\Omega^2 (U, V, W) \tag{9}$$

It is noted that there is no coupling in these equations. However, the displacements in pure shear modes are indeed coupled; the coupling comes through the boundary conditions.

Using eqns (3) in eqns (9), one obtains the governing equations of pure shear modes of vibration in terms of the reduced displacement variables as

$$\{\bar{m}^2 - \lambda^2 \partial_{yy} - \alpha^2 \partial_{zz}\}(\bar{U}, \bar{V}, \bar{W}) = \Omega^2 (\bar{U}, \bar{V}, \bar{W}) \tag{10}$$

The boundary conditions on simply supported or clamped y-sides remain the same as given by eqns (5) and (6). However, on a free y-side, the condition of zero normal traction in eqns (7) is simplified due to eqn (8). The boundary conditions on a free y-side may be written as

$$\lambda \partial_y \bar{U} + \bar{m}\bar{V} = 0, \quad \partial_y \bar{V} = 0, \quad \alpha \partial_z \bar{V} + \lambda \partial_y \bar{W} = 0 \text{ at } Y = 0 \text{ and/or } 1 \tag{11}$$

Similarly, the condition of zero normal traction in eqns (8) is simplified due to eqn (16). The boundary conditions on the lateral surfaces may be written as

$$\alpha \partial_z \bar{U} + \bar{m}\bar{W} = 0, \quad \alpha \partial_z \bar{V} + \lambda \partial_y \bar{W} = 0, \quad \partial_z \bar{W} = 0 \text{ at } Z = 0 \text{ and } 1 \tag{12}$$

The solutions of eqns (18) may be obtained consistent with the boundary conditions and the condition of zero dilatation, eqn (16), which in terms of the reduced displacement variables is

$$-\bar{m}\bar{U} + \lambda\partial_y\bar{V} + \alpha\partial_z\bar{W} = 0 \tag{13}$$

With two opposite sides simply supported and the other two sides having boundary conditions as dual combinations of simply supported, clamped, and free conditions, the total number of rectangular parallelepiped configurations is six. The possible forms of solutions for pure shear modes of vibration of these parallelepipeds are given in Table 1. Following a now-standard notation, the parallelepipeds are designated by four letters ordered to indicate the boundary conditions of sides $x = 0$, $y = 0$, $x = a$, and $y = b$. The letters S, C, and F denote simply supported, clamped, and free conditions, respectively.

The pure shear modes of vibration may be of three types. With dilatation $\theta = 0$ in each case, these modes are: a thickness-twist mode in which the transverse shear stresses $\tau_{yz} = \tau_{zx} = 0$, a torsional mode in which the in-plane shear stress $\tau_{xy} = 0$, and a coupled thickness-twist-torsional mode in which the in-plane shear and either or both of the transverse shear stresses are nonzero. In each of the solutions given in Table 1, such modes are identified.

It needs to be mentioned here that the solutions for simply supported (SSSS) parallelepipeds given in Table 1 are actually included in the work of Srinivas et al. (1970a); these are included here for completeness.

Table 1. Frequency equations for pure shear modes of free vibration of rectangular parallelepipeds simply supported on two opposite sides and free on lateral surfaces

Plate	Modal displacement functions	Range of indices	Mode, frequency (Ω)
SSSS	$u = mA\cos m\pi X \sin n\pi Y \sin k\pi Z$		
	$v = n\lambda A \sin m\pi X \cos n\pi Y \sin k\pi Z$	$m, n = 1, 2, \ldots$	Twist
	$w = -k\alpha A \sin m\pi X \sin n\pi Y \cos k\pi Z$	$k = h\sqrt{(\frac{m}{a})^2 + (\frac{n}{b})^2}$	$\pi\sqrt{2(m^2 + n^2\lambda^2)}$
	$u = n\lambda A \cos m\pi X \sin n\pi Y \cos k\pi Z$		
	$v = -mA \sin m\pi X \cos n\pi Y \cos k\pi Z$		Twist and torsion
	$w = 0$	$m, n, k = 0, 1, 2, \ldots$	$\pi\sqrt{m^2 + n^2\lambda^2 + k^2\alpha^2}$
SCSC,	$u = A \sin n\pi Y \cos k\pi Z$	$m = 0$; $n = 1, 2, \ldots$	Twist and torsion
SSSC	$v = 0$, $w = 0$	$k = 0, 1, 2, \ldots$	$\pi\sqrt{n^2\lambda^2 + k^2\alpha^2}$
SSSF,	$u = A \sin(\frac{2n+1}{2})\pi Y \cos k\pi Z$	$m = 0$	Twist and torsion
SCSF	$v = 0$, $w = 0$	$n, k = 0, 1, 2, \ldots$	$\pi\sqrt{(\frac{2n+1}{2})^2\lambda^2 + k^2\alpha^2}$
SSSF,	$u = mA \cos m\pi X \sin n\pi Y$	$m = n\lambda$	Twist
SFSF	$v = -n\lambda A \sin m\pi X \cos n\pi Y$, $w = 0$	$m, n = 1, 2, \ldots$	$\sqrt{2}\pi m$
SFSF	$u = mA \cos m\pi X \sin k\pi Z$	$m = k\alpha$	Torsion
	$v = 0$, $w = -k\alpha \sin m\pi X \cos k\pi Z$	$m, k = 1, 2, \ldots$	$\sqrt{2}\pi m$
	$u = A \cos n\pi Y \cos k\pi Z$	$m = 0$	Twist and torsion
	$v = 0$, $w = 0$	$n, k = 0, 1, 2, \ldots$	$\pi\sqrt{n^2\lambda^2 + k^2\alpha^2}$

REFERENCE

Srinivas, S., Rao, C. V. J., and Rao, A. K. (1970). An exact analysis for vibration of simply supported homogeneous and laminated thick rectangular plates. *J. Sound Vibr.* **12**, 187-199.

VIBRATION BEHAVIORS OF DEFECTIVE SYSTEMS

Su Huan Chen and Zhong Dong Wang
Department of Mechanics, Jilin University of Technology
Changchun 130025, People's Republic of China

Introduction

The vibration behaviors of linear systems have been well understood and it is assumed that the system has a set of complete eigenvectors to span eigenspace, i. e. the system is nondefective. However, in actual problems, such as general damping systems, flutter analysis of aeroelasticity, rotor system with damping connectors, and so on, the system, called defective system, do not have a set of complete eigenvectors to span the space, do exist and can not be ignored. In this paper, we will start with the vibration behaviors of systems with repeated and close frequencies, and then give those of the defective and near defective systems.

Vibration Behaviors of System with Repeated and Close Frequencies[1]

In engineering, many complex large scale structures, such as an airplane, rocket systems, space station, high tower, bridge and ocean platform, may often have repeated or cluster frequencies. To understand the behaviors of modes of repeated frequencies plays an important role in dynamic design of such structures. In this case, two important characteristics of modes of repeated frequencies may arise: first, if the small changes are made on the system, the multiple frequencies, $\omega_{01} \sim \omega_{0m}$, may be separated into m distinct frequencies, $\omega_1 \sim \omega_m$; second, the modal vectors corresponding to the multiple frequencies may have a jump, that is a large change,

$$\Delta u_i = u_i - u_{0i}, \qquad i = 1, 2, \cdots, m \tag{1}$$

may not be small. We illustrate these behaviors by means of the following example.
Let us consider a two degrees of freedom system and the vibration eigenproblem is

$$\begin{aligned} &[K_1 + \frac{1}{4}(K_2 + K_3)]x_1 + \frac{\sqrt{3}}{4}(K_3 - K_2)x_2 + \omega^2 m x_1 = 0 \\ &\frac{\sqrt{3}}{4}(K_3 - K_2)x_1 + \frac{3}{4}(K_3 + K_2)x_2 + \omega^2 m x_2 = 0 \end{aligned} \tag{2}$$

If $K_1 = K_2 = K_3 = K$, the eigenvalues $\lambda_1 = \omega_1^2$, $\lambda_2 = \omega_2^2$, are identical, that is

$$\lambda_1 = \lambda_2 = \frac{3K}{2m} \qquad U_0 = \begin{bmatrix} 1 & 0 \\ 0 & 1 \end{bmatrix} \tag{3}$$

where U_0 is the modal matrix.

If $K_1 = K_2 = K$ and $K_3 = K + \delta K_3$, the eigenvalues and modal vectors of the perturbed system, are

$$\lambda_1 = \frac{3k + 2\delta K_3}{2m} \qquad \lambda_2 = \frac{3k}{2m}$$

$$U = \begin{bmatrix} \frac{1}{2} & \frac{\sqrt{3}}{2} \\ \frac{\sqrt{3}}{2} & -\frac{1}{2} \end{bmatrix} \tag{4}$$

As can be seen from this example, although the eigenvalue λ_1 has only small change caused by the small change of the system, the eigenvectors have a jump. The reason arising the jump of eigenvectors is that the eigenvectors corresponding to the repeated eigenvalues $u_{0i}(i = 1,2)$ are not unique and the combination of u_{0i} is also the eigenvector corresponding to the multiple eigenvalue λ_{0i}, that is

$$u_{0i} = U_0 \alpha \tag{5}$$

How do we find the expansion coeficients α? If small changes are made on the structure with repeated frequencies, such as the example given by equation (2), the structure may have close frequencies or cluster. In the view of mathematics, the close frequencies are distinct, howerever, the behaviors of vibration modes of close frequencies are similar to those of the repeated frequencies. Although the individual mode of close frequencies is ill—condition, the eigen—subspace corresponding to close frequencies is still well condition, that is if the system has small change, the eigenvectors may have large change, and the eigensubspace has only small change. Because of the ill—condition of modes of close frequencies, the dynamic design, modal identifications, and active control are very difficult to implement for such system. Recently, many research work focused on the dynamic design, modal identification, and active vibration control of structures with close frequencies.

Vibration Behaviors of Defection and Near Defective Systems[2—3]

In the above discussion for the behaviors of modes of repeated or cluster frequencies, we have assumed that the system has a set of complete eigenvectors to span the eigenspace, i. e. the system is nondefective. However, in actural problems, such as general damping systems, flutter analysis of aeroelasticity, rotor system with damping connectors, and so on, the system, called defective system, do not have a set of complete eigenvectors to span eigenspace.

Assume the matrix of system considered is A, the eigenvalue λ has m multiplicity, the number of the linear independent eigenvectors is Gm. If $Gm = m$, the system, A, is nondefective; if $Gm < m$, the system is defective. In this case, the defective matrix A can not be transformed into diagonal by modal matrix. The vibration equation for defective system is as follows:

$$AU = UJ \tag{6}$$

$$A^H V = V J^H \tag{7}$$

$$UV^H = I \tag{8}$$

where $U = [u_1, u_2, \cdots, u_n]$, $V = [v_1, v_2, \cdots, v_n]$ are the generalzed modal matrix, V^H is the conjugate transpose of V, and J is the Jordan form of matrix A. Equation (6) can be written in the following form

$$(A - \lambda I)u_1 = 0 \tag{9}$$

$$(A - \lambda I)u_2 = u_1 \tag{10}$$

$$\cdots \cdots$$

$$(A - \lambda I)u_m = u_{m-1} \tag{11}$$

As an illustrative example, we consider flutter problem of airfoil. The airfoil is replaced by a rigid rectangular panel with two degrees of freedom: a vertical displacement Z and a rotation θ. It is assumed that aerodynamic lift force $p\theta$ is proportional to the angle of attack θ and to the square of the velocity v of flight. The differential equations of motion are

$$\begin{aligned} m_0\ddot{Z} - m_0a_0\ddot{\theta} + C_1Z - p\theta = 0 \\ -m_0a_0\ddot{Z} + m_0(i_0^2 + a_0^2)\ddot{\theta} + C_2\theta = 0 \end{aligned} \tag{12}$$

where m_1 is the mass of the panel of unit length, C_1 and C_2 are stiffness, p is a load parameter propertional to the square of velocity v, i_0 is the radius of gyration. If the velocity v of flight was taken a critical value, the system becomes defective and the flutter occurs.

It should be noted that the defective eigenvalue and eigenvectors are very sensitive with respect to the changes of the system parameters. The small changes of the system parameter may cause the large changes of the defective eigenvectors. For example, given a system with matrix A_1

$$A_1 = \begin{bmatrix} 1 & 1+\varepsilon \\ 0 & 0.9999 \end{bmatrix} \tag{13}$$

A_1 has two linear independent eigenvectors

$$u_1^{(1)} = \begin{bmatrix} 1 \\ 0 \end{bmatrix} \qquad u_2^{(1)} = \begin{bmatrix} 1 \\ \dfrac{0.00001}{1+\varepsilon} \end{bmatrix} \tag{14}$$

where ε is a small parameter. If $\varepsilon \to 0$, $\lambda_1 \to \lambda_2$ and $u_1^{(1)} \to u_2^{(1)}$, that is the system is defective or near defective.

Because of the complecity of the behaviors of the defective modes, the dynamic design, modal identifications, and active control are more difficult than those of systems of repeated or cluster frequencies, and more research work focused on this field.

ACKNOWLEDGEMENTS: This work is supported by the National Natural Science Foundation of China.

References

[1]Chen, Suhaun, Matrix Perturbation Theory in Structural Dynamics, Internation Academic Publisher, 1993.

[2]Xu, T., and Chen, Suhuan, Pertubation Sensitivity of Generalized Modes of Defective System, Computer and Structure, Vol. 52, No. 2, pp. 179～185, 1994.

[3]Chen, Suhuan, and Xu, T., Matrix Perturbation Theory for Linear Vibration Defective Systems, ACTA Mechanica Ainca, Vol. 24, No. 6, pp. 747～752, 1992.

FREE VIBRATIONAL ANALYSIS USING THE RITZ METHOD WITH "ARTIFICIAL" SPRINGS

S.M. Dickinson

Department of Mechanical and Materials Engineering
The University of Western Ontario
London, Ontario, Canada, N6A 5B9

When studying the free vibration of a system, the choice of the method of analysis to be used depends upon a number of things, including the expertise of the investigator, the equipment and software available, the complexity of the system and the accuracy desired. If the geometry of the system is complex or it comprises several components, then the finite element method is often the preferred means of analysis. However, the relative complexity of the formulation, the computer programming required (if a base or commercial package is not available) and the accuracy obtained by its use often renders it less attractive than more classical analytical approaches for systems to which the latter apply. The Ritz method is one such approach and is well recognized as an efficient and accurate method of analysis for the treatment of systems of relatively simple geometry and having few if any discontinuities. There are various ways in which the classical Ritz method can be rendered more versatile than in its standard form and these include the domain decomposition method, the hierarchical (and standard) finite element method and the use of an "artificial" spring approach. It is this last approach with which this paper is concerned.

In his address to the American Mathematical Society, Courant [1] included a discussion of the use of the Ritz method for solving problems with rigid boundaries by treating them as limiting cases of free boundary problems, for which the choice of the coordinate functions can be simpler. The technique was essentially to introduce appropriate artificial springs at the otherwise free boundaries and to permit their stiffnesses to become sufficiently high that the required rigid supports were approximated. The technique has since been employed by numerous researchers for the solution of rigid boundary problems, as in the work of Kao [2] and Mizusawa [3], or for the limiting cases for spring supported systems, as in the work of Warburton and Edney [4], Cortinez and Laura [5] and Kim *et al.* [6]. A similar technique may be used to solve problems of systems comprising two or more components, as follows:

(a) The system under consideration is decomposed into its individual components, the boundaries of each being treated as free.

(b) The displacement for each component is written in terms of coordinate functions chosen to satisfy the geometrical free boundary conditions.

(c) The system is assumed to vibrate freely in simple harmonic motion and the maximum strain and kinetic energies for each component are evaluated in terms of the coordinate functions.

(d) Appropriate "artificial" springs are introduced at the boundaries of the system and at the connections between adjacent components and the maximum strain energy in each spring evaluated, again in terms of the coordinate functions.

(e) The maximum strain and kinetic energies are summed over the entire system and the Ritz minimization procedure carried out to give an eigenvalue problem for a flexibly jointed and supported system.

(f) Should the actual system have any flexible joints between components or at the boundaries, then the appropriate "artificial" springs are given the actual stiffenesses. In order to approximate rigid connections at the boundaries or between components, the stiffnesses of the connecting springs are assigned very high values relative to those of the individual components. The eigenvalue problem is then for the actual system under consideration.

The approach described, which may be construed as a physical interpretation of the penalty function method, has been used by the author and his co-workers to study the free vibration of a number of systems. These include stepped straight and curved, slender beams [7], rectangular plate systems [8], circularly cylindrical shell and plate systems [9] (also treated by Cheng and Nicolas [10] using the same technique), sectorial, annular and circular plates [11,12] (including radial and circumferential slits approximating cracks), plates and shallow shells with curved boundaries [13,14] and shallow rectangular planform shells with slits [15]. Some of these applications will be discussed, illustrating the versatility of the approach, its characteristics and the accuracy of the results achievable. It should be mentioned that, by the introduction of "artificial" springs to approximate rigid connections, the very useful upper bound characteristic of the Ritz approach may appear to be lost. However, it is found that the spring stiffnesses can be permitted to be sufficiently high that the upper bound characteristic is essentially preserved, without computational difficulty.

References

1. R. Courant 1943 *Bulletin of the American Mathematical Society* **49**, 1-23. Variational methods for the solution of problems of equilibrium and vibration.
2. R. Kao 1975 *International Journal of Solids and Structures* **11**, 21-31. Application of Hill functions to two dimensional plate problems.
3. T. Mizusawa 1979 *Journal of Sound and Vibration* **62**, 301-308. Vibration of skew plate by using B-spline functions.
4. G.B. Warburton and S.L. Edney 1984 *Journal of Sound and Vibration* **56**, 537-552. Vibrations of rectangular plates with elastically restrained edges.
5. V.H. Cortinez and P.A.A. Laura 1986 *Journal of Sound and Vibration* **99**, 144-148. Vibrations and buckling of a non-uniform beam elastically constrained at one end with concentrated mass at the other.
6. C.S. Kim, P.G. Young and S.M. Dickinson 1990 *Journal of Sound and Vibration* **143**, 379-394. On the flexural vibration of rectangular plates approached by using simple polynomials in the Rayleigh-Ritz method.
7. J. Yuan and S.M. Dickinson 1992 *Journal of Sound and Vibration* **153**, 203-216. On the use of artificial springs in the Rayleigh-Ritz method for the study of the free vibration of straight and curved beams.
8. J. Yuan and S.M. Dickinson 1992 *Journal of Sound and Vibration* **159**, 39-56. The flexural vibration of rectangular plate systems approached by using artificial springs in the Rayleigh-Ritz method.
9. J. Yuan and S.M. Dickinson 1994 *Journal of Sound and Vibration* **175**, 241-263. The free vibration of circularly cylindrical shell and plate systems.
10. L. Cheng and J. Nicolas 1992 *Journal of Sound and Vibration* **155**, 231-247. Free vibration analysis of cylindrical shell-circular plate system with general coupling and various boundary conditions.
11. J. Yuan, P.G. Young and S.M. Dickinson 1994 *Computers and Structures* **53**, 327-334.

Natural frequencies of circular and annular plates with radial and circumferential cracks.
12. J. Yuan and S.M. Dickinson 1996 *Computers and Structures* **58**, 1261-1264. On the vibration of annular, circular and sectorial plates with cut-outs or on partial supports.
13. P.G. Young and S.M. Dickinson 1994 *Journal of Sound and Vibration* **177**, 93-109. Further studies on the vibration of plates with curved edges, including complicating effects.
14. P.G. Young and S.M. Dickinson 1995 *Journal of Sound and Vibration* **181**, 203-230. Vibration of a class of shallow shells bounded by edges described by polynomials, Part I: Theoretical approach and validation; Part II: Natural frequency parameters for shallow shells of various different planforms.
15. J.A. Crossland and S.M. Dickinson 1997 *Journal of Sound and Vibration* **199**, 513-521. The free vibration of thin rectangular planform shallow shells with slits.

Dynamic Stiffness Vibration Analysis of Non-Uniform Members

Moshe Eisenberger

Faculty of Civil Engineering

Technion - Israel Institute of Technology

Technion City 32000

Israel

Fax: +972-4-8323433

e-mail: cvrmosh@techunix.technion.ac.il

July 2, 1997

Abstract

Solutions for the vibrations of continuous systems composed of prismatic members are widely known. For non-uniform members these are not available, and the common practice is to fall back to approximate numerical techniques for their solotion. The types

of vibrational analysis of non-uniform members that will be covered in this presentation are divided into several classes:

- Second oreder equations including axial vibrations of variable cross section members [2] and torsional vibrations of variable cross section rods.
- Fourth order equations including Euler beam vibrations, torsional vibrations including the effects of warping, composite beams [6,7,8], and beams on elastic foundations [4].
- Coupled equations of motion such as Timoshenko beams [5], coupled flexural torsional vibrations, and Vlasov beams including shear deformations.

For all the above cases the author's exact element method [1,3] for static analysis was expanded to include the inertia terms and the dynamic stiffness matrix was found. Examples will be given for all the above mentioned applications.

References

1. Eisenberger, M., "An Exact Element Method", *Int. Jour. Num. Meth. in Engng.*, Vol. 30, pp. 363-370, 1990.
2. Eisenberger, M., "Exact Longitudinal Vibration Frequencies of a Variable Cross Section Rod", *Applied Acoustics*, Vol. 34, pp. 123-130, 1991.
3. Eisenberger, M., "Exact Solution For General Variable Cross Section Members", *Computers and Structures*, Vol. 41, pp. 765-772, 1991.

4. Eisenberger, M., "Vibration Frequencies for Beams on Variable One and Two-Parameter Elastic Foundation", *Jour. of Sound and Vibrations*, Vol. 176, pp. 577-584, 1994.

5. Eisenberger, M., "Dynamic Stiffness Matrix for Variable Cross Section Timoshenko Beams", *Comm. Appl. Numer. Meth.*, Vol. 11, pp. 507-515, 1995.

6. Abramovich H., Eisenberger, M., and Shulepov, O., "Vibrations of Multi-Span Non-Symmetric Composite Beams", *Composite Engineering*, Vol. 5, pp. 397-404, 1995.

7. Eisenberger, M., Abramovich H., and Shulepov, O., "Dynamic Stiffness Matrix for Laminated Beams Using A First Order Shear Deformation Theory", *Composite Structures*, Vol. 31, pp. 265-271, 1995.

8. Abramovich H., Eisenberger, M., and Shulepov, O., "Vibrations and Buckling of Non-Symmetric Laminated Composite Beams Via The Exact Element Method", *AIAA Jour.*, Vol. 34, pp. 1064-9, 1996.

FREE VIBRATION OF FLEXIBLE MEMBERS

Demeter G. Fertis
Department of Civil Engineering, University of Akron

ABSTRACT

The research work here deals with the free vibration analysis of flexible prismatic and nonprismatic members. During vibration, the beam carries its own weight, as well as other weights that are attached to the member and participate in its vibrational motion. The variation of the mass can be of any arbitrary nature, and its moment of inertia, or stiffness EI, where I is the cross-sectional moment of inertia and E is the Young's modulus, may also vary in an arbitrary manner. Since vibrations of flexible members are taking place with respect to a large static configuration position, it becomes important to locate this position as accurately as possible. The method of the equivalent systems as developed by Fertis and co-workers can be used for this purpose. Therefore, the free vibration analysis here is done in two steps. The first step involves the solution of the Euler-Bernouli nonlinear differential equation, in conjunction with the method of the equivalent systems, in order to establish the static equilibrium configuration and position. From this position, the small vibrations of the member can be determined by using appropriate differential equation that incorporate the effect of the large static deformation. The results are compared by using more than one method to calculate the frequencies. The methodology used here is based on two important transformations. The first one is the replacement of the initial nonlinear system by a mathematically equivalent linear system of identical behavior. The second important transformation is that the equivalent linear system is a straight member that replaces the initial member in its large deflected configuration. In other worlds, we replace a curved nonlinear member by an equivalent linear straight member. Such transformations should create some interesting discussion at the Symposium. These theories may be extended to apply to large vibrational amplitudes and to flexible members that respond inelastically. Several aspects and applications of the general methodology will be discussed, by including mode shape diagnostics of complicated linear and nonlinear systems, if time permits.

FREE VIBRATION ANALYSIS OF RECTANGULAR PLATES WITH ARBITRARILY DISTRIBUTED NON-UNIFORM CLASSICAL EDGE SUPPORTS

By

D.J. Gorman
Department of Mechanical Engineering
University of Ottawa

INTRODUCTION

The problem of obtaining free vibration frequencies and mode shapes for thin rectangular plates with uniform classical edge conditions is one that has been fully resolved for a number of years. The situation pertaining to plates with arbitrary discontinuities in these classical, clamped, simply supported, free, boundary conditions is quite different. Even resolution of the problem of a cantilevered plate with clamping part way along the fixed edge presents the analyst with a formidable challenge [1]. Nevertheless, there is a need to obtain continuum mechanics solutions for this general set of problems and the solution proceedure must be one that is amenable to exploitation by the design engineer. Examples of plates with discontinuities in edge support are often encountered, for example, in the design of electronic circuit boards.

In this paper it is shown how use of the superposition method, and the availability of an extremely limited number of harmonic forced vibration solutions, permits the establishment of Eigenvalues and mode shapes for this most general family of problems. It is shown that almost arbitrarily selected accuracy can be obtained, and certainly, accuracy meeting virtually all realistic design needs.

MATHEMATICAL PROCEEDURE

The superposition method for plate free vibration analysis has been adequately described in many articles in the literature (see for example ref. [2]). It is sufficient to state that all problems of the type under discussion here can be resolved by means of the six building blocks (forced vibration solutions) shown schematically in Figure 1.

Each of the first four building blocks is driven along one edge by a distributed harmonic bending moment. The fifth building block is driven by a concentrated harmonic force located on the plate lateral surface. All non-driven plate edges are free of vertical edge reaction and have zero slope measured normal to the edge. Driven edges are also free of vertical edge reaction.

The spacial distribution of the driving moment of the first building block is expressed in series form as,

$$\frac{M b^2}{a D} = \sum_{m=1,2}^{K} E_m \cos\,(m-1)\,\pi\,\xi \qquad (1)$$

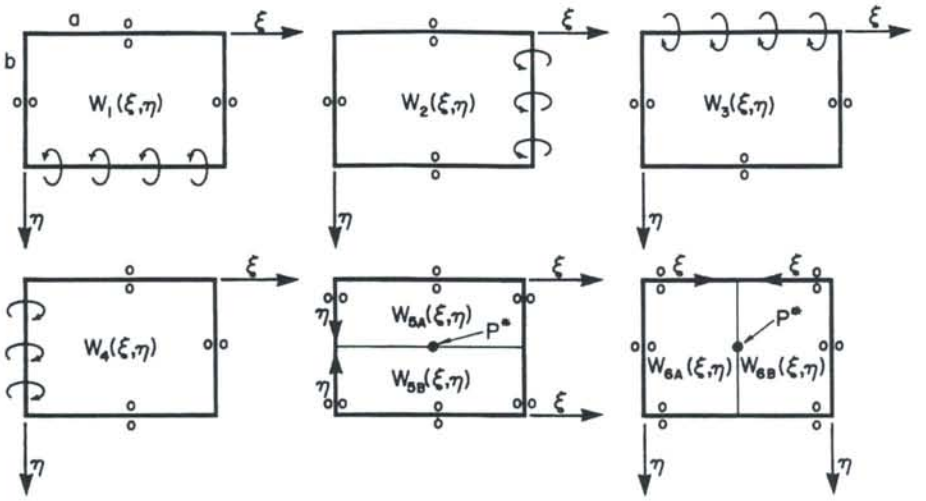

Figure 1. Schematic representation of building blocks utilized in analysis

It is well known that the response of this building block can be written as [2],

$$W(\xi,\eta) = \sum_{m=1,2}^{K} Y_m(\eta)\ \cos\ (m-1)\ \pi\xi \qquad (2)$$

where, for $\lambda^2 < (m\pi)^2$

$$Y_m(\eta) = E_m\left\{\theta_{11\,m}\cosh\ \beta_m\eta + \theta_{12\,m}\cos\ \gamma_m\eta\right\} \qquad (3)$$

and, for $\lambda^2 > (m\pi)^2$

$$Y_m(\eta) = E_m\left\{\theta_{22\,m}\cosh\ \beta_m\eta + \theta_{23\,m}\cosh\ \gamma_m\eta\right\} \qquad (4)$$

ξ and η, are the dimensionless co-ordinates of figure 1, λ^2 is the Eigenvalue and equals $\omega\, a^2\sqrt{\rho/D}$, where ω is the circular frequency, "a" is the plate edge length along the ξ axis, ρ = mass of plate per unit area, and D equals the plate rigidity. All other symbols are defined in Ref. [2].

Solutions for the second, third, and fourth building blocks are readily extracted from that of the first.

The fifth building block is split into two segments and the difference in shear forces across the common boundary is constrained so as to equal shear load associated with the concentrated force P^*. This force is expanded along the common boundary in series form using the DIRAC function. Upon enforcing obvious continuity conditions a solution is obtained for the segments of the fifth building block, which is identical in from to that of the first [2]. The sixth building block differs from the fifth only in that it is split in a different direction.

APPLICATION OF THE SUPERPOSITION METHOD

Consider, for illustrative purposes that we wish to utilize the present method to analyze the free vibration behavior of a conventional cantilever plate. In addition to the first four building blocks above, we superimpose a set of building blocks with concentrated driving forces. A single row of equally spaced forces is distributed along the clamped edge. A second row is then located parallel to the first, but separated from it by 1% of the distance across the plate measured from the clamped edge. Utilizing the above building blocks a solution is obtained for associated Eigenvalues, subject to the condition that there is zero net moment along all plate edges and zero net lateral displacement at all driving force locations. Standard solution techniques are employed [2]. It is found, for example, that Eigenvalues obtained in this way are within about 1 to 1.5% of the known Eigenvalues for cantilever plates. Convergence is found to be rapid, with about 14 terms utilized in the series.

It will now be obvious that by a judicious distribution of single, or double, interrupted rows of point forces the plate can easily be subjected to clamped, simple, or free edge support at any desired regions along the edges. In the full paper the results of comparisons between experimentally measured frequencies and frequencies obtained by this fairly simple theoretical approach are compared. Other questions have had to be addressed. For example, plate response to concentrated forces acting along the edges can be obtained without utilizing the split-plate solution described above. Which approach is best? Also, should building blocks be utilized wherein the plate split-line runs parallel, or normal, to the point-supported edges. All these questions are explored and recommendations made based on the authors experience.

It has been demonstrated in earlier publications that continuous line support along the plate surface can be closely simulated with a row of point supports [3]. It is found here that simple or clamped support along the plate edges can be closely simulated with a single or closely spaced double row of support points, respectively. It is relatively easy to arrive at a reasonable density for point supports, and spacing between point support rows at the boundaries, as the Eigenvalues are well known for all possible combinations of uniform classical edge conditions.

SUMMARY & CONCLUSION

It is demonstrated that the method described constitutes a fairly simple yet quite accurate means for obtaining natural frequencies and mode shapes of plates with arbitrarily distributed classical edge support. Recommendations are made for support point density, separation of support point rows, and the form of split plate solution to be selected. Fortunately, justification for these recommendations is readily demonstrated. The method should prove useful for designers working with such plates.

REFERENCES

1) Gorman, D.J., "An Exact Analytical Approach to the Free Vibration Analysis of Rectangular Plates with Mixed Boundary Conditions", J. of Sound & Vibration, 93 (2), pp. 235-247, 1984.
2) Singal, R.K. and Gorman, D.J., A General Solution for Free Vibration of Rectangular Plates Resting on Fixed Supports and with Attached Masses, A.S.M.E. J. of Electronic Packaging, Vol. 114, pp. 239-245, June 1992.
3) Li, N., and Gorman, D.J., "Free Vibration Analysis of Clamped Rectangular Plates with Line Support along the Diagonals", Journal of Sound and Vibration, 173 (5), pp. 591-598, 1994.

Vibrating Beams Contacting Through a Visco-Elastic Layer: A Mechanical Model for Ultrasonic Motors

Peter Hagedorn

Department of Applied Mechanics
Darmstadt University of Technology
Germany

In this presentation we discuss the nonlinear contact problem between the stator and the rotor of a piezo-electric ultrasonic motor. In a simplified mathematical model this leads to the study of mechanical vibrations of two beams in intermitent contact, with a visco-elastic layer on the surface of one of the beams. The regions of contact between the two beams as well as the contact pressure and the frictional forces are calculated using Fourier Series and assuming COULOMB friction.

Ultrasonic traveling wave motors are a new type of small drives ([1],[2],[3],[4],[5]). Considerable effort has been spent during the last years in the design and optimization of these motors. High frequency mechanical vibrations are generated in the stator by piezoceramic elements polarized in a suitable way and to which an appropriate alternate voltage is applied. Traveling bending waves are generated in the stator in this manner. The rotor is then pressed against the stator by means of a disk spring, often with the stator coated with a visco-elastic friction layer. Due to the kinematics of the stator vibrations, the rotor turns in a direction opposite to that of the traveling wave in the stator (see [6] for details). Ultrasonic traveling wave motors typically produce high torques at low rotational speeds.

In the bending vibrations of the stator and of the rotor, contact between the two parts occurs in small contact regions only. A realistic mathematical model of the contact between the stator and the rotor is necessary for a reliable analysis of the motor, which is needed for the optimization of its performance.

For a simplified treatment, here the ultrasonic traveling wave motor is substituted by a *linear* motor. The stator is modeled as an elastically supported BERNOULLI-EULER beam, whose motion in the axial direction is restricted. The slider is also elastically supported and pressed against the stator, which is coated with a viscoelastic friction layer.

In previous studies the slider was assumed as rigid, which may be a reasonable assumption for certain cases ([1],[7]). However, a more realistic model has to include the elasticity of both the stator and the slider. This becomes particularly important for thin sliders (or rotors) and a high prestress between slider and stator. Therfore, in this paper the slider is modeled as an *axially moving* BERNOULLI-EULER beam.

It turns out, that the contact problem formulated for the linear motor and analyzed in this paper contains many of the essential features of the rotating motor. It therefore represents a useful model for parameter studies and optimization of ultrasonic travelling wave motors.

References

[1] Schmidt, J.P., Hagedorn, P., Bingqi, M.A, *Note on the Contact Problem in an Ultrasonic traveling wave motor*, Journal of Non-Linear Mechanics, Vol. 31, No. 6, pp. 915-924 **155** (1), 31-46, 1996.

[2] Hagedorn, P., Konrad, W., Wallaschek J., *Travelling Wave Ultrasonic Motors, Part II: A Numerical Method for the Flexural Vibrations of the Stator*, Journal of Sound and Vibration, **168** (1), 115-122, 1993.

[3] Sashida, T., Kenjo, T., *An Introduction to Ultrasonic Motors*, Oxford Science Publications, Claredon Press, Oxford, 1993.

[4] Ueha, S., Tomikawa, Y., *Ultrasonic Motors: Theory and Applications*, Oxford Science Publications Claredon Press, Oxford, 1993.

[5] Wallaschek, J., *Piezoelectric Ultrasonic Motors*, Journal of intelligent Material Systems and Structures, Vol. 6, Jan 1995.

[6] Hagedorn, P., Wallaschek J., *Travelling Wave Ultrasonic Motors, Part I: Working Principle and Mathematical Modelling of the Stator*, Journal of Sound and Vibration, **155**(1), 31-46, 1992.

[7] Cao, X., Wallaschek, *Estimation of tangential stresses in the stator/rotor contact of traveling wave motors using visco-elastic foundation models*, In Contact Mechanics II, Computational Techniques, pp. 53-61. Computational Mechanics Publications, Southhampton, Boston (1995)

IN-PLANE VIBRATIONS OF ARCHES WITH VARYING CURVATURE AND CROSS-SECTION

C. S. Huang — National Center for Research on Earthquake Engineering, Taiwan.
Y. P. Tseng — Department of Civil Engineering, Tamkang University, Taiwan.
K. Y. Nieh — Department of Civil Engineering, Tamkang University, Taiwan.

Curved beams play an important role in various structural applications such as arch bridges, roof structures, piping systems, and aerospace structures. Because of their great importance, a vast literature has been published on the dynamic analysis of planar arches(see the review articles [1], [2], [3], and [4]). In this presentation, an accurate solution for analyzing in-plane vibrations of arches having variable curvature and cross-section is proposed. The effects of shear deformation and rotary inertia are taken into account. The solution for free vibration, which, basically, is a analytical solution, is obtained by using the dynamic stiffness method, in which the local dynamic stiffness matrix is established from a general series solution in terms of polynomials. The series solution is formulated by modifying the solution given by Suzuki and Takahash [5], which was established by applying the well-know method of Frobenius. The Laplace transform is applied to time variable and incorporates the dynamic stiffness method to find the transient responses of arches. The solution provides accurate responses of displacement components as well as stress resultants.

The solution for free vibration is verified by a convergence study for a fixed-fixed semi-elliptic arch and a comparison with the results provided by Suzuki et al. [6]. Then, the solution is applied to solve for the natural frequencies of parabolic arches with a complicated variation of cross-section defined by (see Fig. 1)

$$I(x) = \frac{I_c}{[1-(1-\eta^*)\dfrac{|x-l_1|}{l_1}]\cos\phi_x} \tag{1}$$

where I_c is the second moment of the area of cross-section at the middle point of arch, l_1 is a half of the span length , ϕ_x is the angle between the tangent of the centroidal axis and a horizontal axis. The value of the parameter η^* is between 0 and 1. This type of parabolic arch has been frequently designed in civil engineering.

To show the validity of the solution for forced vibration, a parabolic arch with the variation of cross-section defined by eq.(1) subjected to a sinusoidal loading with finite duration at the middle point of arch is analyzed. In the analysis, the effect of damping is also considered. The frequency of the sinusoidal loading is chosen to be very close to one of the natural frequencies of the arch under consideration so that one can see the process of resonance.

Finally, the free vibration of a multiple-span highway arch bridge is analyzed to demonstrate the versatility of the dynamic stiffness matrix developed above in practical engineering,. The deck of the bridge is modeled by straight beam elements. Hence, the analysis is accomplished by using the dynamic stiffness matrices for arches and straight beams. In the analysis, the effects of the shapes of arches on the frequencies are shown.

References:

1. Chidamparam, P. and Leissa, A. W. (1993). "Vibrations of planar curved beams, rings, and arches." *Applied Mechanics Reviews* 46(9), 467-483.

2. Laura, P. A. A. and Maurizi, M. J. (1987). "Recent research on vibrations of arch-type structures." *The Shock and Vibration Digest* 19 (1), 6-9.

3. Markus, S. and Nanasi, T.(1981). "Vibration of curved beams." *The Shock and Vibration Digest* 13 (4), 3-14.

4. Auciello, N. M. And Rosa, M. A. De. (1994). "Free vibrations of circular arches—a review", *Journal of Sound and Vibration*, 176(4), 433-458.

5. Suzuki, K. and Takahashi, S. (1982). "In-plane vibrations of curved bars with varying cross-section." *Bulletin of the Japanese Society of Mechanical Engineer* 25(205), 1100-1107 .

6. Suzuki, K., Miyashita, Y., Kosawada, T., and Takahashi, S. (1985). "In-plane impluse response of a curved bar with varying cross-section" *Bulletin of the Japanese Society of Mechanical Engineer* 28(240), 1181-1187.

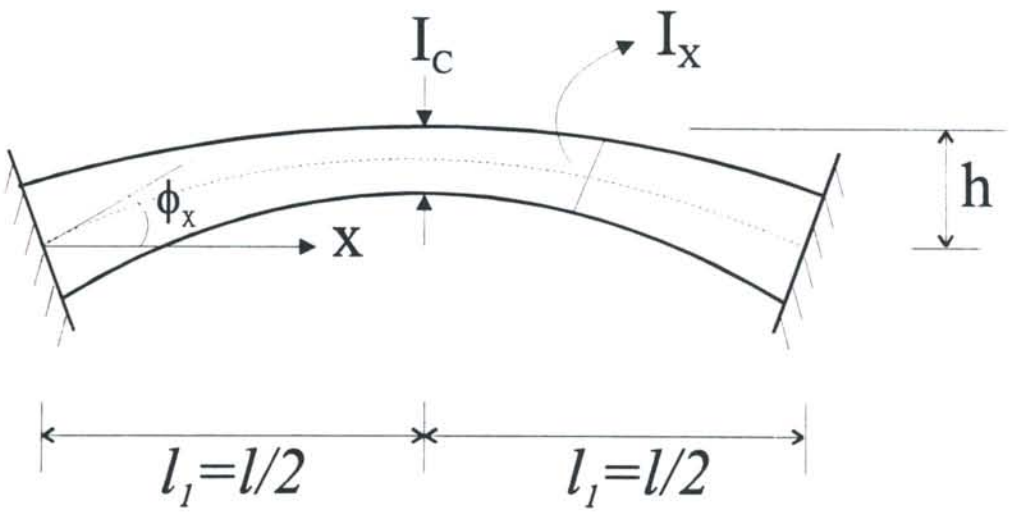

Figure1. A sketch of parabolic arch with varying cross-section.

Vibrations of Thick Free Circular Plates Revisited

James R. Hutchinson
Civil and Environmental Engineering Department
University of California, Davis CA 95616

Introduction

This paper is intended to clarify some of the points made in Ref. 1. In that paper a series solution was used as a basis of comparison for Mindlin plate theory and a modification of a solution method proposed by Pickett. At the time Ref. 1 was written the number of terms used in the series was severely limited by the available computer. Newer computers allow use of many more terms in the series and hence much greater accuracy. The improved accuracy is used to clarify the previous results.

Series Solution

The series solution, which is described in detail in Ref. 2, combines terms which identically satisfy the differential equations of three dimensional linear elasticity. The solution forms are grouped in three series. Two of the series are summations of terms in the axial direction and the third is the sum of terms in the radial direction. Boundary conditions on the shear stress τ_{rz} at the top, bottom and edge of the plate and on $\tau_{\theta z}$ at the top and bottom of the plate are satisfied identically. The boundary conditions on the stress σ_r at the edge, σ_z at the top and bottom, and $\tau_{r\theta}$ at the edge are satisfied by orthogonality. This process leads to a system of homogeneous simultaneous equations whose coefficients are transcendental functions of the natural frequency. Zeros of the determinant of this set of equations give the natural frequencies. The order of the matrix is the number of terms in the radial direction (NR) plus twice the number of terms in the axial direction (NZ). Parameters in the problem are the thickness to diameter ratio h, the circumferential wave number n, and Poisson's ratio ν. The effects of varying Poisson's ratio were adequately covered in Ref. 1 so ν is taken as 0.3 in this paper.

Modified Pickett Method

The modified Pickett method (see Ref. 1) also involves combining terms which identically satisfy the differential equations of three dimensional linear elasticity. The boundary conditions at the top and bottom of the plate are satisfied identically and the boundary conditions at the edges are approximated by setting the resultants M_r, $M_{r\theta}$ and Q_r to zero.

Mindlin Plate Theory

The Mindlin plate theory assumes that normals remain straight but not normal to the mid surface. This formulation leads to an undetermined shear coefficient K. In Ref. 1 it was shown that by matching the exact infinite plate solution for straight-crested flexural waves of long wave length with the Mindlin plate solution a shear coefficient of $5/(6\text{-}\nu)$ resulted. To determine if that shear coefficient had meaning for circular plates, plots were made of the shear coefficient which would make the series solution and the modified Pickett solution match as a function of the thickness to diameter ratio (h). A typical plot from Ref. 1 is shown in Fig. 1. To produce this figure the series solution was limited to 20 terms in each of the three series. This provided sufficient accuracy for the comparison with the Mindlin solution for large h but for smaller h the accuracy wasn't sufficient. In Ref. 1 it was stated, "The reason for the for the exact solution being cut off for small h is two fold: first ... as the plate becomes thinner more terms are needed for equivalent accuracy; and second as the plate becomes thinner, greater accuracy in the frequency is necessary to compute a correct shear coefficient." In this paper the two causes for loss of accuracy is investigated.

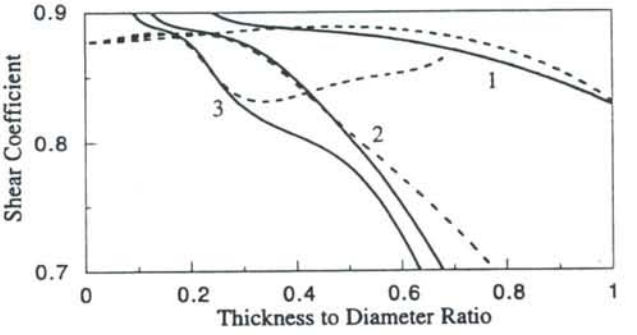

Fig. 1 Shear coefficient vs. thickness to diameter ratio for $n = 0$. Series (——) modified Pickett (---)

Increased Series Size

Increasing the number of terms in each of the series will greatly improve the accuracy of the solution. In Ref. 2 it was shown how the order of the matrix could be reduced to just the number of terms in the radial direction. It was also shown in Ref. 2 that the optimum convergence took place when the ratio of NZ to NR equaled the thickness to diameter ratio h. This work, however, involves small h so NZ should be smaller than NR. Therefore, the order of the matrix was reduced, in a similar manner to Ref. 2, to twice the number of terms in the axial direction . The computer program for finding the frequencies was rewritten to make use of this improvement.

Causes of Lack of Accuracy

The two causes for lack of accuracy for small h is investigated in this section. Table 1 was constructed to investigate convergence and in particular to see the effect of h on the convergence. The nondimensional frequencies in this table are the frequency times the outer radius divided by the shear velocity.

Table 1. Convergence of frequencies for increasing number of terms. NZ and NR refer to the number of terms in the axial and radial directions respectively. Mindlin and modified Pickett solutions are shown for comparison. The Mindlin solution uses K = 5/(6-ν).

		h = 0.05		h = 0.10		h = 0.15	
NZ	NR	Mode 1	Mode 2	Mode 1	Mode 2	Mode 1	Mode 2
4	20	0.498669	1.831930	0.851241	3.075969	1.185550	3.901710
20	100	0.436154	1.766014	0.832208	3.059589	1.176493	3.894039
40	200	0.433726	1.763785	0.831604	3.059075	1.176209	3.893798
60	400	0.433116	1.763228	0.831458	3.058951	1.176144	3.893743
120	60	0.433001	1.763124	0.831426	3.058924	1.176125	3.893727
160	800	0.432962	1.763088	0.831416	3.058915	1.176120	3.893723
200	1000	0.432943	1.763071	0.831412	3.058912	1.176118	3.893721
Mindlin		0.432909	1.762946	0.831368	3.057512	1.175930	3.889495
Pickett		0.432910	1.763044	0.831405	3.058997	1.176134	3.894141

It can be seen that the convergence is slightly more rapid for the higher values of h, although the difference in convergence is not very significant.

The sensitivity of the Mindlin solution was investigated by considering the percentage change in the frequency due to a one percent change in the shear coefficient. A plot of the frequency sensitivity is shown in Fig. 2 for the $n = 0$ case. This plot shows that the sensitivity for all modes approaches zero as h approaches zero. Which means that, for a thin plate, any shear coefficient will produce the appropriate frequency. Putting numbers to the plot, at $h = 0.05$ the sensitivity in the first mode is 0.007% and in the second mode is 0.04%. As a numerical example, in the table above the first mode 200x1000 term solution at $h = 0.05$ agrees with the Mindlin solution to four significant figures. The Mindlin solution is based on K = 0.877 whereas matching the frequency 0.432943 would require a K = 0.886. For this reason in the plots of the shear coefficients which match the series solution, only values of h higher than 0.05 are considered in this paper.

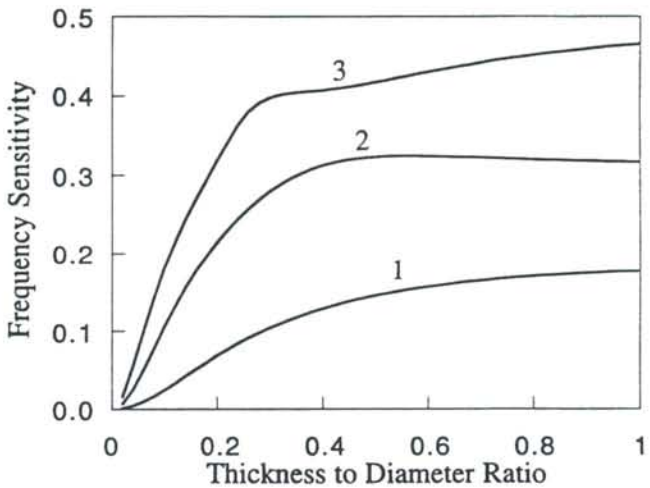

Fig. 2 Percent change in frequency for a one percent change in shear coefficient vs. thickness to diameter ratio.

Accurate Results

Plots of the shear coefficient which would be required in the Mindlin plate theory to make it match the series solution are shown in Figs. 3, 4, 5 and 6. Also shown in the figure is the shear coefficient of $5/(6\text{-}\nu)$ i.e. 0.877 for comparison. To produce the numbers used for these plots from $h = 0.05$ to $h = 0.10$, 1000 terms were used in the radial direction. From $h = 0.11$ to $h = 0.15$, 750 terms were used in the radial direction. From $h = 0.16$ to $h = 0.20$, 500 terms were used in the radial direction. In all of these cases the number of terms in the axial direction was taken as NR x h rounded to the next highest integer. From $h = 0.21$ to $h = 1.00$, 200 terms were used in each of the series.

It can be seen in Figs. 3-6 that for most cases the shear coefficient approaches $5/(6\text{-}\nu)$ as the thickness to diameter ratio goes to zero. If one compares Fig. 3 with Fig. 1 it can be seen that for small h the new solution follows the modified Pickett solution very closely. If one were to compare Figs. 4-6 with the figures in Ref. 1 the same would be seen to be true. It can be seen that as h approaches zero most of the curves approach the shear coefficient $5/(6\text{-}\nu)$. The notable discrepancies are the fundamental modes for the $n = 2$ and $n = 3$ cases. This same discrepancy takes place when the modified Pickett method is employed as shown in Ref.1.

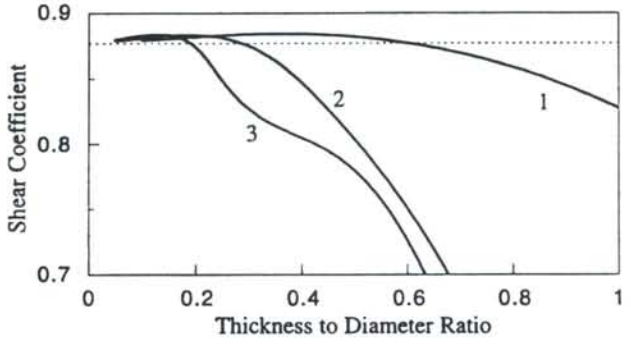

Fig. 3 Shear Coefficient vs. thickness to diameter ratio for $n = 0$.

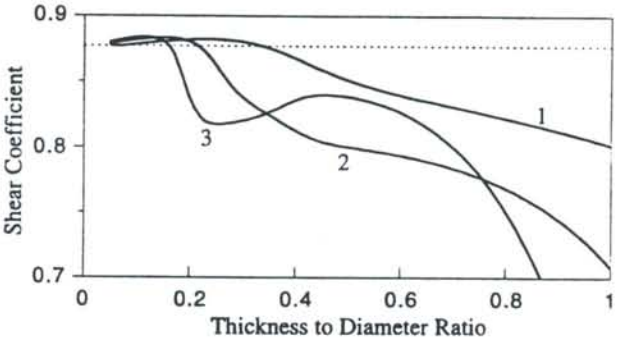

Fig. 4 Shear Coefficient vs. thickness to diameter ratio for $n = 1$.

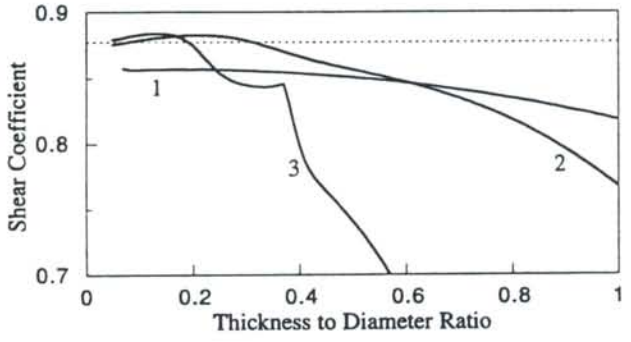

Fig. 5 Shear Coefficient vs. thickness to diameter ratio for $n = 2$.

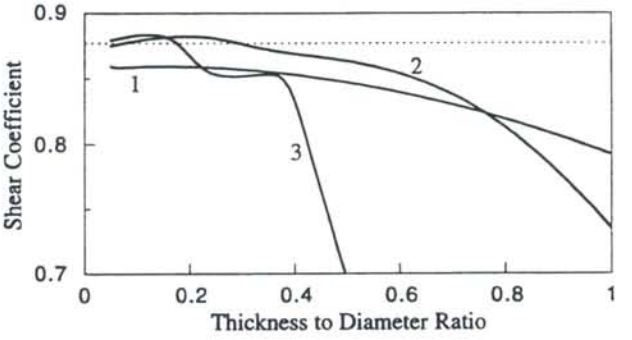

Fig. 6 Shear Coefficient vs. thickness to diameter ratio for $n = 3$.

References

1 Hutchinson J.R. "Vibrations of Thick Free Circular Plates, Exact Versus Approximate Solutions," *ASME Journal of Applied Mechanics*, Vol. 51, 1984, pp. 581-585.

2 Hutchinson J.R. "Vibrations of Solid Cylinders," *ASME Journal of Applied Mechanics*, Vol. 47, 1980, pp.901-907.

On the Application of Rayleigh's Principle and the Ritz Method - Some Points to Ponder

S. Ilanko
Department of Mechanical Engineering, University of Canterbury, New Zealand.

The purpose of this paper is to discuss two interesting issues related to the application of Rayleigh's principle and the Ritz method. These are: (a) the total potential energy of a statically axially loaded Euler-Bernoulli beam; (b) on the use of asymptotically aproximate partially restrained models in the analysis of constrained beams and plates to overcome some limitations on the choice of permissible functions.

Total Potential Energy of an Axially Loaded Beam

The total potential energy of an axially loaded thin beam undergoing small amplitude flexural vibration consists of three components: (1) the strain energy associated with the flexural stiffness of the beam; (2) the potential energy associated with the straining of the supports (applicable for flexible supports only); (3) the additional potential energy due to the static axial force in the beam. The first two components are easily explained and readily found in text books. Although the additional potential energy due to static axial force distribution has been widely used [1,2] its derivation is available only for beams subject to longitudinally dynamically free [3] and fully restrained cases [4]. The typical text book derivations assume that the beam is free to move axially during vibration, and the potential energy associated with the axial force is then found by calculating the work done by the end loads which for a beam subject to a compressive force P results in the equation

$$V_P = -\int_0^L \frac{1}{2} P(v')^2 dx \qquad (1)$$

Sine the end loads P move towards each other by $\int_0^L \frac{1}{2}(v')^2 dx$ the work done by P gives the above expression. For a statically axially loaded beam subject to an longitudinally restrained conditions (such as in cases where the axial force results from temperature changes), the additional potential energy comes from extra strain energy due to the stretching (or release of stretching) of the neutral plane and is available in the literature. For partially longitudinally restrained beams, the additional potential energy consists of the potential energy of the supports (or end loads) as well as the non-flexural component of strain energy. This may be derived from first principles, in terms of the lateral and longitudinal dynamic displacements (v, u respectively). For small displacements, the functions of longitudinal displacement u that appear in the strain energy of the beam and the potential energy of the end loads cancel each other, and the resulting expression is the same as equation (1). This should be expected, since the Newtonian equation of motion for an axially loaded beam does not depend on longitudinal conditions. The derivations also allow for the effect of body forces and the axial force may vary along the beam. The result is not new, and indeed it has been used in the vibration analysis gravity loaded beams and rotating beams. However, to the author's knowledge, the only general derivations in the literature are based on the equations of motion and variational principles. The approach described here is simpler, and the required potential energy expression can be obtained with little manipulation. From author's experience, undergraduate students find these derivations easy to follow.

Rayleigh-Ritz Analysis of Beams Using Asymptotic Models

One of the requirements of the Rayleigh-Ritz procedure is that the displacement functions used must not violate the geometric constraints. For some problems, for example a simply supported plate subject to some point supports, this introduces the additional task of finding suitable permissible functions. If the point support is flexible, sine functions are permissible and inclusion of additional strain energy of equivalent springs would be the only extra work involved. By increasing the "stiffness" of the equivalent springs until it asymptotically approaches a "rigid" support is one way of obtaining an estimate of the natural frequencies of the actual system. However, this only gives an upper bound to the approximate model, and may not be sufficiently accurate due to numerical problems associated with the use of very high values for the stiffness.

Another possible way to approach the "rigid" support is to add a point mass and increase its magnitude until it becomes sufficiently "massive" to restrain the motion of the system at the support fully. Since the natural frequencies decrease with mass, the frequencies of this asymptotically approximate model will approach the frequencies of the actual model from above. This then leads to the question, whether true upperbounds of the natural frequencies of a constrained system can be obtained using an asymptotically approximate model where supports are replaced with masses of very large magnitude.

References:

1. T. Yokoyoma 1988 Int. J. Mech. Sci. 30(10), 743-755. Free Vibration charateristics of rotating Timoshenko beams.

2. B. Schäfer 1985 Ingenieur-Archiv 55, 66-80. Free vibrations of a gravity loaded clamped-free beam.

3. H. McCallion 1973 Vibration of Linear Mechanical Systems. London: Longman Publications.

4. R.V. Southwell 1969 An Introduction to The Theory of Elasticity. New York: Dover Publications.

Free Vibration of Skew Laminated Plates

Rakesh K. Kapania*, Andrew E. Lovejoy† and P. Mohan‡
Department of Aerospace and Ocean Engineering
Virginia Polytechnic Institute and State University
Blacksburg, VA 24061-0203

Abstract

Plate free vibrations have been extensively studied in the literature. These studies have progressed from thin to thick isotropic plates, isotropic plates to thin laminated plates, and finally to thick laminated plates. Most early studies involving quadrilateral plates focussed on rectangular planforms. However, skew and trapezoidal plates find wide use, especially in aircraft structures. Additionally, the growing use of structures fabricated from composite materials has facilitated the development of methods for the analysis of these structures.

The number of papers which study the free vibration of quadrilateral plates is quite voluminous, an in-depth review of theories and approaches is found in Lovejoy and Kapania[1]. Early methods to analyze laminated plate focused on the Classical Laminate Theory (CLT), which involves many simplifying assumptions, e.g., the neglect of transverse shear and normal stress. Only a small portion of the studies presented in the literature since 1986 focuses on skew and/or trapezoidal laminated plates.

Laminated, parallelogram plates have been studied by Iyengar and Umaretiya[2], Ng and Das[3] and Narita[4]. Reference 2 uses characteristic beam functions and/or trigonometric functions in the Galerkin Method for the analysis of plates simply-supported on 2 edges and clamped on the remaining edges. Clamped plates of sandwich construction were studied by Ng and Das[3], also using the Galerkin method. Using the power series in the Rayleigh-Ritz method, cantilever plates were studied by Narita[4]. More recently, Hadid and Bashir[5] present results for the clamped, skew, orthotropic plate calculated using the spline-integral method. Symmetrically laminated, clamped, skew plates have been studied by Hosokawa, Terada and Sakata[6]. The Green function, expressed as a power series, is approximately integrated over small regions of the plate. Frequencies and mode shape nodal patterns are presented for a number of stacking sequences and skew angles. Liew and Lam[7] studied isosceles trapezoidal, anisotropic plates with various boundary conditions using the Rayleigh-Ritz method utilizing two-dimensional orthogonal polynomials. Kapania and Singhvi[8,9] provide a method for the analysis of skew, trapezoidal, thin, laminated plates through the use of Chebychev polynomials in the Rayleigh-Ritz method. The method used is applicable to plates having arbitrarily supported edges, however, only cantilever plates were extensively studied, with frequency results for a number of stacking sequences and planforms being studied. In a subsequent study[10], these authors studied the sensitivity of natural frequency of these plates to various shape variables.

---

* Professor

† Graduate student, Currently, Research Scientist for Analytical Services and Materials, Inc, 107 Research Drive, Hampton, VA 23666.

‡ Graduate Research Assistant

Kapania and Mohan[11] presented free vibration analysis of laminated skew cantilever plates using a flat shell element obtained by combining the Discrete Kirchhoff Theory (DKT) plate bending element and a membrane element similar to the Allman element, but derived from the Linear Strain Triangular (LST) element. Both lumped and consistent mass matrices were employed. Since for the DKT element the transverse displacement is not explicitly defined over the interior, the determination of the consistent mass matrix is not straight-forward. Consistent mass matrix was obtained using the shape functions given by Specht[12] for the transverse displacement and the standard quadratic interpolation functions in area coordinates for the in-plane displacement components. The flat shell element[11] is currently being applied to study the free vibration of laminated rhombic plates which have inclusion angle that is more than 90^o. For such angles, a singularity occurs at those corners[13]. Results from this ongoing study will be presented at the conference.

In laminated or single layer plates in which the transverse shear modulus is small compared to the extensional modulus, as well as in thick plates, transverse shear has a pronounced effect and cannot be neglected. The assumption of Kirchhoff, where transverse shear stiffness is considered to be infinite, results in an over-estimation of the natural frequencies. Laminated, isosceles, trapezoid, cantilever plates were analyzed by Krishnan and Deshpande[14] by means of finite elements. Finite elements, based on the FSDT, are used by both Lakshminarayana, Rajagopal, Ramamurthy, and Joshi[15], and Lee and Lee[16] to study skew, laminated plates, but results are presented only for thin plates. The authors have published papers[1,17,18] regarding the vibration of thick, skew, trapezoidal laminated plates having numerous supports. Chebychev polynomials are implemented in the Rayleigh-Ritz method as applied to the First-Order Shear Deformation Theory (FSDT). Natural frequencies and mode shapes are presented for numerous stacking sequences and planforms for cantilever plates[1,17] and point supported plates[18]. Most recently, Wang[19] has also used the FSDT and Rayleigh-Ritz method, however, B-splines are the chosen functions. At present, the authors are comparing the performance of the Chebychev based Ritz method to that of Wang's B-spline based method. These comparisons will also be presented at the conference.

References

1. Lovejoy, A. E., and Kapania, R. K., "Natural Frequencies and an Atlas of Mode Shapes for Generally-Laminated, Thick, Skew, Trapezoidal Plates," Center for Composite Materials and Structures, Virginia Polytechnic Institute and State University, *CCMS- Report 94-09*, 1994.

2. Iyengar, N. G. R., and Umaretiya, J. R., "Transverse Vibrations of Hybrid Laminated Plates." *Journal of Sound and Vibration*, Vol. 104, 1986, pp. 425-435.

3. Ng, S. S. F., and Das. B., "Free Vibration and Buckling Analysis of Clamped Skew Sandwich Plates by the Galerkin Method." *Journal of Sound and Vibration*, Vol. 107, 1986, pp. 97-106.

4. Narita, Y., "Free Vibration Analysis of Cantilevered Composite Plates of Arbitrary Planform." *JSME International Journal*, Vol. 33, 1990, pp. 291-296.

5. Hadid, H. A., and Bashir, M. H. M., "Free Vibration of Beams and Oblique Panels by Spline-Integration Method." *Journal of Sound and Vibration*, Vol. 189, No. 1, 1996, pp. 3-12.

6. Hosokawa, K., Terada, Y., and Sakata, T., "Free Vibration of Clamped Symmetrically Laminated Skew Plates." *Journal of Sound and Vibration*, Vol. 189, No. 4, 1996, pp. 525-533.

7. Liew, K. M., and Lam, K. Y., "A Rayleigh-Ritz Approach to Transverse Vibration of Isotropic and Anisotropic Trapezoidal Plates Using Orthogonal Plate Functions," *International Journal of Solids and Structures*, Vol. 27, No. 2, 1991, pp. 189-203.

8. Kapania, R. K., and Singhvi, S., "Free Vibration Analysis of Generally Laminated Tapered Skew Plates," *Composites Engineering*, Vol. 2, No. 3, 1992, pp. 197-212.

9. Singhvi S., and Kapania, R. K., "Analysis Shape Sensitivities and Approximations of Modal Response of Generally Laminated Tapered Skew Plates," Center for Composite Materials and Structures, VPI&SU, CCMS-91-20, Nov. 1991.

10. Singhvi, S., and Kapania, R. K., "Analytical Shape Sensitivities and Approximations of Modal Response of Generally Laminated Tapered Skew Plates," *Journal of Aircraft*, Vol. 30, No. 3, 1993, pp. 423–426.

11. Kapania, R. K., and Mohan, P. ,"Static, Free Vibration and Thermal Analysis of Composite Plates and Shells Using a Flat Triangular Shell Element," *Computational Mechanics-an International Journal*, Vol. 17, 1996, pp. 343-357.

12. Specht, B.,"Modified Shape Functions for the Three Node Plate Bending Element Passing the Patch Test," *International Journal for Numerical Methods in Engineering*, Vol. 26, pp. 705-715, 1988.

13. McGee, O. G., Leissa, A. W. and Huang, C. S., "Vibrations of Cantilever Skewed Plates with Corner Stress Singularities," *International Journal for Numerical Methods in Engineering*, Vol. 35, pp. 409-424, 1992.

14. Krishnan, A., and Deshpande, J. V., "A Study on Free vibration of Trapezoidal Plates," *Journal of Sound and Vibration*, Vol. 146, No. 3, 1991, pp. 507-515.

15. Lakshminarayana, H. V., Rajagopal, P., Ramamurthy, M. R., and Joshi, A., "Vibration Characteristics of a Swept Composite Wing Panel: Finite Element Analysis and Experimental Verification," *Journal of the Aeronautical Society of India*, Vol. 37, No. 4, 1985, pp. 289-295.

16. Lee, I., and Lee, J. J., "Vibration Analysis of Composite Plate Wing," *Computers and Structures* , Vol. 37, No. 6, 1990, pp. 1077-1085. 1350, Vol. 3, New Orleans, LA, April 10-13, 1995, pp. 1604-1618.

17. Kapania, R. K., and Lovejoy, A. E., "Free Vibration of Thick Generally Laminated Cantilever Quadrilateral Plates," *AIAA Journal*, Vol. 34, No. 7, July 1996, pp. 1474-1486.

18. Lovejoy, A. E., and Kapania, R. K., "Free Vibration of Thick Generally Laminated Quadrilateral Plates with Point Supports," *Proceedings, 37th AIAA/ASME/ASCE/AHS/ASC Structures, Structural Dynamics, and Materials Conference*, AIAA 96-1346, Salt Lake City, UT, April 15-17, 1996, pp. 248-258.

19. Wang, S., "Free Vibration Analysis of Skew Fibre-Reinforced Composite Laminates Based on First-Order Shear Deformation Plate Theory." *Computers and Structures*, Vol. 63, No. 3, 1997, pp. 525-538.

LARGE AMPLITUDE FREE VIBRATION OF COMPOSITE LAMINATED SHALLOW SHELLS

Yukinori KOBAYASHI, Gen YAMADA and Syogo KIMURA
Division of Mechanical Science, Hokkaido University, Sapporo, 060, Japan

INTRODUCTION

Since fiber reinforced plastic (FRP) has been used widely to improve the characteristics of structures recently, many researchers have attacked nonlinear problems of laminated composite shells.[1)-7)] In this paper, the Ritz method and Galerkin's procedure are used to solve the governing equations for the nonlinear vibration of laminated composite shallow shells based upon the first order shear deformation theory (FSDT). The Ritz method is used to determine the trial function for Galerkin's procedure, because it is difficult to find the suitable trial function that satisfy the boundary conditions except the case of simply-supported shells. Eigenfunctions for the linear free vibration are used to express the displacements, approximately, in the nonlinear analysis of the shell. Applying Galerkin's procedure and eliminating variables except transverse displacement, the governing equations are reduced to an elliptic ordinary differential equation in time. The period of vibration for the shell is calculated by integrating the equation. The present method is applied to a clamped shallow shell which has a rectangular planform.

ANALYSIS

Figure 1 shows a shallow shell which has a rectangular boundary and principal curvature radii R_x and R_y. The thickness of the shell is h and lengths of edges are a and b. The displacement components are u, v and w in the x, y and z directions, respectively. The principal directions of elasticity are denoted as 1- and 2-axes and the 3-axis is coincident to the z-axis. The angle between 1- and x- axes is θ. Applying FSDT, the displacement field of the shell may be expressed as

$$u = u_0 + z\,\psi_x, \quad v = v_0 + z\,\psi_y, \quad w = w_0, \tag{1}$$

where u_0, v_0 and w_0 are the displacements at the midsurface, and ψ_x and ψ_y are the rotations of the midsurface about the y and x axes, respectively. The classical lamination theory is used to obtain the elastic rigidities. Assuming $1+z/R_i \fallingdotseq 1$ $(i=x, y)$, the equations of motion of the shell are derived as

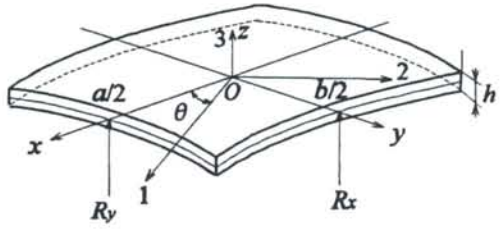

Fig.1 Coordinate system of a shallow shell

$$\frac{\partial N_x}{\partial x}+\frac{\partial N_{xy}}{\partial y}+\frac{Q_x}{R_x}=\rho h\ddot{u}_0,\quad \frac{\partial N_{xy}}{\partial x}+\frac{\partial N_y}{\partial y}+\frac{Q_y}{R_y}=\rho h\ddot{v}_0,$$

$$-\frac{N_x}{R_x}-\frac{N_y}{R_y}+\frac{\partial Q_x}{\partial x}+\frac{\partial Q_y}{\partial y}+\frac{\partial}{\partial x}(N_x w_{0,x}+N_{xy}w_{0,y})+\frac{\partial}{\partial y}(N_y w_{0,y}+N_{xy}w_{0,x})=\rho h\ddot{w}_0, \tag{2}$$

$$\frac{\partial M_x}{\partial x}+\frac{\partial M_{xy}}{\partial y}-Q_x=\frac{\rho h^3}{12}\ddot{\psi}_x,\quad \frac{\partial M_y}{\partial y}+\frac{\partial M_{xy}}{\partial x}-Q_y=\frac{\rho h^3}{12}\ddot{\psi}_y,$$

where N_x, N_y, N_{xy} are inplane force resultants, M_x, M_y, M_{xy} are moment resultants and Q_x and Q_y are shear force resultants. The shear correction factor is introduced to obtain the shear force resultants and the value 5/6 is used in this paper. In–plane and rotational inertia terms are neglected in the following analysis. Linear free vibration of the shell is solved by the Ritz method prior to the nonlinear analysis, then eigenfunctions of the linear free vibration are used to express the displacements, approximately, in the nonlinear analysis of the shell. Displacements are expressed approximately as

$$U_0=\sum_{i=0}^{I}\sum_{j=0}^{J}a_{ij}U_{xi}(\xi)U_{yj}(\eta)U(\tau),\quad V_0=\sum_{k=0}^{K}\sum_{l=0}^{L}b_{kl}V_{xk}(\xi)V_{yl}(\eta)V(\tau),\quad W_0=\sum_{m=0}^{M}\sum_{n=0}^{N}c_{mn}W_{xm}(\xi)W_{yn}(\eta)W(\tau),$$
$$\psi_x=\sum_{o=0}^{O}\sum_{p=0}^{P}d_{op}\Psi_{xxo}(\xi)\Psi_{xyp}(\eta)\Psi_x(\tau),\quad \psi_y=\sum_{q=0}^{Q}\sum_{r=0}^{R}e_{qr}\Psi_{yxq}(\xi)\Psi_{yyr}(\eta)\Psi_y(\tau) \tag{3}$$

by using the trial functions

$$U_{xi}=\xi^i(1-\xi^2),\quad U_{yj}=\eta^j(1-\eta^2),\quad V_{xk}=\xi^k(1-\xi^2),\quad V_{yl}=\eta^l(1-\eta^2),$$
$$W_{xm}=\xi^m(1-\xi^2),\quad W_{yn}=\eta^n(1-\eta^2),$$
$$\Psi_{xxo}=\xi^o(1-\xi^2),\quad \Psi_{xyp}=\eta^p(1-\eta^2),\quad \Psi_{yxq}=\xi^q(1-\xi^2),\quad \Psi_{yyr}=\eta^r(1-\eta^2), \tag{4}$$

which satisfy the geometrical boundary conditions for the clamped shell. Following nondimensional parameters are introduced to simplify the analysis:

$$\xi=\frac{2x}{a},\quad \eta=\frac{2y}{b},\quad U_0=\frac{u_0}{h},\quad V_0=\frac{v_0}{h},\quad W_0=\frac{w_0}{h},$$
$$\tau=\frac{1}{a^2}\sqrt{\frac{D_0}{\rho h}}\,t,\quad D_0=\frac{E_2h^3}{12(1-\nu_{12}\nu_{21})}, \tag{5}$$

where τ is nondimensional time, ρ is the mass density of the shell and E_2 is the Young's modulus in the direction of 2–axis and ν_{12} and ν_{21} are Poisson's ratios.

The displacements for the nonlinear vibration are expressed approximately by using the linear eigenfunction for the fundamental vibration mode. Applying Galerkin's procedure and eliminating variables except transverse displacement, the governing equations are reduced to an elliptic ordinary differential equation in time.

$$\frac{d^2W}{d\tau^2}+\alpha_1W+\alpha_2W^2+\alpha_3W^3=0. \tag{6}$$

The period of free vibration of the shell is calculated by integrating the equation (6) numerically.

RESULTS AND DISCUSSION

Accuracy of results by the present method depends on the number of series (3), namely, convergence of eigenfunctions for the linear free vibration. Table 1 shows convergence characteristics of fundamental frequency and frequency ratios for three layered cross-ply and angle-ply shells made of graphite/epoxy with square planform. Increasing the number of series $M\times N$, linear natural frequencies λ converge rapidly. Frequency ratios, nonlinear frequency ω_N over linear one ω_L, are tabulated for nondimensional amplitudes W=1 and 2. They change slightly, however, the values have enough converged if we use more than $M\times N$=5×5 for the cross-ply shell and $M\times N$=6×6 for the angle-ply shell.

Figure 2 shows the effect of amplitude upon frequency for the three layered shallow shells having various fiber angles with square planform. The cross-ply shells and the angle-ply shell with θ=15° exhibit a hard spring behavior. The angle-ply laminated shells whose fiber angles are 30° and 45° exhibit a "soft spring" response for small vibration amplitudes (i.e., the frequency decreases with increasing amplitude). As the amplitude increases further, a hard spring behavior appears.

Table1 Convergence characteristics of frequency parameters $\lambda = \omega a^2\sqrt{\rho h/D_0}$ and frequency ratios of the shells (E_1/E_2=15.4, G_{12}/E_2=0.79, G_{23}/E_2=0.5, ν_{12}=0.3, $R_x/a=R_y/b$=15, h/a=0.02)

	0°/90°/0°			30°/−30°/30°		
$M\times N$	λ	W=1	W=2	λ	W=1	W=2
3×3	100.5	1.216	1.759	97.64	1.181	1.682
4×4	100.3	1.211	1.760	92.59	1.030	1.406
5×5	100.7	1.217	1.773	91.61	0.887	1.165
6×6	100.7	1.216	1.773	91.48	0.920	1.221
7×7	100.7	1.215	1.770	91.44	0.924	1.230

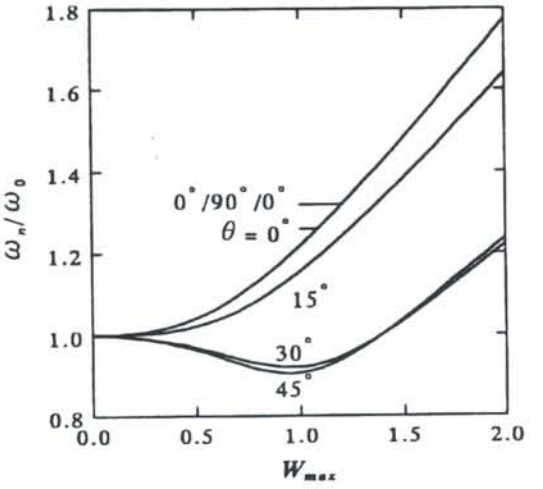

Fig.2 Frequency ratios for various fiber angles ($\theta/-\theta/\theta$, $R_x/a=R_y/a$=15, h/a=0.02)

REFERENCES

1. J.N. Reddy and K. Chandrashekhara, Geometrically non-linear transient analysis of laminated, doubly-curved shells, *Int. J. Non-linear Mech.* **20**, 79-90, (1985).
2. C.Y. Chia, Nonlinear vibration and postbuckling of unsymmetrically laminated imperfect shallow cylindrical panels with mixed boundary conditions resting on elastic foundation, *Int. J. Eng. Sci.* **25**, 427-441 (1987).
3. Y.M. Fu and C.Y. Chia, Multi-mode nonlinear vibration and postbuckling of anti-symmetric imperfect angle-ply cylindrical thick panels, *Int. J. Non-linear Mech.* **24**, 365-381 (1989).
4. Y.M. Fu and C.Y. Chia, Non-linear vibration and postbuckling of generally laminated circular cylindrical thick shells with non-uniform boundary conditions, *Int. J. Non-linear Mech.* **28**, 313-327 (1993).
5. R.A. Raouf and A.N. Palazotto, Nonlinear dynamic response of anisotropic, arbitrarily laminated shell panels: an asymptotic analysis, *Composite Struct.* **18**, 163-192 (1991).
6. R.A. Raouf and A.N. Palazotto, Nonlinear free vibrations of symmetrically laminated, slightly compressible cylindrical shell panels, *Composite Struct.* **20**, 249-257 (1992).
7. R.K. Kapania and C. Byum, Vibrations of imperfect laminated panels under complex preloads, *Int. J. Non-linear Mech.* **27**, 51-62 (1992).

VALIDITY OF THE MULTIPLE-SCALE SOLUTION FOR A SUBHARMONIC RESONANCE RESPONSE OF A BAR WITH A NONLINEAR BOUNDARY CONDITION

W. K. LEE, M. H. YEO AND S. S. BAE
Department of Mechanical Engineering, Yeungnam University,
Gyongsan 712-749, Korea

In order to analyze nonlinear vibrations of structural elements, many have used the method of multiple scales, which has been known to give a uniformly valid approximation as long as a specific system parameter is small. However, we cannot rely fully on the approximation, because there is no criterion on how small the parameter should be. Thus checking numerically and/or experimentally the validity of the approximation is essential, especially when the approximation disagrees with our intuition.

For instances, according to Nayfeh and Asfar[1], Hadian and Nayfeh[2], and Lee and Kim[3], secondary resonance responses can always be excited for all large value of the frequency detuning parameter, but 'physically this is not the case' as stated by Nayfeh and Asfar[1]. The reason for the statement is as follows. The increase in the parameter causes the excitation frequency to meet another natural frequency, and then system is governed by a primary resonance corresponding to the natural frequency rather than the secondary resonance. The analysis of the primary resonance starts with a different assumption on the magnitude of the excitation amplitude from the case of the secondary resonance. Thus we have to abandon the approximation for the secondary resonance when the parameter escapes from some range of the parameter, which the analysis doesn't tell us. Eventually, we have to rely on the numerical and/or experimental means to estimate the range.

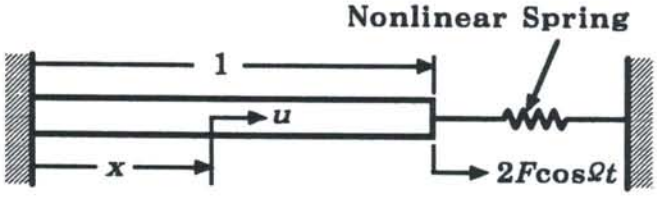

Fig. 1 A schematic diagram of a bar with a nonlinear boundary condition.

In this study, to check the validity of the approximate responses for the secondary resonance we examine the longitudinal response of a bar with a nonlinear boundary condition as shown in Fig. 1. One end of the bar is clamped and the other end is constrained by a nonlinear spring to a harmonic excitation.

The governing equation of motion of the structural system is given by

$$\frac{\partial^2 u}{\partial x^2}=\frac{\partial^2 u}{\partial t^2}+2\varepsilon\mu(x)\frac{\partial u}{\partial t} \tag{1}$$

$$u=0 \text{ at } x=0, \quad \frac{\partial u}{\partial x}+\alpha u+\varepsilon u^3=2F\cos\Omega t \text{ at } x=1 \tag{2, 3}$$

Using the method of multiple scales, Nayfeh and Asfar[1] obtained a uniform first-order expansion of the solution for the third-order subharmonic resonance ($\Omega=3\omega_n+\sigma$, where $\sigma=\varepsilon\hat{\sigma}$ is a detuning parameter and $\hat{\sigma}=O(1)$) as follows.

$$u(x,t)=a_n G(x,\omega_n)\cos\left(\frac{1}{3}\Omega t-\frac{1}{3}\gamma\right)+2\Lambda G(x,\Omega)\cos\Omega t+O(\varepsilon) \tag{4}$$

where

$$G(x,\omega)=\frac{\sin\omega x}{\sin\omega}, \quad \Lambda=\frac{F\sin\Omega}{\Omega\cos\Omega+\alpha\sin\Omega} \tag{5, 6}$$

The natural frequencies ω_n, poles of Λ, are given by the following characteristic equation.

$$\omega\cos\omega+\alpha\sin\omega=0 \tag{7}$$

The nth mode amplitude a_n of the subharmonic response with the frequency $\Omega/3$ is given by the steady state($a_n'=0$, $\gamma'=0$) of the system of autonomous ordinary differential equations

$$a_n'=-\mu_n a_n-\frac{3\Gamma_n\Lambda}{4\omega_n}a_n^2\sin\gamma \tag{8}$$

$$a_n\gamma'=\hat{\sigma}a_n-\frac{9\Gamma_n}{8\omega_n}a_n^3-\frac{9\Gamma_n\Lambda^2}{\omega_n}a_n-\frac{9\Gamma_n}{4\omega_n}a_n\sum_{r\neq n}^{\infty}a_r^2-\frac{9\Gamma_n\Lambda}{4\omega_n}a_n^2\cos\gamma \tag{9}$$

where μ_n and Γ_n are given by

$$\mu_n=\Gamma_n(\sin^2\omega_n)^{-1}\int_0^1\mu(x)\sin^2\omega_n x\,dx \tag{10}$$

$$\Gamma_n=4\omega_n\sin^2\omega_n(2\omega_n-\sin2\omega_n)^{-1} \tag{11}$$

In order to check the validity of the solution given by the equation (4), we solve the nonlinear problem (1)~(3) by using the finite difference method with $\Delta t=(2\pi/\Omega)/3000$ and $\Delta x=0.01$. In this study we consider the case of $\Omega\approx3\omega_1$ ($n=1$) and { ε, μ_1, α}={0.01, 0.1, 0.3}. The natural frequencies are { ω_1, ω_2, ω_3, ···}={1.7414, 4.7751, 7.8920, ···}.

Using equations (8) and (9) and stability criteria, we have plotted the amplitude-detuning parameter response curves in Fig. 2, where solid and doted lines denote, respectively, stable and unstable responses. There exist a stable zero-amplitude response and one pair of nonzero-amplitude responses. The pair has the stable and unstable branches. Since the zero-amplitude response is stable, the system has at most two stable responses. In this case, the long-term response of the system depends on the initial condition. The symbols Δ and o obtained by the finite difference analysis denote, respectively, the zero-amplitude and nonzero-amplitude responses. One of difficulties in obtaining numerical solutions of the boundary and initial value problem is to choose proper initial conditions. Each of these initial conditions implies 200 numbers (one velocity and one displacement at each of 100 points ($\Delta x=1/100$)

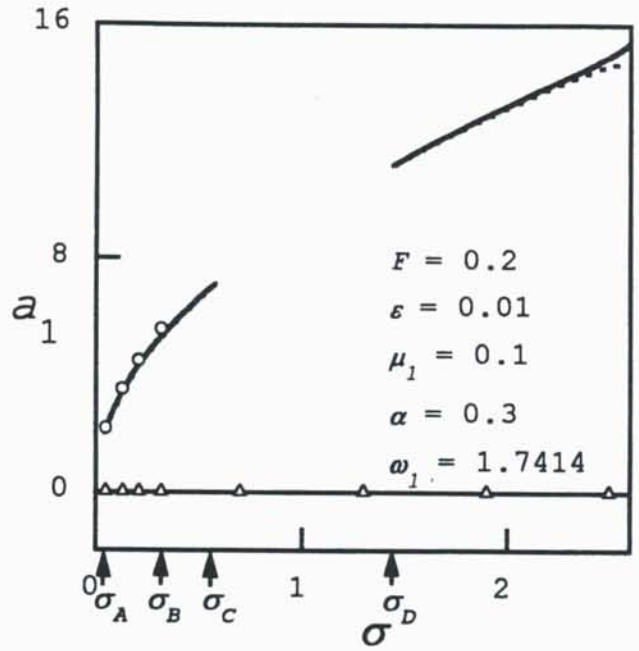

Fig. 2 Variation of the amplitude of subharmonic responses with the detuning parameter σ. ——, Stable; ···; unstable. Numerical solutions: ○, nonzero-amplitude resonance solution; △, zero-amplitude resonance solution.

along the bar). In this study, for convenience, we use the stable solutions (solid lines in the figures) obtained analytically to choose proper initial conditions.

The Fig. 2 shows three saddle-node bifurcation points, σ_A, σ_C and σ_D. Because of the zero-amplitude response, jump phenomenon occurs at each of these bifurcation points. The figure shows that the amplitude of the stable nonzero-amplitude response increases with the detuning parameter σ. However, we can easily expect that this result is physically invalid. As σ increases and the excitation frequency Ω increases up to ω_3 (σ=2.668), the effect of the subharmonic resonance should disappear. The result from the finite difference analysis shows that the approximate solution for the nonzero-amplitude response is valid only for a very limited region of σ ($\sigma_A < \sigma < \sigma_B$) as expected. Of course, the invalidness of the solution for large σ may not be so crucial because it is well known that the effect of the resonance is meaningful in a limited region of σ. However, this result is in a marked contrast to the cases of the primary resonance[4, 5] where the first-order approximations expect very well that the nonzero-amplitude resonance reponses exist for a limited region of σ.

References

[1] A. H. Nayfeh and K. R. Asfar, 1986, *Journal of Sound and Vibration*, 105, 1-15. Response of a Bar Constrained by a Nonlinear Spring to a Harmonic Excitation.

[2] J. Hadian and A. H. Nayfeh, 1990, *Journal of Sound and Vibration*, 142, 279-292. Modal Interaction in Circular Plates.

[3] W. K. Lee and C. H. Kim, 1995, *ASME Journal of Applied Mechanics*, 62, 1015-1022. Combination Resonances of a Circular Plate with Three-Mode Interaction.

[4] A. H. Nayfeh and D. T. Mook, 1979, *Nonlinear Oscillations*. New York: John Wiley.

[5] W. K. Lee and C. S. Hsu, 1994, *Journal of Sound and Vibration*, 171, 335-359. A Global Analysis of an Harmonically Excited Spring-Pendulum System with Internal Resonance

SOME MISCONCEPTIONS IN MEMBRANE, PLATE, AND SHELL VIBRATION ANALYSIS

by

Arthur W. Leissa
Ohio State University
Columbus, Ohio, USA

The classical equation of motion for a planar membrane stretched uniformly in all directions is

$$T\nabla^2 w + p = \rho h \frac{\partial^2 w}{\partial t^2} \tag{1}$$

Where T is the uniform inplane tension and p is a distributed transverse pressure. If the R.H.S. of (1) is zero one has a statically loaded membrane; if p = 0 the free vibration problem is described; and if neither is zero, one has the dynamic response situation, including forced vibration.

All is well for the above problems if T is sufficiently large, the displacement (w) is sufficiently small (so that T does not change significantly), the membrane slope is small (a required assumption to arrive at the linear form of (1)), and that p is distributed (i.e., not a concentrated force). For the static problem it is well known that the harmonic functions which are solutions of (1) become singular at a concentrated force. That is, the solution for the static, concentrated force yields infinite deflection at the loading point. Even if one were to generalize (1) to permit large slopes, the slope at the point load would still be infinite.

This rather obvious result does not seem to enter the thinking of some people who solve dynamic problems. For example, one sees published papers for free vibration frequencies and mode shapes of membranes having point supports in the interior and/or at the boundary. Others exist for the forced vibrations of membranes subjected to concentrated exciting forces. But neither type of problem is a proper one. Clearly, whether an exciting force is static or dynamic does not change the character of the membrane deflection (infinite) at the loading point. Similarly, if the concentrated force is reactive (the point support), instead of active, the membrane cannot not supply any resistance (or stiffness).

As a specific example, consider the free vibration of an annular membrane with outer radius "a" and inner radius "b". This problem has a well-known exact solution in terms of Bessel functions. The table below summarizes fundamental values of the nondimensional frequency $\omega a \sqrt{\rho h / T}$ as one varies b/a. The mode is an axisymmetric one.

b/a	0.40	0.20	0.10	0.02	0.00
$\omega a \sqrt{\rho h / T}$	5.183	3.816	3.314	2.884	2.405

For b/a = 0, the value of 2.405 is the same as that for a complete circular membrane of radius "a." That is, the point support does not increase the frequency. One achieves the value in the table either by taking limiting values of the Bessel functions in the frequency equation, or by numerically approaching b/a = 0 with the computer program.

On the other hand the table also shows that if one supports the membrane additionally along a very small interior circle of 1/50 the diameter of its outer diameter, the frequency is significantly increased (20 percent) from that of the supposed "point support." In the published papers for point supported membranes no exact solution is achieved. The approximate solutions result in distributing the pressure over a small, but finite, area, causing natural frequency increases in a similar manner.

For nonplanar membranes (i.e., membrane shells) the problem is the same. The curved membrane cannot support a point load, either. (This is one of the serious defects of the membrane theory of shells.)

A similar problem arises for plates, but in a different manner. Classical thin plate theory does give finite deflections under point loads (but infinite bending moments) for the static problem. Therefore, point-loaded or point-supported plates are sensible dynamic problems, as well. However, consider now a concentrated bending moment applied to either an interior or exterior point. Timoshenko presented the static solution for an interior concentrated moment (see Theory of Plates and Shells, Second Ed., 1959, p. 326, equation (207)). But he never bothered to mention that the slope $(\partial w / \partial r)$ due to the point moment at the loading point becomes infinite, even with the smallest moment (M_o). Therefore, the classical plate has no resistance to concentrated bending moments, as the classical membrane has no resistance to concentrated transverse forces. Thus, plates with exciting point moments (interior or boundary), or point rotation constraints (e.g., "point clamps") are meaningless in vibration or other dynamic problems. The same can be said for shells, even when the classical, eighth order, bending theory is used.

Another type of singularity has existed in plate and shell vibration problems since classical plate theory was first formulated more than a century ago. This singularity exists at sharp corners where edges intersect. A few examples are shown below:

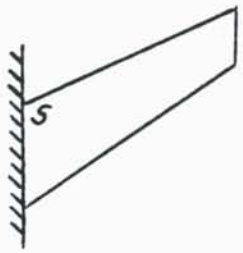

cantilevered
skew

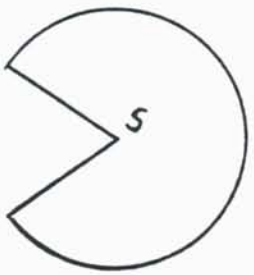

free
sectorial

simply supported
parallelogram

The existence and strength of the moment singularities at a sharp corner depends upon the types of intersecting edges and their included angle. Corners with singularities are marked "S" in the sketches above. Until recently, these singularities have typically been ignored in solving plate vibration problems. But they must be accounted for if one wants to obtain accurate frequencies, especially the lowest (and most important) ones.

In another direction let us consider the "beam functions" that are often used with the Rayleigh and Ritz methods to determine approximate frequencies for quadrilateral plates or shell panels. They were introduced by Ritz himself (1909) in his only paper that dealt with plate vibrations --- the completely free square plate. For this problem one uses the products of "beam functions" (the eigenfunctions of vibrating beams) which are those for free-free beams.

But, consider an edge x = constant. If it is free, in the limit, as sufficient products of beam functions are taken, the following free edge boundary conditions must be approached:

$$\frac{\partial^2 w}{\partial x^2} + \nu \frac{\partial^2 w}{\partial y^2} = 0, \quad \text{and} \quad \frac{\partial^3 w}{\partial x^3} + (2-\nu)\frac{\partial^3 w}{\partial x \partial y^2} \tag{2}$$

arising from zero edge moment and Kelvin-Kirchhoff edge reactions, respectively. The beam functions guarantee that $\partial^2 w/\partial x^2 = 0$ and $\partial^3 w/\partial x^3 = 0$ along the entire edge. However, then the first of (2) implies that $\partial^2 w/\partial y^2 = 0$ for all y, or the edge can have no curvature in the y-direction. It therefore must remain straight, which is unrealistic. The beam functions impose a similar undesirable constraint upon the higher derivative term $\partial^3 w/\partial x \partial y^2$ in (2). With these constraints the Ritz method will converge, but to <u>incorrect</u> upper bound frequencies.

Finally, a lot of people think that a single "Rayleigh-Ritz method" exists. There are two methods. The one accredited to Raleigh (see his <u>Theory of Sound</u>, 1877) uses a single assumed mode shape and calculates the corresponding frequency by equating maximum potential energy to maximum kinetic energy in a cycle of free vibration. The Ritz method utilizes a series of admissible functions, and determines the coefficients of the series by minimizing the frequency so as to obtain the best possible upper bounds. To my knowledge, Rayleigh (an Englishman) was unaware of this extension, and Ritz (a German) did not mention Rayleigh. The methods are separate in origin, and altogether different in application.

Vibration of Deep Cylindrical Shells: A Three-Dimensional Elasticity Approach

C. W. Lim and S. Kitipornchai
Department of Civil Engineering, The University of Queensland, Queensland 4072, Australia
K. M. Liew
School of Mechanical and Production Engineering, Nanyang Technological University, Singapore

Abstract– The three-dimensional elastic analysis of vibration of deep cylindrical shells is treated here. Transverse extensibility usually neglected in plate and shell higher-order theories has been considered. The natural frequencies and vibration mode shapes have been obtained via a three-dimensional displacement-based extremum energy principle. The excessive requirement of memory and computation has been overcome without sacrifying numerical accuracy. The effects of subtended angle and aspect ratio have been concluded for shells with various boundary conditions.

1. Introduction

Vibration of thick plates and shells have been conventionally solved by the first-order (Reissner, 1945) and higher-order theories (Reddy and Liu, 1984). Solutions to vibration of thick shallow shells have been presented by Lim and Liew (1995) and Liew and Lim (1996) for singly-curved and doubly-curved shells with arbitrary boundary conditions. Three-dimensional elastic solutions are particularly scarce and almost all the investigations are concerned with rods and beams (Hutchinson, 1981), parallelepiped (Hutchinson and Zillmer, 1983; Leissa and Zhang, 1983) and cylinders (Hutchinson, 1980; Liew *et al.*, 1995b).

This paper investigates the free vibration of thick, deep cylindrical shells using a three-dimensional displacement-based extremum energy principle. The strain energy integral considers transverse extensibility neglected in first-order and higher-order theories. The p-Ritz method is employed and the three-dimensional displacement field is characterized by a cylindrical coordinate system with orthogonal displacement components. The conventional numerical shortcoming of excessive memory and computation have been overcome by classifying the vibration modes into various symmetry classes. The effects of subtended angle and aspect ratio have been investigated for shells with various boundary conditions.

2. Theory and Formulation

Consider an isotropic, deep and thick cylindrical shell with length a, midsurface radius R, subtended angle θ_o, thickness t as shown in Fig. 1. An orthogonal cylindrical coordinate system (r, θ, z) is defined with r the radial coordinate, θ the angular coordinate and z-axis parallel to the axis of cylindrical shell. The orthogonal displacement components are u_r, u_θ and u_z.

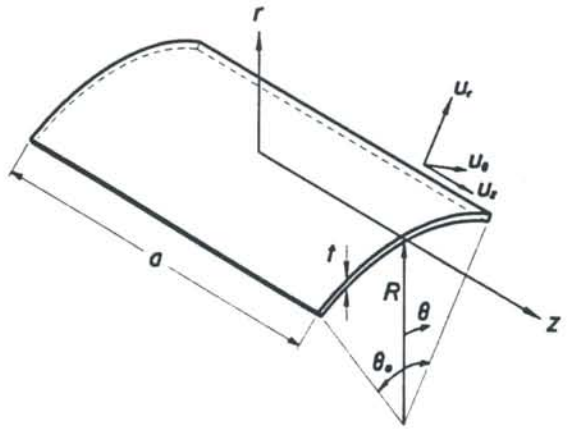

Fig. 1. Geometry of a deep cylindrical shell.

For linear and elastic free vibration, the strain energy of a three-dimensional solid is

$$U = \frac{1}{2}\int\int\int_V \Big[(\Delta+2G)\left(\epsilon_{rr}^2+\epsilon_{\theta\theta}^2+\epsilon_{zz}^2\right) + 2\Delta\left(\epsilon_{rr}\epsilon_{\theta\theta}+\epsilon_{\theta\theta}\epsilon_{zz}+\epsilon_{zz}\epsilon_{rr}\right) + G\left(\gamma_{\theta z}^2+\gamma_{zr}^2+\gamma_{r\theta}^2\right)\Big] r\, dr\, d\theta\, dz \quad (1)$$

where V is volume, G is shear modulus and

$$\Delta = \frac{\nu E}{(1+\nu)(1-2\nu)} \quad ; \quad G = \frac{E}{2(1+\nu)} \quad (2a,b)$$

in which E is the Young's modulus.

The normal and shear strain-displacement relations are

$$\epsilon_{rr} = \frac{\partial u_r}{\partial r} \quad ; \quad \epsilon_{\theta\theta} = \frac{1}{r}\frac{\partial u_\theta}{\partial \theta} + \frac{u_r}{r} \quad (3a,b)$$

$$\epsilon_{zz} = \frac{\partial u_z}{\partial z} \quad ; \quad \gamma_{\theta z} = \frac{\partial u_\theta}{\partial z} + \frac{1}{r}\frac{\partial u_z}{\partial \theta} \qquad (3c,d)$$

$$\gamma_{zr} = \frac{\partial u_z}{\partial r} + \frac{\partial u_r}{\partial z} \qquad (3e)$$

$$\gamma_{\theta z} = \frac{1}{r}\frac{\partial u_r}{\partial \theta} + \frac{\partial u_\theta}{\partial r} - \frac{u_\theta}{r} \qquad (3f)$$

The kinetic energy is

$$T = \frac{\rho}{2}\int_V \left[\left(\frac{\partial u_r}{\partial t}\right)^2 + \left(\frac{\partial u_\theta}{\partial t}\right)^2 + \left(\frac{\partial u_z}{\partial t}\right)^2\right] dV \qquad (4)$$

where ρ is the mass density per unit volume.

For linear, small deformation vibration, the displacement components u_r, u_θ, u_z assume temporal simple harmonic functions with U_r, U_θ, U_z the displacement amplitude functions and ω the angular frequency of vibration. The displacement amplitude functions for midsurface and thickness deformations of a vibrating thick cylindrical shell can be expressed by a set of three-dimensional (3D) p-Ritz functions. These functions are the products of 2D p-Ritz functions $\phi_r(\theta,z)$, $\phi_\theta(\theta,z)$, $\phi_z(\theta,z)$ for midsurface deformation and 1D p-Ritz functions $\psi_r(r)$, $\psi_\theta(r)$, $\psi_z(r)$ for thickness deformation. The displacement amplitude functions are

$$U_r(r,\theta,z) = \sum_{i=1}^{m}\sum_{j=1}^{n} c_r^{ij}\,\phi_r^i(\theta,z)\,\psi_r^j(r) \qquad (5a)$$

$$U_\theta(r,\theta,z) = \sum_{i=1}^{m}\sum_{j=1}^{n} c_\theta^{ij}\,\phi_\theta^i(\theta,z)\,\psi_\theta^j(r) \qquad (5b)$$

$$U_z(r,\theta,z) = \sum_{i=1}^{m}\sum_{j=1}^{n} c_z^{ij}\,\phi_z^i(\theta,z)\,\psi_z^j(r) \qquad (5c)$$

in which c_r^{ij}, c_θ^{ij}, c_z^{ij} are unknown coefficients.

An energy functional is defined as

$$\Pi = U_{max} - T_{max} \qquad (6)$$

According to the Ritz principle

$$\frac{\partial \Pi}{\partial c_\alpha^{ij}} = 0 \quad ; \quad \alpha = r,\theta \text{ and } z \qquad (7)$$

which leads to the governing eigenvalue equation

$$\left(\boldsymbol{K} - \Lambda^2 \boldsymbol{M}\right)\{C\} = \{0\} \qquad (8)$$

where

$$\Lambda = \frac{\lambda}{\theta_o} \quad ; \quad \lambda = \omega b\sqrt{\frac{\rho}{E}} \qquad (9a,b)$$

are the dimensionless frequency parameters.

3. The 1D and 2D p-Ritz Functions

The midsurface and thickness displacements denoted by $u_r(r,\theta,z)$, $u_\theta(r,\theta,z)$ and $u_z(r,\theta,z)$ are truncated finite series given in Eqs. (5a-c). The midsurface deformation admissible functions are sets of geometrically-compliant 2D polynomials $\phi_r(\theta,z)$, $\phi_\theta(\theta,z)$ and $\phi_z(\theta,z)$ derived such that the geometric boundary conditions are satisfied at the outset. They are composed of the product of a series simple two-dimensional polynomials and boundary-compliant basic functions (Lim and Liew, 1995; Liew and Lim, 1996). Similarly, the 1D thickness admissible functions $\psi_r(r)$, $\psi_\theta(r)$ and $\psi_z(r)$ are the products of sets of 1D polynomials and appropriate basic functions.

Classification of vibration modes is possible by grouping terms with odd and even powers in $\phi_r(\theta,z)$, $\phi_\theta(\theta,z)$ and $\phi_z(\theta,z)$ (Lim and Liew, 1995; Liew and Lim, 1996). This tremendously reduces the number of terms in each series and thus the determinant size of the eigenvalue equation is considerably smaller. Huge computational effort can be saved as will be discussed in detail in the next section.

4. Results and Discussion

The convergence characteristics of dimensionless frequency parameter λ has bee studied for CFFF (cantilevered), CFCF and CCCC shells. Satisfactory convergence of λ has been reached for admissible functions with $p_{\theta z} \times p_r = 10 \times 4$. All the eigenvalues converge downwards as expected because the Ritz method overestimates stiffness and vibration frequency and underestimates displacement.

Classification of modes has significant effect on the efficiency of algorithm as the determinant size of the eigenvalue problem can be greatly reduced and tremendous numerical computation can been saved while maintaining the same level of numerical accuracy. Details of vibration mode classification can be found in Lim and Liew (1995) and Liew and Lim (1996).

A comparison of frequency parameters with finite element solutions (FEM) is presented in Table 1. As observed, the p-Ritz solutions agree well with the FEM solutions and agreement is particu-

larly excellent with the solutions using HX8M elements. This is understood as the HX8M elements are 3D elements which consider transverse extensibility similar to the present analysis. It should be emphasized here that it takes between 1.5 hours to 4 hours to obtained a converged FEM solution using LUSAS while it takes less than a minute to obtain solutions as accurate using the present p-Ritz approach with mode symmetry classification.

4. Conclusions

A new analysis using a three-dimensional elasticity approach for free vibration of thick, deep cylindrical shells has been developed. An energy functional with spatial integrals for strain and kinetic energy components have been formulated. The two-dimensional p-Ritz admissible functions (Lim and Liew, 1995; Liew and Lim, 1996) have been generalized to three-dimensional functions.

Convergence of vibration frequencies has been examined while excellent comparison with finite element solutions has been recorded. Classification of vibration modes tremendously reduces the matrix determinant size. Much computation effort can been saved while maintaining the same level of accuracy.

Table 1. Comparison of λ for a cylindrical shell with $\nu = 0.3$, $h/b = 0.2$ and $\theta = 180°$.

Sources	Mode Sequence Number			
	S-1	S-2	A-1	A-2
	CFFF and $a/b = 1$			
FEM†	0.34079	1.1483	0.40619	0.69750
FEM‡	0.34295	1.1476	0.40706	0.70120
3D	0.34299	1.1347	0.40676	0.70092
	CFFF and $a/b = 2$			
FEM†	0.093042	0.48893	0.15497	0.26706
FEM‡	0.093433	0.49583	0.15507	0.26792
3D	0.093425	0.49122	0.15509	0.26772
	SS-1	SA-1	AS-1	AA-1
	CFCF and $a/b = 1$			
FEM†	1.3101	1.1981	2.6625	2.5794
FEM‡	1.3386	1.2269	2.7589	2.6855
3D	1.3235	1.2141	2.7000	2.6257
	CFCF and $a/b = 2$			
FEM†	0.47587	0.45196	1.0668	0.99628
FEM‡	0.48591	0.45796	1.1029	1.0281
3D	0.47935	0.45416	1.0754	1.0040
	CCCC and $a/b = 1$			
FEM†	2.8071	2.2988	3.6263	3.5733
FEM‡	2.9055	2.3672	3.6855	3.6826
3D	2.8696	2.3383	3.6567	3.6346
	CCCC and $a/b = 2$			
FEM†	2.5140	1.7504	2.5110	2.1692
FEM‡	2.6422	1.8477	2.5243	2.2680
3D	2.6034	1.8174	2.5144	2.2341

† LUSAS: 30 × 30 QTS8 thick shell elements
‡ LUSAS: 15 × 15 × 6 HX8M 3D isoparametric solid elements

References

Hutchinson, J. R., Vibrations of solid cylinders, *J. Applied Mech.*, **47**, 901-907, 1980.

Hutchinson, J. R., Transverse vibration of beams: Exact versus approximate solutions, *J. Applied Mech.*, **48**, 923-928, 1981.

Hutchinson, J. R., and Zillmer, S. D., Vibration of a free rectangular parallelepiped, *J. Applied Mech.*, **50**, 123-130, 1983.

Leissa, A. W., and Zhang, Z. D., On the three-dimensional vibrations of the cantilevered rectangular parallelepiped, *J. Acous. Soc. Ame.*, **73**, 2013-2021, 1983.

Liew, K. M., Hung, K. C., and Lim, M. K., Vibration of stress-free hollow cylinders of arbitrary cross section, *J. Applied Mech.*, **62**(3), 718-724, 1995.

Liew, K. M., and Lim, C. W., A higher-order theory for vibration of doubly-curved shallow shells, *J. Applied Mech.*, **63**(3), 587-593, 1996.

Lim, C. W., and Liew, K. M., A higher order theory for vibration of shear deformable cylindrical shallow shells, *I. J. Mech. Sci.*, **37**(3), 277-295, 1995.

Reddy, J. N., and Liu, C. F., A Higher-order Shear Deformation Theory of Laminated Elastic Shells, *I. J. Eng. Sci.*, **23**, 319-330, 1985.

Reissner, E., The effect of transverse shear deformation on the bending of elastic plates, *J. Applied Mech.*, **12**, A69-A77, 1945.

Axisymmetric vibration of circular plates by axisymmetric finite element- A 3-D approach

Chorng-Fuh Liu
Department of Mechanical Engineering
National Sun Yat-Sen University
Kaohsiung, Taiwan, R.O.C.

Plate theories are conventionally employed in vibration analysis of circular plates. However, plate theories are two-dimensional approximation of 3-D elasticity. It is to be expected that such approaches may not satisfactorily describe the real behavior. Therefore, an approach using axisymmetric finite element to analyses the axisymmetric vibration of circular plate is proposed. The advantage of the approach is twofold. First, it is based three-dimensional elasticity, no approximations or assumptions are imposed, and behavior in the thickness direction of circular plates can be explored. Secondly, boundary conditions can be imposed exactly.

Results of analyses by the present method are given in [1] wherein, five different boundary conditions are considered and are shown here in Fig. 1. Among them there are four types of simply supported conditions representing possible realistic constrained situations. Part of the results are shown in table 1, from which we may find that constraining the bottom of the outer edge of circular plates in both the radial and the transverse directions, i.e. ss-3, leads to significantly different prediction of the frequency parameters compared to the other three simply-supported conditions of the present study and of those based on plate theories. This is a simple support which is just as likely to be encountered in practical situations as one at the midplane of the plate(e.g. ss-1), but, to the knowledge of the author, has not yet been reported in literature. Another noteworthy aspect is the appearance of some vibration modes that are different from the conventional flexural modes and are named as "straining modes". They are so called because, from their mode shapes, the tensile and compressive behaviors of the circular plate itself in the radial and axial direction are more obvious than the flexural motion of the plate. Fig. 2 shows the first 10 axisymmetric modes of a circular plate with clamped boundary condition. Obviously, the 4^{th}, 6^{th}, 8^{th} and 10^{th} modes are the straining modes, and such modes are impossible to be seen through plate-theory-based approaches. Some similar types of vibration modes have been shown to appear in the 3-dimensional vibration analyses[2,3] of cantilevered rectangular parallelepipeds, and rods and beams with uniform boundary conditions. From the mode shapes of the present results, it is possible that straining modes may dominate the dynamic stresses developed during vibration, e.g., the straining modes can enhance the possibility of crack extension.

From the above observation, we may therefore come to the conclusion that, to have a complete solution or to show all the facets of vibration of circular plates, 3-dimensional analyses should be conducted, and the results of 1-D and 2-D theories should be used with caution.

Reference:

1. C. F. Liu and G.T. Chen, A simple finite element analysis of axisymmetric vibration of annular and circular plates, Int. J. Mech. Sci., vol. 37, no. 8, pp. 861-871, 1995

2. A. W. Leissa and Z. D. Zhang, On the three-dimensional vibration of cantilevered rectangular parallelepiped, J. Acou. Soc. Am., vol. 73, pp. 2013-2021, 1983.
3. A. W. Leissa and J. So, Comparsion of vibration frequencies for rods and beams from one-dimensional and three-dimensional analyses, J. Acou. Soc. Am., vol. 98, pp. 2122-2135, 1995

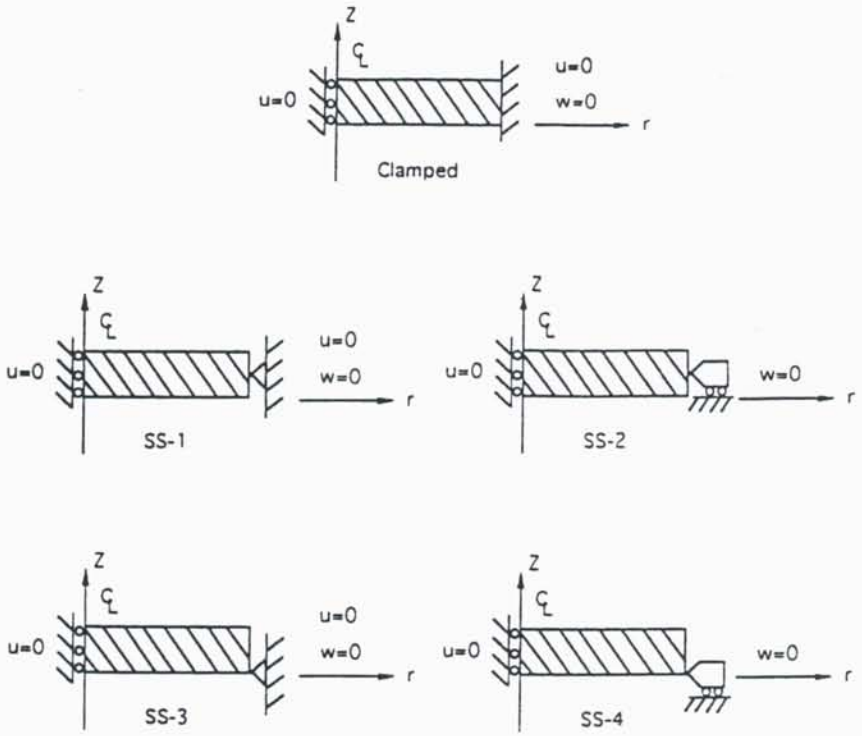

Fig. 1 Boundary condition used.

a/h	4	5	10	20	50	
Mode 1	4.733	4.802	4.901	4.926	4.934	Present SS1
	4.725	4.795	4.897	4.925		MARC SS1
	4.733	4.802	4.901	4.926	4.934	Present SS2
	6.874	7.082	7.409	7.526	7.582	Present SS3
	6.874	7.082	7.409	7.526		MARC SS3
	4.664	4.762	4.893	4.925	4.934	Present SS4
	4.696	4.777	4.894	4.925	4.935	
					4.935	
					4.935	by different plate theories
					4.935	
Mode 2	24.042	25.599	28.452	29.383	29.665	Present SS1
	24.042	25.599	28.452	29.383	29.665	Present SS2
	23.910	26.414	30.878	32.310	32.767	Present SS3
	22.839	24.876	28.322	29.362	29.663	Present SS4
	23.254	24.994	28.240	29.323	29.720	
					29.720	by different plate theories
					29.727	

Table 1. Non-dimensional frequencies ϖ for simply supported isotropic circular plates

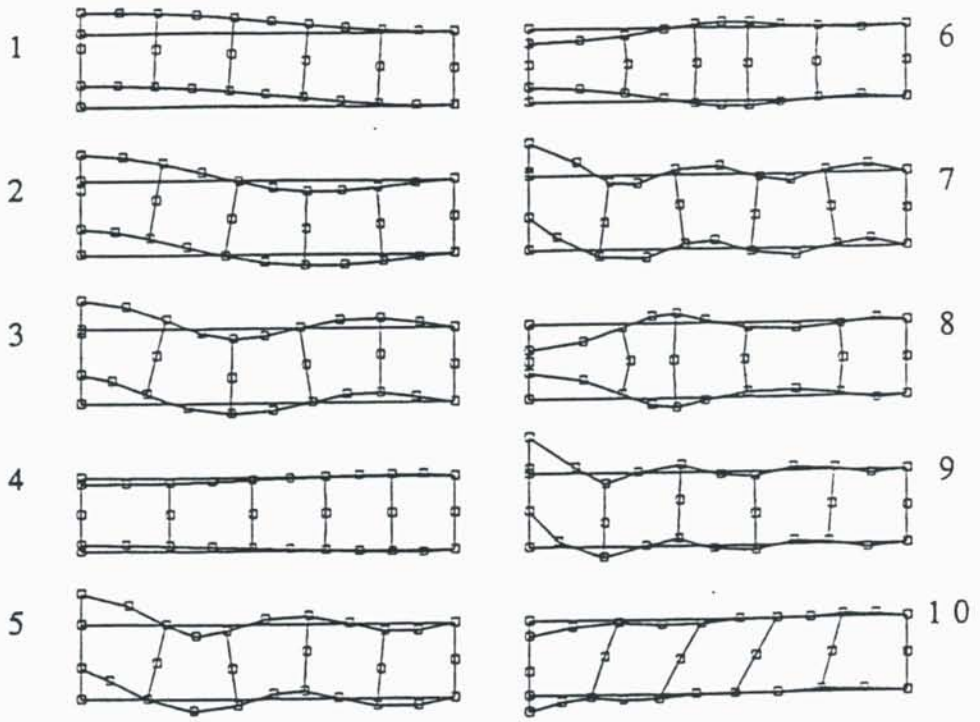

Fig. 2 The first 10 mode shapes with clamped boundary condition

Modelling Unsteady Aeroelastic Behavior of Wings

J. A. Luton, S. Preidikman, and D. T. Mook
Department of Engineering Science and Mechanics
Virginia Polytechnic Institute and State University
Blacksburg, Virginia 24061-0219

Modelling the aeroelastic behavior of wings, either responses to sudden changes in wind velocity (gusts) or self–excited responses to high wind speeds (flutter), is rendered somewhat challenging by the following set of circumstances: To solve for the flow around the wing and, subsequently, the distributed aerodynamic loads acting on it, one must know the position and velocity (state) of the wing and their histories in order to impose boundary conditions on the flowfield. On the other hand, to solve for the state of the wing, one must know the current aerodynamic loads as well as the history of motion leading up to the present state.

The traditional approach to breaking this apparent impasse is to assume certain characteristics for the flowfield, such as simple harmonic motion in the case of flutter, and to solve the problem in the frequency domain. Though such approaches are rather dependable for predicting the onset of an instability, they are obviously limited; for example, they cannot predict post–flutter behavior reliably.

The present approach is to consider the structure and the flowing air to be elements, or subsystems, of a single dynamic system and to integrate all the equations of motion simultaneously and interactively. The problem is solved in the time domain. As an example, we consider a very high aspect ratio, very flexible wing, such as the wing on a high–altitude, long–endurance reconnaissance airplane. Such wings can be structurally modeled as beams. The example wing is represented and the governing equations in dimensionless variables are given in figure 1. Overdots denote derivatives with respect to time, and primes denote those with respect to position. D_b and D_t are rigidities and W is the weight of the wing per unit of length; in dimensionless variables they decrease as the speed increases. q_b and q_t have the same values at all speeds.

The wing is modeled as a beam with no torsional–flexural structural coupling. There is torsional–flexural aerodynamic coupling. $\phi(y,t)$ is the flexural twist angle, $v(y,t)$ is the transverse deflection, and $u(y,t)$ is the axial displacement resulting from the deflection. In the equation for v the radius of curvature is represented by a two–term (nonlinear) expansion. The distributed aerodynamic torque Q_t and loading Q_b are functions of the current state as well as the history of the motion. There are no formulas for Q_t and Q_b; they are obtained from a computer program that can reliably provide time–accurate forces acting on a streamlined body executing an arbitrary motion, something that no simple formula can do. The aerodynamic model is inherently nonlinear. The procedure is to numerically couple these three partial–differential equations with the computer code that provides the aerodynamic loads and solve for ϕ, v, u, Q_t and Q_b as functions of y and t, for arbitrary initial disturbances, airspeeds, and in some cases motions of the ailerons (not shown) simultaneously and interactively.

In figure 2, some numerical results are represented. Here the wind speed is near critical, and the response is a limit cycle. The tip deflection is around 20% of the semi–span. In the case of the airplane called *Condor*, this tip deflection corresponds to about six meters. At speeds sufficiently below the critical the fast Fourier transforms of the numerical results show the presence of two frequencies in the decaying response to an arbitrary disturbance. As the wind speed approaches the critical, the two frequencies merge, as one would expect from classical treatments, and a limit cycle evolves, as one would *not* expect from classical treatments. As the wind speed increases further and reaches a point sufficiently above the critical, the limit cycle breaks down, and the amplitude of the response begins to increase while its frequency begins to decrease. The noticeable evolution of organized (one–frequency, constant–amplitude) motion, which occurs as the wind speed increases toward the critical, is symptomatic of impending flutter and can be used to trigger active control of the ailerons to suppress the instability.

This example as well as others will be used to explain the procedure, demonstrate the considerable capability of this type of approach to modeling aeroelastic behavior, and provide some new insight into the physics of actively controlled, unsteady, and unstable aeroelastic behavior.

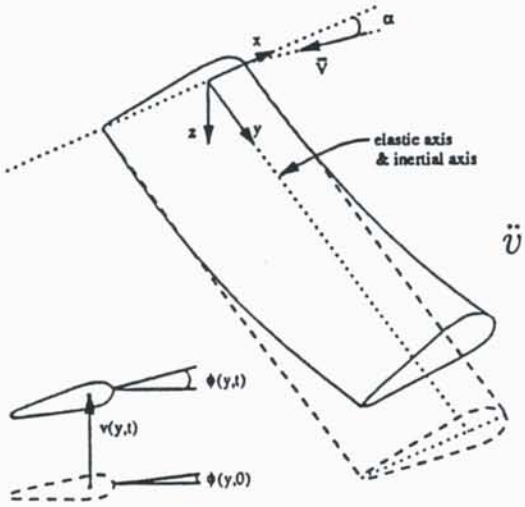

$$\ddot{\phi} - D_t\phi'' = q_t Q_t$$

$$\ddot{v} + D_b v'''' - D_b\left(2v'^2 v'''' + 10v'v''v''' + 3v''^3\right) = q_b Q_b - W - \frac{1}{2} q_b Q_b v'^2$$

$$u(y,t) = -\frac{1}{2}\int_0^y v'^2 dy$$

$$D_b = -\frac{EI}{mL_c^2 V^2},\quad D_t = \frac{GJ}{V^2 J_0},\quad q_b = \frac{\rho L_c^2}{2m},\quad q_1 = \frac{\rho L_c}{2J_0},\quad W = \frac{gL_c}{V^2}$$

$$\phi(0,t) = 0\ \ \phi'(L,t) = 0,\ \ v(0,t) = 0,\ \ v'(0,t) = 0,\ \ v''(L,t) = 0,\quad v'''(L,t) = 0$$

$$Q_t = Q_t(v, \dot{v}, \phi, \dot{\phi}, \text{ and their histories}),\quad Q_b = Q_b(v, \dot{v}, \phi, \dot{\phi}, \text{ and their histories})$$

$$\delta_{c,TE}(t) = G_1\dot{v}(0.95L,t) + G_2\dot{\phi}(0.95L,t),\quad \delta_{c,LE}(t) = G_3\dot{v}(0.95L,t) + G_4\dot{\phi}(0.95L,t)$$

$$\ddot{\delta} + 2\xi\omega_n\dot{\delta} + \omega_n^2\delta = \omega_n^2\delta_c$$

Figure 1. A high–aspect–ratio wing modeled as beam, governing equations, boundary conditions, and feedback–control laws.

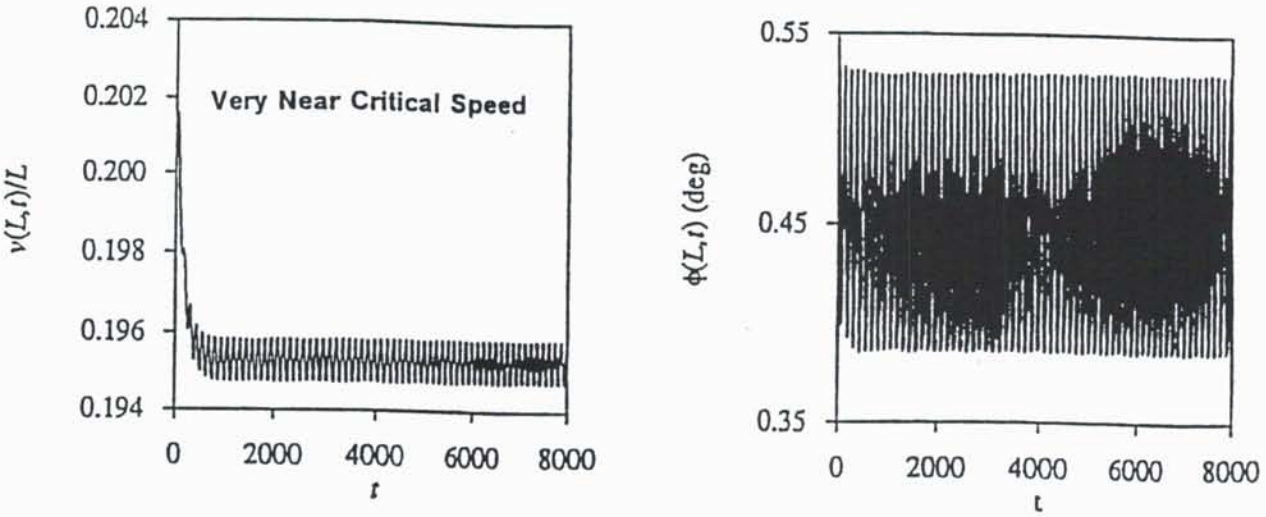

Figure 2. The response of the wing in twist, ϕ, and bending, v, to an initial disturbance near the critical speed. Limit–cycle behavior.

Experiments on Chaotic Vibration of a Shallow Cylindrical Shell-Panel with an In-plane Elastic-Support at Boundary

Ken-ichi Nagai
Department of Mechanical Engineering
Gunma University, 1-5-1 Tenjincho, Kiryu, Gunma, 376, Japan
Takayuki Hata
ANEST IWATA Co, Ltd., Yokohama, 223, Japan
Takao Yamaguchi
SUBARU Research Center Co, Ltd., Ota, Gunma, 373, Japan

1. Introduction

Experimental results are presented on chaotic vibrations of a shallow cylindrical shell-panel with square boundary subjected to lateral excitations. The boundary of the shell is arranged to be a simply-supported edge and an elastic support in an in-plane direction. Three types of shells with different curvature are examined. Changing the exciting frequency, the frequency regions are examined carefully where chaotic responses are generated. The chaotic responses of the shell are confirmed by the Fourier spectrum analysis, the Poincaré projection onto phase plane and the maximum Lyapunov exponent. Stability boundaries of the chaotic vibration are clarified. Moreover, interactions of the mode of vibration generated in the chaos are discussed.

2. Shell-Panel and Boundary Condition

Figure 1 shows the shell-panel and the supporting frame. A test shell of phosphor bronze sheet with thickness h=0.205 mm is rolled to a cylindrical surface with radius R. The shell is cut to a square form of length a=b=140 mm. Physical quantities are obtained as mass density ρ=8.88×10^3 kg/m^3, Young's modulus E =99.5 GPa and Poisson's ratio $\nu = 0.33$. The radii of the shells are measured as R=4350 mm, R=2220 mm and R=1760 mm, respectively.

To compose the simply-supported boundary condition, the rounded edge of the shell is connected to the supporting frame by wrapping and pasting thin films along the boundary alternately. Consequently, elasticity of the thin film acts as an elastic constraint in the in-plane direction.

3. Vibration test and Procedure

The shell was excited periodically by the vibration exciter through the shell frame. Measuring the relative displacement of the shell to the supporting frame by two laser displacement sensors, the responses of the shell are recorded. The following non-dimensional notations are introduced.

$$\xi = x/a,\ \eta = y/b,\ \alpha = a^2/Rh,\ \beta = a/b,\ w = W/h,\ p_d = a_d \rho a^4/D,\ q_s = Q_s a^2 \beta/Dh,\ \tau = \Omega_0 t,\ \omega = 2\pi f/\Omega_0 \quad (1)$$

$$D = Eh^3/12(1-\nu^2),\ \Omega_0 = (1/a^2)\sqrt{D/\rho h} \quad (2)$$

Where, D is the bending rigidity of the shell. α is the non-dimensional shell curvature. β is the aspect ratio of the length of the rectangular boundary. p_d is the non-dimensional intensity of distributed load due to the periodic acceleration a_d. q_s is the non-dimensional static load by the concentrated load Q_s. ω and τ are the non-dimensional exciting frequency and the non-dimensional time, respectively. f is the exciting frequency.

4. Results and Discussions

The aforementioned shells of $\alpha = 23$, $\alpha = 43$ and $\alpha = 54$ are tested. Figure 2 shows the static deflection w of the shell under the concentrated force q_s. w is measured at the point ξ =0.57 and η =0.43 of the shell. The shell shows the character of soft-hardening spring. For the typical shell of $\alpha = 43$, the negative slope appears in the restoring force. It will cause a snap-through buckling by an ultimate level of q_s. Figure 3 shows the frequency response curves. w_{rms} is the root mean square value of the periodic response. ω is the non- dimensional exciting frequency. In the figure, the regions of the chaotic vibration are assigned by the named chaos. In the figure, $(m,n{:}j)$ denotes the type of resonance response, in which (m,n) is generated mode of vibration, while, j indicates the type of resonance. The integer m and n imply predominant half wave number of the deflection in the x-direction and y-direction, respectively. For example, (2,1:1) means the principal resonance of the mode (2,1), while, (1,1:1/2) means the sub-harmonic resonance of 1/2 order with the mode (1,1). $(m,n{:}2)$ and $(m,n{:}3)$ mean the super- harmonic resonance of 2 and 3 orders, respectively. Figure 4 shows the time progresses of the chaos of the shell under the forcing amplitude $p_d = 1500$. The time history has no periodicity and exhibits complicated movement. The Poincaré maps of the chaos are recorded more than 6000 points at phase delay θ =60 degree measured from the maximum amplitude of the exciting force. Figure 5 shows the maps at ω=48.7, ω=45.6 and ω=35.8. The phase plane of the deflection w and the velocity $w_{,\omega\tau}$ is measured at ξ=0.57 and η=0.43. The projection on the map changes by the variation of exciting frequency. The maximum Lyapunov exponent λ of the chaos is shown in Figure 6. The maximum Lyapunov exponent converges to non-integer constant values more than e=6. This implies that number of vibration mode related to the chaos exceeds more than three predominantly.

5. Conclusion

The main results can be summarized as follows:

(1) The violent chaotic vibrations are generated close to the responses of principal resonance, sub-harmonic resonance, super-harmonic resonance and internal resonance, respectively. These responses are corresponded to lower modes of vibration relatively.

(2) In the shell of small curvature, the chaos is emerged accompany with the internal resonance. While, the shell of larger curvature, the chaos is generated due to the dynamic snap-through and the condition of internal resonance.

(3) As the curvature of the shell increases, the maximum Lyapunov exponent grows to a large magnitude. Furthermore, the mode interactions to the chaos are found to be of complicated.

References

1. Nagai, K., 'Experimental study of chaotic vibration of a clamped beam subjected to periodic lateral forces', *Trans. of Japan Soci. of Mech. Engrs* **56**-525, 1990, 1171-1177 (in Japanese).
2. Nagai, K. and Yamaguchi, T., 'Chaotic vibrations of a post-buckled beam carrying a concentrated mass (1st Report, Experiment)', *Trans. of Japan Soci. of Mech. Engrs* **60**-579, 1994, 3733-3740 (in Japanese).
3. Yamaguchi, T. and Nagai, K., 'Chaotic vibrations of a post- buckled beam carrying a concentrated mass (2nd Report, Theoretical Analysis)', *Trans.o f Japan Soci. of Mech. Engrs* **60**-579, 1994, 3741-3748 (in Japanese).
4. Nayfeh, A.H., Raouf, R.A. and Nayfeh, J.F.,'Nonlinear response of infinitely long circular cylindrical shells to subharmonic radical loads', *J.of Applied Mech.*, **58**, 1991, 1033- 1041.
5. Maestrello, L., Frendi, A. and Brown,D.E., 'Nonlinear vibration and radiation from a panel with transition to chaos', *AIAA J.*, **30**-11, 1992, 2632-2638.
6. Nagai, K. and Yamaguchi, T.,'Chaotic oscillations of a shallow cylindrical shell with rectangular boundary under cyclic excitaion', *High Pressure Technology, PVP*- Vol. **297**, 1995, ASME, 107-115.
7. Yamaguchi, T. and Nagai, K. , 'Chaotic Vibrations of a Cylindrical Shell-Panel with an In-plane Elastic-Support at Boundary', *Nonlinear Dynamics* (to be appeared).
8. Wolf, A., et al., 'Determining Lyapunov exponents from a time series', *Physica* **16**D ,1985, 285-317.

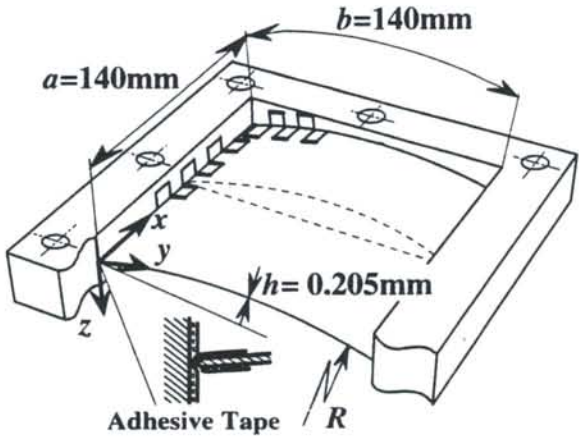

Figure. 1. Shallow cylindrical shell-panel

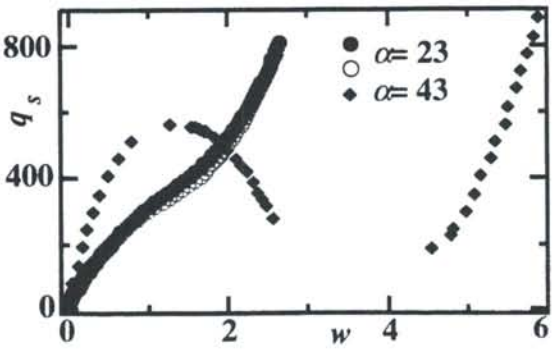

Figure.2 Static deflection of the shells

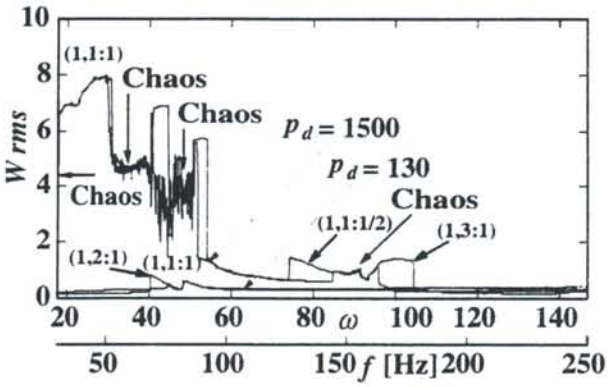

Figure.3 Frequency responses curves of the shell
α=43, ξ = 0.57, η = 0.43

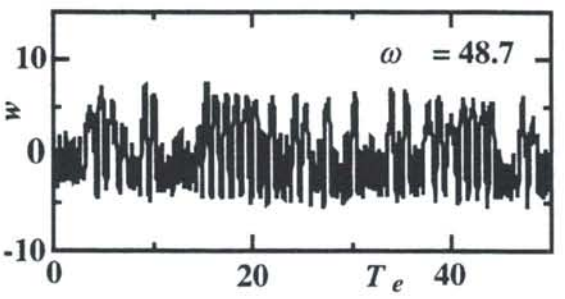

Figure.4 Time history of displacement distribution
α=43, p_d=1500, ξ = 0.57, η = 0.43

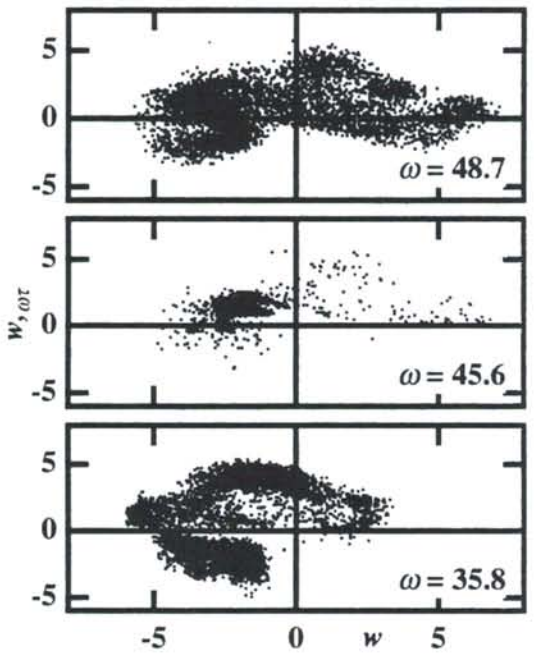

Figure.5 Poincaré map of the shells
α=43, p_d=1500, θ = 60, ξ = 0.57, η = 0.43

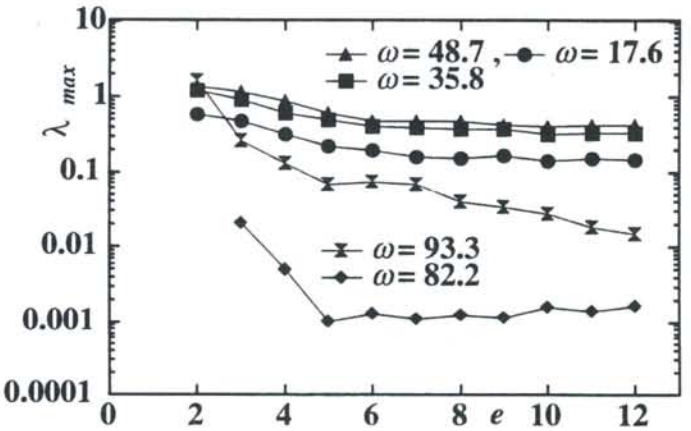

Figure.6 Maximum Lyapunov exponent of the shells
α=43, p_d=1500, ξ = 0.57, η = 0.43

Analysis and Optimal Design of Column Using Earthquake Force for Controlling Vibrations

Kosuke Nagaya* and Toshiyuki Fukushima*

**Department of Mechanical Engineering, Gunma University*
Kiryu, Gunma 376, JAPAN

This paper presents a method of vibration control for a column carrying a mass at its tip subjected to earthquakes. A vibration isolation mechanism consisting of gear train for the column is presented. Theoretical analysis for the column is developed, and to validate the method and analysis, experimental tests are carried out for a model of the present mechanism. It is clarified that the vibration displacements and the moments in the column are reduced significantly in comparison with the general column without the mechanism. In the present column, energies for controlling vibrations are not required, because the earthquake force is utilized as a control force. Therefore, the column has advantages as compared with the columns having active vibration control system.

1. Introduction

In the Hanshin-Awaji earthquake in Japan, a number of structures and buildings were destroyed. To reduce vibrations of structures and buildings, two methods are popular in practical use. One is the vibration isolation method. Recently a number of studies have been reported by use of the method [1-3].But the vibration isolation system is expensive, so the method has not been utilized thoroughly. The other method is to strengthen the structures. The method is simple because the strength of structures increases with their thickness, but a cost also increases with the thickness. Columns without wall used high-way bridges and parking were destroyed in the earthquakes as just mentioned. If the columns are destroyed, buildings are also destroyed, so it is important to prevent destruction of columns used such structures. Gravity forces of the building apply to the column, so the bending moment at the base becomes significantly large when the deflection at the tip occurs due to an earthquake. Hence, it is important to prevent the tip displacement of the column under earthquakes.

The earthquake has significantly large energy, so if its energy is applicable to the control energy, the vibration can be reduced without increasing the thickness of column. But the studies on this standpoint has not been reported. From this situation, this paper presents a method for reducing the tip displacement of the column by using an earthquake force as a control force. To transform the earthquake force to the control force, a gear train mechanism is inserted in the hollow column. In the mechanism, an inertia force of the mass at the tip of the column is transformed into a control moment. The theoretical analysis has been developed on the proposed vibration control system. To validate the present method and analyses , experimental tests have been performed.

2. Principle of the Column

Figure 1 depicts a geometry of a hollow column having a gear train mechanism inside. The center of the gear 2 is rigid joined to an end of a rigid bar 1 whose other end is rigid joined to the tip of the column. The gear 2 engages into the middle gear 3 whose center is pin joined to the column. The gear 3 makes the rotation of the gear 4 whose center is rigid joined to the column as shown in Fig.1. In this mechanism, if the tip of the column moves in the right direction, since the gear 2 moves in the right direction, the gear 3 rotates in the clockwise direction. Then the gear 4 rotated in the counterclockwise direction. Since the center of the gear 4 is rigid joined to the column, restoring moment M_4 is generated. The moment reduces the deflection of the column. In this system, if the gear 4 is small in comparison with the gear 2, the angle of rotation of the gear 4 is larger than that of gear 2, so the moment M_4 increases with the gear ratio.

3. Theoretical Analysis and Experiment

Theoretical analysis has been developed for the column with the gear mechanism by using the transfer

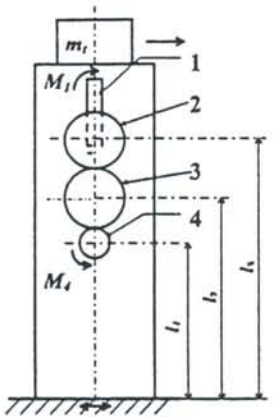

Fig.1 Geometry of the present column

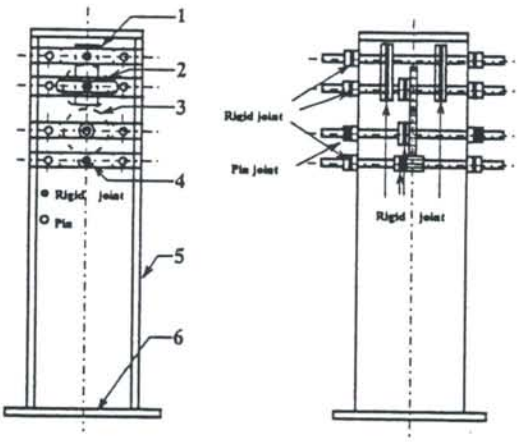

Fig.2 Column used in the experiment.

matrix method. The analysis is omitted here, and the numerical results are shown. for a model. Fig.2 shows the model used both the numerical calculation and experiments. In the model, the column is made of two flat steel plates (hereafter it is called as the column plate) with a base plate and a top plate. The top plate is pin joined to the column plates, so the resisting moment between the top plate and the column plate does not occur. Three gears are inserted between two column plates, whose centers are rigid joined to their shafts. The shafts are pin joined or rigid joined to the slender side plates whose ends are pin joined to the sides of column plates. The black dot denotes the rigid joint and the white dot the pin joint. There is a slit in the side plate for the upper gear (gear 2), so the shaft of the gear 2 moves in both right and left directions, but the rotation is restricted because the shaft is rigid joined to the rigid arm 1.

A mass lies on the top of the column, and the base is excited by the oscillator. The displacement of the mass was measured by the non-contact displacement sensor. The strains at two points ($x=l_0=0.025$[m], and $x=l_1=0.338$[m]) from the base were measured by the strain meter.

Figure 3 shows the comparison between the theoretical results and experimental data for the frequency response of the bending moments at the base. It is seen that the resonance frequency of the present column increases, and the peak value at the resonance frequency decreases due to the friction among gears. Especially, the moments of the present column are significantly smaller than those of the general column for low frequencies less than the resonance frequency. It is ascertained that the analytical results are in good agreement with the experimental data.

4 Optimal Design

There are optimal values for the radii of gears, length . of the arm, so to have the large control effects, the optimal design is of importance. In the design of the column, the bending moment at the base becomes maximum when the principal frequency of the earthquake is less than the first resonance frequency. If the gear train is inserted in the column, the reaction force Q increases with the control force. Then the gear teeth becomes large. Then, to have the optimal values of the parameters as just mentioned, the following cost function is applied:

$$J = \alpha_1 \int_{\omega_1}^{\omega_2} |M(\omega)| d\omega + \alpha_2 \int_{\omega_1}^{\omega_2} |Q(\omega)| d\omega$$

(1)

where $M(\omega)$ is the bending moment at the base, $Q(\omega)$ is the reaction force shown in Fig1, ω the principal angular frequency of the earthquake, ω_1 and ω_2 the lower- and upper bound of the considered frequency region, α_1 and α_2 the weighting coefficients. Consider a hollow square cross section column with length =300mm, width =300mm, height = 4000mm, mass = 505 kg. The mass of 1000 kg lies on the tip of the column. Numerical calculations for the optimal design are carried out using the data as just

mentioned. In this calculation, the considered frequency region is taken from 2Hz to 4.5Hz in which principal frequencies of the earthquake in Japan are included. Figure 4 illustrates the frequency response for the moment at the base of the column. It can be seen that the resonance frequency increases for the curve after optimization. Especially, the moments in the considered frequency range (2 Hz to 4.5Hz) are significantly smaller than those without gears.

4. Conclusion

The present article provides an intelligent column in which the earthquake force is transformed to the control force for reducing vibrations of the column without using sensors. Theoretical expression for obtaining the displacement and moment in the column has been presented. To validate the method and the analysis, experimental tests have been performed for a model of the column. A method of optimal design for the column has been also presented. It is clarified that the present column is applicable for reducing vibrations of the column under earthquakes.

References

[1] Fujita, T., 1989, Seismic Isolation Rubber Bearings for Nuclear Facilities, Proc. 1st Int. Seminar on Seismic Base Isolation for Nuclear Power Facilities (A Post-Conf. Seminar of SMiRT-10) , 268-295.

[2] Teramura, A., Takeda, T., Thunoda, T., Seki, M., Kageyama, M., and Nohata, A., 1988, Study on Earthquake Response Characteristics of Base Isolated Full Scale Building, Proc. 9th World Conf. Earthq. Eng., Vol.V, 693-698.

[3] Yasaka, A., Koshida, II., and Iizuka, M., 1988, Base Isolation System for Earthquake Protection and Vibration Isolation of Structures, ibid., 6 99-704

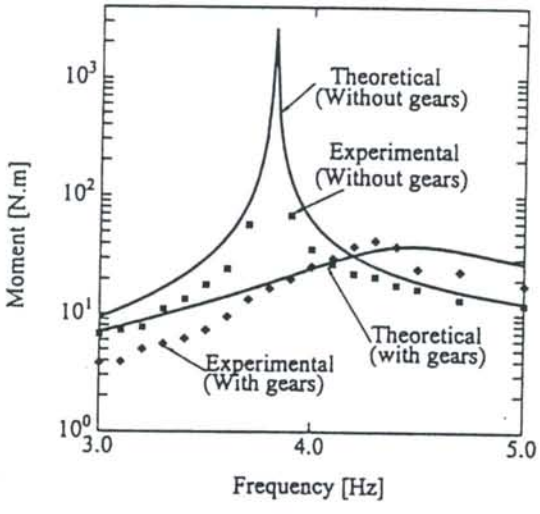

Fig.3 Comparison between the tip displacements of the present column and those of a usual column without gears.

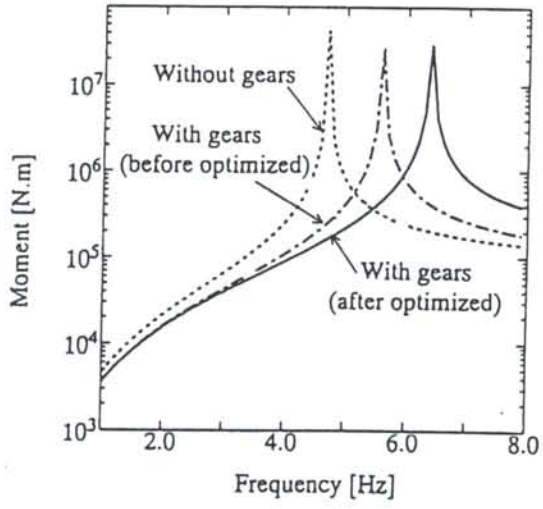

Fig.4 Comparison between base moments of the present optimal column and those of a usual column without gears.

Analytical solution to the mode shape differential equation of some non-uniform Euler-Bernoulli beams

S.Naguleswaran
Department of Mechanical Engineering, University of Canterbury, Christchurch, New Zealand

Summary

Non-uniform beam elements occur in aeronautical, aerospace, civil, mechanical and robot engineering applications and the lateral vibration of such beams has been the topic of investigation by several researchers. The variation in beam cross-section may be continuous or discontinuous. Numerical methods like Rayleigh-Ritz, Galerkin, finite element method etc have been used to obtain the natural frequencies. If the mass per unit length and the flexural rigidity vary continuously then for some Euler-Bernoulli non-uniform beams the mode shape differential equation admit analytical solution. Frequencies, mode shape details etc obtained by analytical methods may be used to judge/validate results obtained by numerical methods.

Consider an Euler-Bernoulli beam whose mass per unit length and flexural rigidity at the 'big' end are $m(\ell)$ and $EI(\ell)$ respectively. If the variation of mass per unit length and flexural rigidity are continuous then $m(x) = \phi_1(x)m(\ell)$, $EI(x) = \phi_2(x)EI(\ell)$ where $\phi_1(x)$ and $\phi_2(x)$ are continuous functions of x. A 'complete' beam is in the range $0 \le x \le \ell$. A 'truncated' beam has the portion of length $\alpha\ell$ removed from a 'complete' beam and is in the range $\alpha\ell \le x \le \ell$. For the beam vibrating at a natural frequency ω if the amplitude at coordinate x is y(x), then the bending moment M(x), shearing force Q(x) and the equation of motion are

$$M(x) = \phi_2(x)EI(\ell)d^2y(x)/dx^2, \quad Q(x) = -\,dM(x)/dx, \quad dQ(x) + \phi_1(x)m(\ell)\omega^2y(x) = 0 \qquad (1,2,3)$$

and the mode shape differential equation is

$$d^2[\phi_2(x)EI(\ell)d^2y(x)/dx^2]/dx^2 - \phi_1(x)m(\ell)\omega^2y(x) = 0 \qquad (4)$$

This equation subject to the boundary conditions may be solved numerically but analytical solution is not available for all combinations of $\phi_1(x)$ and $\phi_2(x)$.

Consider the case $\phi_1(x) = (x/\ell)^q$ and $\phi_2(x) = (x/\ell)^p$ with $p > 0$ and $q > 0$. Such beam elements occur in engineering applications. For example (p, q) = (0, 0) is a uniform beam, (p, q) = (3, 1) is a uniform wedge, (p, q) = (4, 2) is a uniform cone or pyramid beam and (p, q) = (1, 1) is a beam of constant depth and linearly varying breadth. The author will review several publications on the lateral vibration of the beams of the above types.

It is prudent to express the governing equations in dimensionless form with the introduction of the dimensionless variables $X = x/\ell$, $Y(X) = y(x)/\ell$, $M(X) = M(x)\ell/EI(\ell)$, $Q(X) = Q(x)\ell^2/EI(\ell)$, $\mu = m(\ell)\omega^2\ell^4/EI(\ell)$ and the operator $D^n = d^n/dX^n$. One gets

$$M(X) = X^pD^2Y(X), \quad Q(X) = -\,D[X^pD^2Y(X)] \qquad (5,6)$$

and the dimensionless mode shape differential equation

$$D^2[X^pD^2Y(X)] - \mu X^qY(X) = 0 \qquad (7)$$

For a 'complete' beam equation (7) is applicable in the range $0 \le X \le 1$ and for a 'truncated' beam in the range $\alpha \le X \le 1$. Equation (7) is linear with regular singularity at $X = 0$ and the general solution will consist of the superposition of four independent solution functions. The four constants of integration are now eliminated from the boundary conditions to yield the frequency

equation which will have an infinite number of roots. A 'complete' beam will be 'sharp' ended and cannot sustain a bending moment or shearing force at this end and the frequency equation is a 2x2 determinant equated to zero. No such restriction is needed at the 'small' end of a 'truncated' beam and the frequency equation is a 4x4 determinant equated to zero.

Brief description of some of the special cases of equation (7) follows. If (p, q) = (0, 0) is a uniform beam and the solution of $D^4Y(X) - \mu Y(X) = 0$ is

$$Y(X) = C_1\sin\mu^{1/4}X + C_2\cos\mu^{1/4}X + C_3\sinh\mu^{1/4}X + C_4\cosh\mu^{1/4}X \quad (8)$$

It can be shown that equation (7) admit Bessel's function based solution if the exponents p and q satisfy the relation

$$(p+q)(p-q-2)(p-q-6)(3p-q-8) = 0 \quad (9)$$

and the corresponding solution is

$$Y(X) = X^a[C_1J_n(b\beta X^{1/b}) + C_2Y_n(b\beta X^{1/b}) + C_3I_n(b\beta X^{1/b}) + C_4K_n(b\beta X^{1/b})] \quad (10)$$

where $\beta = \mu^{1/4}$, $a = (2-p-q)/4$, $b = 4/(4-p+q)$, $n^2 = [(2-p-q)^2 + 2(p+q)(p-q-2)]/(4-p+q)^2$.

For certain combinations of p and q Y(X) and/or DY(X) are singular at X = 0.
If p = q + 4, the mode shape differential equation degenerates to the Cauchy differential equation

$$X^4D^4Y(X) + 2pX^3D^3Y(X) + p(p-1)X^2D^2Y(X) - \mu Y(X) = 0 \quad (11)$$

Fortuitously the coefficients are such that the solution is as follows

$$Y(X) = X^{(3-p)/2}\{C_1\sinh[\gamma_1\ln(X)] + C_2\cosh[\gamma_1\ln(X)] + C_3\sin[\gamma_2\ln(X)] + C_3\cos[\gamma_2\ln(X)]\} \quad (12)$$

where $\gamma_1 = \{2(p-2)+2[(p-2)^2 + 4\mu]^{1/2} + (3-p)^2\}^{1/2}$, $\gamma_2 = \{-2(p-2)+2[(p-2)^2 + 4\mu]^{1/2} - (3-p)^2\}^{1/2}$

Values of p exist for which Y(X) and/or DY(X) is singular at X = 0.

Apart from application to engineering the mode shape differential equation (7) is mathematically interesting. The method of Frobenius is used to solve it but each combination of p and q calls for individual treatment. Consider the polynomial

$$Y(X,c) = \sum a_{n+1}(c)X^{c+n\xi} \quad (13)$$

where c is an undetermined exponent, ξ is the exponent factor and n = 0, 1, 2.....∞. It can be shown that Y(X,c) is a solution of equation (7) if ξ and the coefficients $a_{n+1}(c)$ are chosen as follows

$$\xi = 4 - p + q, \quad P_{n+2}(c)a_{n+2}(c) - \mu a_{n+1}(c) = 0 \quad (14,15)$$

$$P_{n+1}(c) = [c+n\xi][c+n\xi-1][c+n\xi-2+p][c+n\xi-3+p] \quad (16)$$

and c is a root of the indicial equation

$$P_1(c) = c(c-1)(c-2+p)(c-3+p) = 0 \quad (17)$$

Choice of $a_1(c) = 1$ will not result in loss of generality. The four solution functions are $Y(X,c)_{c=0,1,2-p,3-p}$ and for brevity let

$$[Y(X,0)\ \ Y(X,1)\ \ Y(X,2-p)\ \ Y(X,3-p)] = [E(X)\ \ F(X)\ \ G(X)\ \ H(X)] \quad (18)$$

If the four functions are independent and unbounded the solution of equation (7) is

$$Y(X) = C_1E(X) + C_2F(X) + C_3G(X) + C_4H(X) \quad (19)$$

where the constants of integration are determined from the boundary conditions. The method of solution need be modified if the indicial equation (17) has coincident roots or if one or more of the solution functions are unbounded and this occurs in equation (16) if $P_{n+2}(c) = 0$. Here the general solution will have functions with logarithmic terms. It will be shown that solution functions with

logarithmic terms occur if the ratio of the difference between any two roots of the indicial equation (17) to the exponent factor is an integer. If $p - q > 4$, the four solution functions will be in descending powers of X and therefore singular at $X = 0$. The writer will discuss these aspects at the symposium but examples are briefly discussed below.

Consider a beam of rectangular cross-section of constant depth and breadth proportional to X^s. The exponent factor $\xi = 4$ and therefore for all positive values of s two or more solution functions are not singular at $X = 0$ and the natural frequencies of 'complete' beams may be calculated. Logarithmic terms will occur in up to two solution function/s if s is a positive integer except multiples of 4. From equation (9) for $s = 4$ the solution can also be expressed in terms of Bessel's functions.

Consider a non-uniform wedge. This is a beam of rectangular cross-section of constant breadth and depth proportional to X^s. From equation (9) the solution for a wedge with $s = 1$ can also be expressed in terms of Bessel's functions. The mode shape differential equation, the exponent factor and the indicial equation of a non-uniform wedge are

$$D^2[X^{3s}D^2Y(X)] - \mu X^s Y(X) = 0, \quad \xi = 4 - 2s, \quad c(c-1)(c-2+3s)(c-3+3s) = 0 \qquad (20,21,22)$$

If the indicial equation has coincident roots four independent solution functions will not eventuate and here one needs

$$\partial Y(X,c)/\partial c = X^c \ln(X) + \sum a_{n+2}(c) X^{c+(4-2s)(n+1)} \psi_{n+2}(X,c),$$

$$\psi_{n+2}(X,c) = \psi_{n+1}(X,c) - 1/[c+(4-2s)(n+1)] - 1/[c+(4-2s)(n+1)-1] - 1/[c+(4-2s)(n+1)-2+3s]$$

$$- 1/[c+(4-2s)(n+1)-3+3s], \quad \psi_1(X,c) = \ln(X) \qquad (23,24,25)$$

If $s = 1/3$, three solution functions are $Y(X,c)_{c=0,1,-1}$ and the fourth is $[\partial Y(X,c)/\partial c]_{c=0}$. If $s = 2/3$ two solution functions are $Y(X,c)_{c=0,1}$ and the other two are $[\partial Y(X,c)/\partial c]_{c=0,1}$. If $s = 1$ although the indicial equation has three distinct roots only two independent solution eventuate and the solution corresponding to the third root is unbounded. The general solution is derived with a slightly different approach. It will be shown that unbounded solution functions occur if $s = 2 - 1/(2n+2)$, $2 + 4/(2n-1)$, $2 + 3/(2n-1)$, $2 + 1/(2n+2)$, $2 + 5/(2n-1)$, $2 - 4/(2n+5)$, $2 - 5/(2n+5)$, $2 - 3/(2n+5)$. Note that for $s = 2$, the mode shape differential equation degenerates to a Cauchy differential equation. If $s \geq 2$, $Y(X)$ is singular at $X = 0$ and the natural frequencies of such 'sharp' ended wedges cannot be calculated. For $s \geq 1.5$ $DY(X)$ is singular at $X = 0$. This contradict the linear Euler-Bernoulli theory of bending. Frequencies of 'sharp' ended wedge beams with $2 \geq s \geq 1.5$ are therefore be subject to this limitation. The general solution is applicable to 'truncated' non-uniform wedge beams since the solution is not singular at the 'small' end. Further discussion is reserved for the symposium.

A non-uniform cone beam is formed by rotation of the curve $y = Ax^s$ about the x-axis.
Aspects of the unusual properties of the non-uniform wedge beams are found here along with some additional facets.

Numerical methods like Rayleigh-Ritz, Galerkin, finite element method etc are very useful tools in the study of lateral vibration of non-uniform beams. Analytical solution however highlight the deficiencies in study based on linear Euler-Bernoulli theory of bending and it may not be possible to obtain such information from numerical methods.

A number of references are available and will be surveyed at the symposium.

VIBRATION ANALYSIS OF THREE DIMENSIONAL COMPOSITES IN CYLINDRICAL COORDINATES CONSIDERING ARBITRARY BOUNDARY CONDITIONS

Yoshihiro NARITA
Department of Mechanical Engineering, Hokkaido Institute of Technology,
7−15 Maeda, Teine, Sapporo 006, Japan

Abstract− The objective of the present paper is to propose a semi−analytical method, based on the three dimensional theory of orthotropic elasticity, for the free vibration problem of laminated composites expressed in cylindrical coordinates. The method is based on the Ritz method, but unlike conventional Ritz methods, it can accommodate arbitrary boundary conditions on each face. Numerical results are given for natural frequencies of a wide class of geometry, ranging from solid cylinders and thin shells to flat solid cirular and annular plates, and the applicability of the present method, which cannot be obtained by the two dimensional theories, is widely demonstrated.

INTRODUCTION

With the increasing demands for fibrous composites in structural applications, it is becoming essential to understand vibrational characteristics of composite components. Although many references are found on vibrations of composite shells and plates, the majority of them are based upon the *two dimensional* approach, which is either the classcical thin plate/shell theories or the thick shear deformation theories to account for the transeverse shear effect. It is desirable however to use the *three dimensional* approach for problems of very thick laminates and for testing results from the two dimensional theories. Unfortunately, few three dimensional solutions are available for such purposes in the literature, particularly when arbitrary boundary conditions are concerned.

In the present analysis, the strain and kinetic energies are formulated in cylindrical coordinates by using the three dimensional stress−strain and strain−displacement relations. After applying the variational principle to the functional (the sum of the strain and kinetic energies), a set of linear homogeneous equations containing eigenvalues (i.e., frequency parameters) is derived in terms of coefficients of displacements. The displacement functions are given to satisfy prescribed kinetic boundary conditions by using the boundary index previously introduced in [1][2]. Numerical examples are presented for natural frequencies of laminated composite solid cylinders and thin shells, and are compared to existing results. Also by taking on specific aspect ratios, results were obtained for flat soid circular and annular plates. Such wide applicability of the present single solution is well demonstrated, which cannot be accomplished by the two dimensional theories.

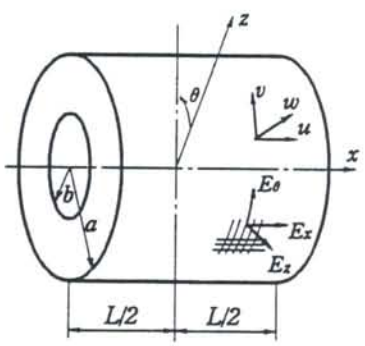

Fig 1. Coordinate system and dimension of thick circular cylindrical composite.

METHOD OF ANALYSIS

Figure 1 shows the geometry and coordinate system used in the analysis. The x axis is taken along the center of circular cross−section of the cylinder, and the θ and z axes are in the circumferential and radius directions, respectively. The outer and inner radii are denoted by a and b, respectively, and the length of the cylinder is L. The principle material axes are assumed to be parallel to the x, θ and z axes, and it is stacked as cross−ply laminates in the z direction. Under these assumptions, the stress−strain relation in the k−th layer is given by

$$\begin{Bmatrix} \sigma_x \\ \sigma_\theta \\ \sigma_z \\ \tau_{\theta z} \\ \tau_{xz} \\ \tau_{x\theta} \end{Bmatrix}^{(k)} = \begin{bmatrix} Q_{11} & Q_{12} & Q_{13} & 0 & 0 & 0 \\ Q_{12} & Q_{22} & Q_{23} & 0 & 0 & 0 \\ Q_{13} & Q_{23} & Q_{33} & 0 & 0 & 0 \\ 0 & 0 & 0 & Q_{44} & 0 & 0 \\ 0 & 0 & 0 & 0 & Q_{55} & 0 \\ 0 & 0 & 0 & 0 & 0 & Q_{66} \end{bmatrix}^{(k)} \begin{Bmatrix} \varepsilon_x \\ \varepsilon_\theta \\ \varepsilon_z \\ \gamma_{\theta z} \\ \gamma_{xz} \\ \gamma_{x\theta} \end{Bmatrix} \tag{1}$$

where $Q_{ij}^{(k)}$ $(i,j=1,2,\ldots 6)$ are elastic constants defined by moduli of elasticity and Poisson's ratios (See references [3][4]). The maximum displacements in the x, θ and z directions during infinitesimal vibration are denoted by u, v and w, respectively, and the strains are expressed in terms of the displacements. By using the relations, the maximum strain and kinetic energies are obtained by summing up energies for all layers and are written in the form

$$\left.\begin{aligned} U_{max} &= \frac{1}{2}\sum_{k=1}^{K}\int \{\varepsilon\}^T[Q]^{(k)}\{\varepsilon\} z\, dx d\theta dz \\ T_{max} &= \frac{1}{2}\omega^2\sum_{k=1}^{K}\int \rho\{u\ v\ w\}\begin{Bmatrix} u \\ v \\ w \end{Bmatrix} z\, dx d\theta dz \end{aligned}\right\} \tag{2}$$

with

$$\{\varepsilon\} = \left\{u_{,x},\ \frac{(w+v_{,\theta})}{z},\ w_{,z},\ \frac{(w_{,\theta}-v)}{z}+v_{,z},\ u_{,\theta}+w_{,x},\ v_{,x}+\frac{u_{,\theta}}{z}\right\}^T \tag{3}$$

where ρ is the mass per unit volume, ω is the radian frequency, and $(,x)$, $(,\theta)$, $(,z)$ denote differentiation with respect to x, θ and z axes, respectively. For clarity of the analysis, nondimensional quantities are introduced, such as $\xi = x/(L/2)$, $\delta = \{2z-(a+b)\}/(a+b)$ and $\Omega = \omega a(\rho/4E_2)^{1/2}$ (frequency parameter). The displacements are then assumed in the form

$$\left.\begin{aligned} u(\xi,\theta,\delta) &= \sum_{i=0}^{I-1}\sum_{j=0}^{J-1} A_{ij}X_i(\xi)Z_j(\delta)\cos N\theta \\ v(\xi,\theta,\delta) &= \sum_{k=0}^{I-1}\sum_{l=0}^{J-1} B_{kl}X_k(\xi)Z_l(\delta)\sin N\theta \\ w(\xi,\theta,\delta) &= \sum_{m=0}^{I-1}\sum_{n=0}^{J-1} C_{mn}X_m(\xi)Z_n(\delta)\cos N\theta \end{aligned}\right\} \tag{4}$$

where A_{ij}, B_{kl} and C_{mn} are unknown coefficients, N is the circumferential wave number, and $X(\xi)$ and $Z(\delta)$ are specific polynomials having boundary indeces that allow assumed solutions (4) to meet desired boundary conditions [1][2]. In the case of $u(\xi,\theta,\delta)$, X_i and Z_j are

$$\left.\begin{aligned} X_i(\xi) &= \xi^i(\xi+1)^{bc1u}(\xi-1)^{bc2u} \\ Z_j(\delta) &= \delta^j(\delta+1)^{bc3u}(\delta-1)^{bc4u} \end{aligned}\right\} \tag{5}$$

where *bc1u* ~ *bc4u* are indeces to constrain the u displacement on the surface *1* ~ *4* (*1*: left end surface at $x=-L/2$, *2*: right end surface at $x=L/2$, *3*: inner surface at $z=b$, *4*: outer surface at $z=a$). Substitution of 0 or 1 into the index *bc1u* ~ *bc4u* makes the displacement unconstrained (free) or constrained (fixed) on each face.

For the example of hollow cylinders (shells), all the displacements on outer and inner surfaces are made free (*bc3u=bc3v=bc3w=bc4u=bc4v=bc4w=0*) and the other indeces are

Both ends simply supported		Both ends clamped	
$bc1u=bc2u=0$	(u is free on both ends)	$bc1u=bc1v=bc1w=1$	(u, v and w are
$bc1v=bc1w=bc2v=bc2w=1$	(v and w are fixed)	$bc2u=bc2v=bc2w=1$	all fixed)

On the other hand, for flat circular(annular) plates ($L << a$), all the displacements on both ends (i.e., plate surfaces) are set free ($bc1u=bc1v=bc1w=bc2u=bc2v=bc2w=0$) .

Following the Ritz method procedure, the functional $F=T_{max}-U_{max}$ is extremized for a stationary value: $\partial F/\partial A_{ij} = \partial F/\partial B_{kl} = \partial F/\partial C_{mn} = 0$. This yields a set of linear equations in terms of $\{A_{ij}, B_{kl}, C_{mn}\}$ and the eigenvalues of the system give frequency parameters Ω .

NUMERICAL RESULTS AND DISCUSSIONS

Table I presents comparisons of the present 3D results with those obtained in other references. The values are compared in Table I(a) with the finite element results in reference [4] for the three-layerd thin shells. The FEM values are based on the classical thin shell theory (CTST). For thicker shells where the transverse shear effect is not negligible, the first-order shear deformation shell theories (FSDST) may be used for better accuracy in the two dimensional analysis. In Table I(b), the present results are compared to those obtained by the transfer matrix method (TMM) and FSDST [5]. The present parameters Ω are again in good agreement with the reference values given for a fixed N (=0). For all the values in the table (except for one case), the present ones are slightly lower than the others, and this seems to reflect the fact that the 3D analysis allows more flexibilities in the thickness direction than the 2D theories.

Table I. Comparison of frequency parameters Ω for cross-ply laminated cylindrical shells ([0°/90°/0°])

B.C.	Method	Ω			
(a) Classical thin shell theory (CTST) (a/H=50.5, a/L=0.2525)					
		(N=4)	(N=3)	(N=5)	(N=2)
$S-S$	FEM[4]	0.07484	0.08312	0.09459	0.1299
	Present	0.07469	0.08302	0.09444	0.1298
		(N=4)	(N=5)	(N=3)	(N=6)
$C-C$	FEM[4]	0.09459	0.1059	0.1089	0.1363
	Present	0.09443	0.1057	0.1088	0.1359
(b) First-order shear deformation shell theory (FSDST)* (N=0)					
$S-S$ (a/H=10.5, a/L=1.05)					
	TMM[5]	1.530	2.244	3.323	
	Present	1.529	2.232	3.304	
$S-S$ (a/H=5.5, a/L=1.1)					
	TMM[5]	1.742	2.680	3.814	
	Present	1.735	2.675	3.857	

* : $E_1=20E_2$, $G_{12}=0.65E_2$, $G_{23}=0.5E_2$, $\nu_{12}=0.25$

REFERENCES

1. Narita, Y. and et al , *AIAA J.*, 30 (1992), 790. 2. Turvey, T.J. and Marshall, I.H., *Buckling and Postbuckling of Composite Plates*, Chapman and Hall, 1995, 51. 3. Vinson, J.R. and Sierakowski, R.L., *The Behavior of Structures Composed of Composite Materials*, Martinus Nijihoff Publishers, Dordrecht, 1986. 4. Narita, Y., Ohta, Y. and Saito, M., *Compos. Struct.*, 26 (1993), 55. 5. Yamada, G., Kobayashi, Y. and Ohta,Y., *Trans. JSME* (in Japanese), 57C (1991), 27.

On the Discretization of Weakly Nonlinear Continuous Systems

Walter Lacarbonara and Ali H. Nayfeh
Department of Engineering Science and Mechanics
Virginia Polytechnic Institute and State University
Blacksburg, VA 24061-0219

Abstract

Methods for the study of weakly nonlinear continuous systems are discussed. Approximate solution procedures based on discretization via the Galerkin method are contrasted with direct application of the method of multiple scales to the integro-partial-differential equations and boundary conditions governing nonlinear planar vibrations of a buckled beam around its first buckled deflection. The case of primary resonance ($\Omega \approx \omega_n$), where Ω is the excitation frequency and ω_n is the natural frequency of the nth mode of the beam, is investigated. Frequency-response curves are generated using both approaches and contrasted with experimentally obtained frequency-response curves. It is shown that the discretization can lead to erroneous quantitive as well as qualitative results if the discretization is not performed by using a complete set of basis functions that satisfy the boundary conditions.

In the great majority of recent works on forced nonlinear vibrations of distributed-parameter systems, it has been a common practice to use the Galerkin method to discretize them by taking as trial functions only the eigenmodes that are directly or indirectly excited. This discretization procedure has two drawbacks. First, by minimizing the residuals, one discards the nonlinear terms that are orthogonal to the eigenmodes assumed in the expansion. Second, the shape of the motion is fixed *a priori*. On the contrary, by attacking directly a distributed-parameter system with a reduction method, such as the method of multiple scales, one does not assume the form of the solution a priori.

Troger and Steindl (1991) [1] showed that, in the context of snap-buckling problems, discretization techniques, such as the Rayleigh-Ritz and Galerkin methods, can lead to qualitatively

erroneous bifurcation diagrams. By applying the direct procedure to several weakly nonlinear distributed-parameter systems with quadratic and cubic nonlinearities (e.g., relief valves, suspended cables, surface waves, cylindrical shells), Nayfeh, Nayfeh, and Mook (1992) [2], Nayfeh, Nayfeh, and Pakdemirli (1994) [3], and Chin and Nayfeh (1996) [4] showed that finite-degree-of-freedom discretization can lead to erroneous results.

In this paper, we first discretize the governing integro-partial-differential equation by using the Galerkin method assuming that only the nth mode is excited. Then, we apply the method of multiple scales to the resulting discretized equation to determine an approximation for the frequency-response equation characterizing periodic motions. Next, we attack directly the governing equation and associated boundary conditions by using the method of multiple scales.

"Small" finite-amplitude transverse vibrations of a homogeneous Euler-Bernoulli, buckled beam subjected to a uniform harmonic excitation are governed by

$$\ddot{u} + 2\mu\dot{u} + u^{iv} + P_1 u'' - b^2\phi'' \int_0^1 \phi' u' dx - \frac{1}{2} b\phi'' \int_0^1 u'^2 dx \qquad (1)$$
$$-bu'' \int_0^1 \phi' u' dx - \frac{1}{2} u'' \int_0^1 u'^2 dx = F(x)\cos(\Omega t + \tau)$$

where the prime and overdot indicate differentiation with respect to x and t, respectively, $\phi(x)$ is the first buckling mode, and b represents the buckling level. The frequency-response equation characterizing periodic asymmetric oscillations around the first buckled deflection are given by

$$\sigma = -\alpha_e a^2 \pm \left(\frac{f^2}{4\omega^2 a^2} - \mu^2 \right)^{\frac{1}{2}} \qquad (2)$$

where σ denotes a detuning parameter expressing the nearness of the resonance and α_e has different expressions depending on whether it is evaluated by the discretization or the direct procedure. Figure 1 shows that the results obtained with discretization are qualitatively as well as quantitatively different from those obtained with the direct approach. The discretization procedure predicts a hardening behavior whereas the direct approach predicts a softening behavior, in agreement with the experimental results. Figure 2 shows the experimentally obtained frequency-response curve generated by setting the buckling amplitude at the same level used to calculate the curves in Figure 1. Clearly, the experimentally obtained frequency-response curve exhibits a softening behavior, in agreement with the direct approach and in disagreement with the discretized approach.

References

1. Troger, H. and Steindl, A., *Nonlinear Stability and Bifurcation Theory*, Springer-Verlag, Wien, 1991.

2. Nayfeh, A. H., Nayfeh, J. F., and Mook, D, T., 'On methods for continuous systems with quadratic and cubic nonlinearities,' *Nonl. Dyn.* **3**, 145–162, 1992.

3. Nayfeh, A. H., Nayfeh, S. A., and Pakdemirli, M., 'On the discretization of weakly nonlinear spatially continuous systems', in *Nonlinear Dynamics and Stochastic Mechanics*, W. Kliemann and N. Sri Namachchivaya, eds., 1994.

4. Chin, C. and Nayfeh, A. H. 1995, 'Bifurcation and chaos in externally excited circular cylindrical shells', *Journal of Applied Mechanics* **63**(3), 565–574, 1996.

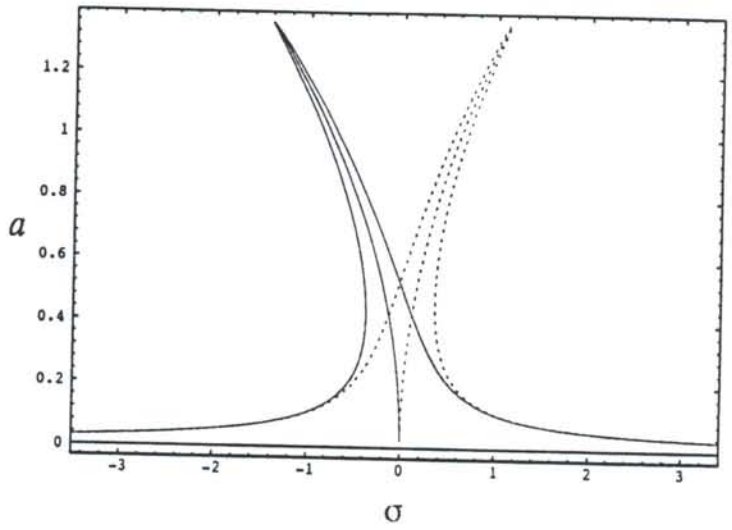

Figure 1: Frequency-response curves in the case of primary resonance of the first mode. Solid (dashed) lines denote the curve obtained with the direct (discretization) approach: $b = 0.11$ *in*.

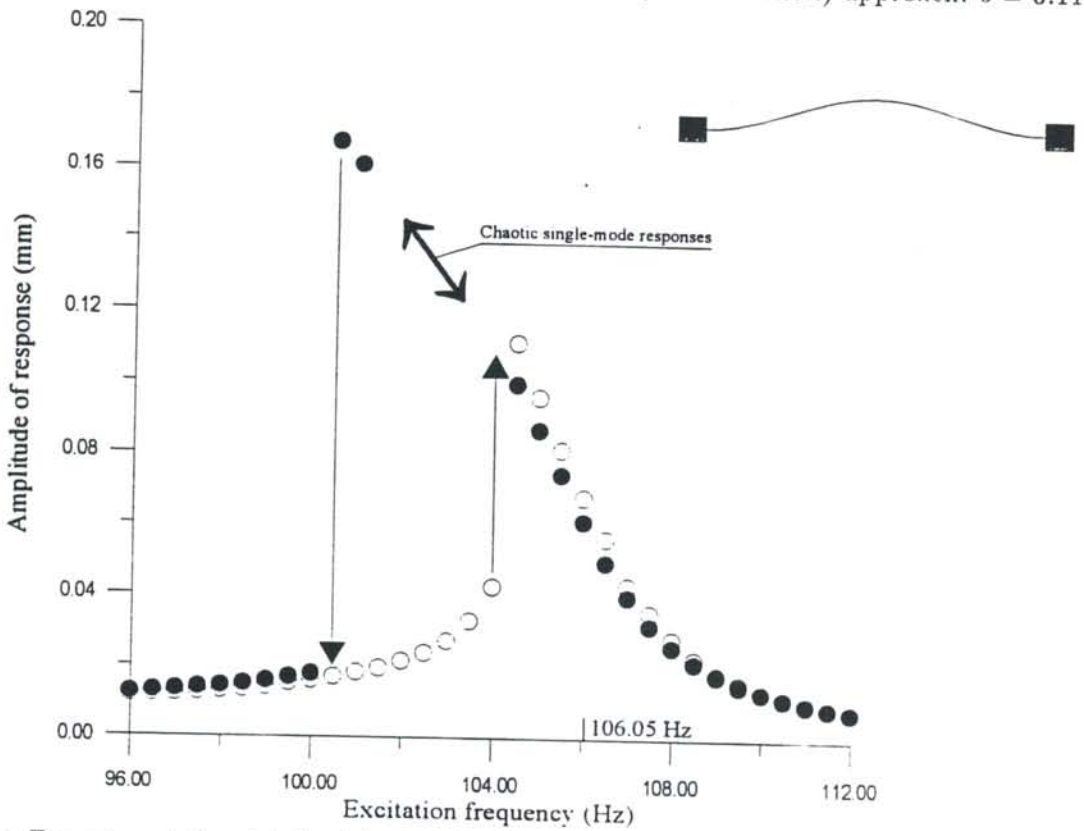

Figure 2: Experimentally obtained frequency-response curve in the case of primary resonance of the first mode: $b = 0.11$ *in*. $\ell = 11$ *in*. $A = 0.01$ in^2. $I = 3.33\text{x}10^{-7}$ in^4. $E = 3\text{x}10^7$ *psi*. $m = 7.3\text{x}10^{-6}$ lbm/in. ∘ (•) indicates forward (reverse) sweep.

DAMPING PROPERTIES OF TWO-LAYERED CURVED STRUCTURES WITH AN UNCONSTRAINED VISCOELASTIC LAYER

A. Okazaki

Department of Engineering Physics
Chubu University , Kasugai, Japan

1. INTRODUCTION

One of the simple methods of reducing the resonance amplitudes of structures is to coat their surface with a high damping viscoelastic material. Damping properties of two-layered flat structure are almost independent of boundary conditions and modes of vibration, and the ratio of the loss factor η of a two-layered structure to the loss factor η_E of a viscoelastic material is given by

$$\frac{\eta}{\eta_E} = \frac{eh\left(4h^2+6h+3\right)}{1+eh\left(4h^2+6h+3\right)}, \qquad (1)$$

where h is the thickness ratio, and e is the Young's modulus ratio of the elastic viscoelastic layers [1,2,3].

However, damping properties of curved structures are different from those of flat structures. The primary reason for this is that, for curved structures, flexural and extensional deformations are coupled with each other. It is shown that loss factors of two-layered cylindrically curved structures are generally less than those of flat beams and plates, and depend on sectional shapes, frequencies, modes of vibration and boundary conditions as well as on the Young's modulus and thickness each layer.

2. ANALYTICAL MODEL

Figure 1 shows the geometrical dimensions of two-layered cylindrically curved structures. Layer 1 and 2 are taken to be the elastic layer and the viscoelastic layer respectively. It is assumed that the energy dissipation primarily occurs in the viscoelastic layer. The analyses are carried out, using the equations of motion on the basis of the Flügge's shell theory[4].

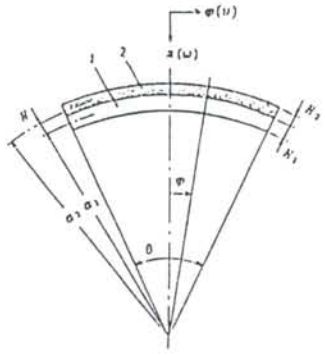

(a) A cylindrically curved beam

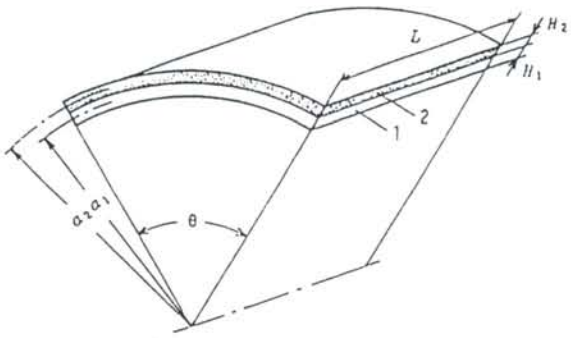

(b) A cylindrically curved plate

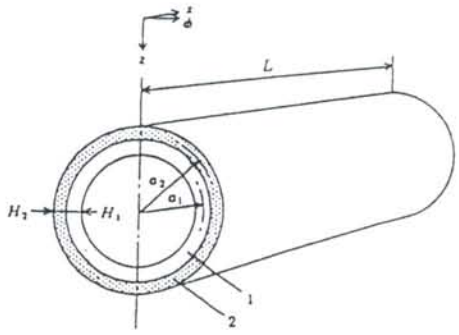

(c) A cylindrical shell

Fig.1 The geometrical dimensions of two-layered cylindrically curved structures.

3. NUMERICAL RESULTS

3.1 CURVED BEAM

Figures 2 and 3 show the variation of η/η_E with θ for the following boundary conditions: Both ends are simply supported (S-S), clamped (C-C), freely supported (F-F), and hinged supported (H-H). One end is clamped and other end is free (C-F). As shown in Fig.3(b), damping characteristics of symmetric vibration modes of a F-F beam and a H-H beam are strikingly different from those of other beams. These differences are related to the existence of the extensional deformation. In the case of the mode of inextensional deformation, η/η_E remains almost constant even if θ increases.

3.2 CURVED PLATE

Figures 4, 5 and 7 show the variation of η/η_E with θ for the following boundary conditions: (1) All edges are simply supported (SSSS). (2) All edges are clamped (CCCC). (3) Straight edges are simply supported, and curved edges are freely supported (SFSF). (4) Straight edges are clamped, and curved edges are freely supported (CFCF). The analysis for a CCCC plate and a CFCF plate is carried out by the use of Kantorovich method[5].

η/η_E of a curved plate is usually smaller than that of a flat plate, and the decrease of the loss factor with bending depends on the aspect ratio $\xi = L/a_1\theta$, the thickness-length ratio $\zeta = (H_1 + H_2)/2a_1\theta$, mode of vibration and boundary conditions.

3.3 CYLINDRICAL SHELL

The variation of η/η_E with $\Lambda(= L/ma_1, m$: longitudinal half-wavenumber) for different circumferential wavenumbers n is shown in Fig.8. Boundary conditions are taken as simply supported. η/η_E depends on the length parameter Λ and the wavenumber n. η/η_E for two-layered thin cylindrical shells with large values of Λ are practically independent of Λ, and their approximate values can be generated from the equations

$$n = 0, 1 \quad : \frac{\eta}{\eta_E} = \frac{eh}{1+eh}, \tag{2}$$

$$n \geq 2 \quad : \frac{\eta}{\eta_E} = \frac{eh\left(4h^2+6h+3\right)}{1+eh\left(4h^2+6h+3\right)}. \tag{3}$$

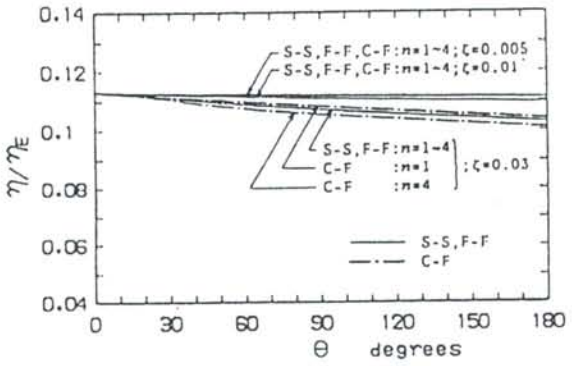

Fig.2 The variation of η/η_E with θ for S-S, F-F and C-F beams ($h = H_2/H_1 = 1, e = E_2/E_1 = 0.01$).

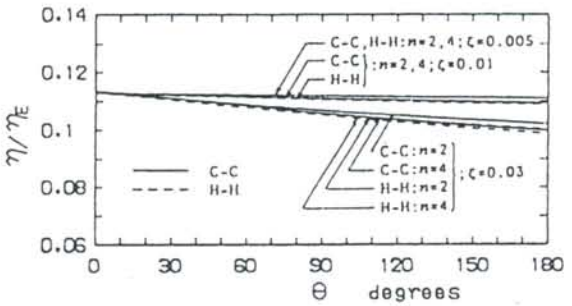

(a) Antisymmetric modes [$n = 2, 4$]

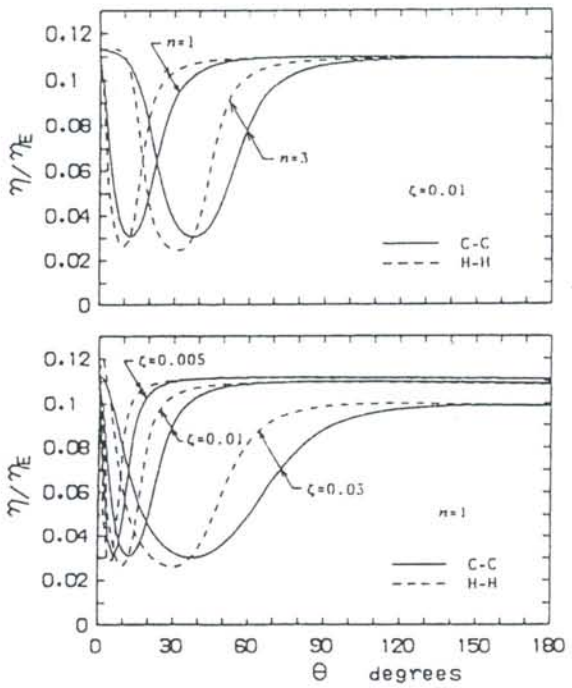

(b) Symmetric modes [$n = 1, 3$]

Fig.3 The variation of η/η_E with θ for C-C, and H-H beams ($h = H_2/H_1 = 1, e = E_2/E_1 = 0.01$).

REFERENCES

1. H.Oberst and K.Frankenfeld 1952 *Acustica* 2, AB181. Über die Dämpfung der Biegeschwingungen dünner Bleche durch fest haftende Beläge.
2. N.Ren and Y.Y.Yu 1967 *AIAA J.* 5-4, 797. Flexural and Extensional Vibrations of Two-Layered Plates.
3. F.Abdulhadi 1969 *Shock and Vib. Bull.* 40 Part 2, 93. Transverse Vibrations of Laminated Plates with Viscoelastic Layer Damping.
4. W.Flügge 1962 *Stresses in Shells.* Berlin: Springer Verlag.
5. L.V.Kantorovich and V.I.Krylov 1964 *Approximate Methods of Higher Analysis.* Interscience Publishers Inc..

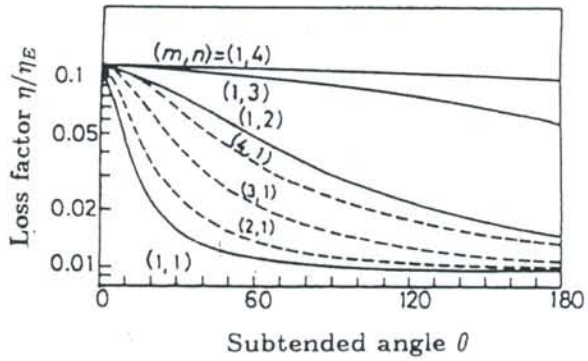

Fig.4 The variation of η/η_E with θ for a SSSS plate ($\xi = L/a_1\theta = 1, \zeta = (H_1+H_2)/2a_1\theta = 0.01, h = H_2/H_1 = 1, e = E_2\left(1-\nu_1^2\right)/E_1\left(1-\nu_2^2\right) = 0.01$).

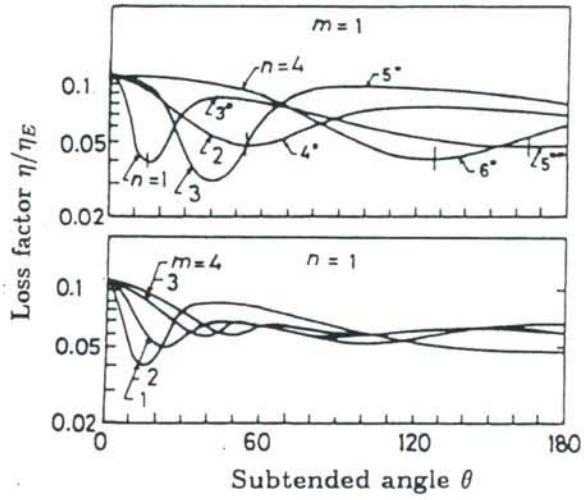

Fig.5 The variation of η/η_E with θ for a CCCC plate ($\xi = 1, \zeta = 0.01, h = 1, e = 0.01$).

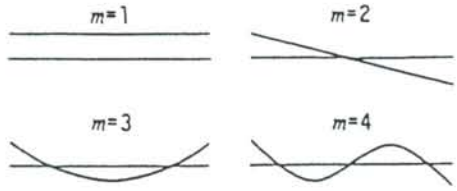

Fig.6 Mode shapes of a curved edges freely supported plate.

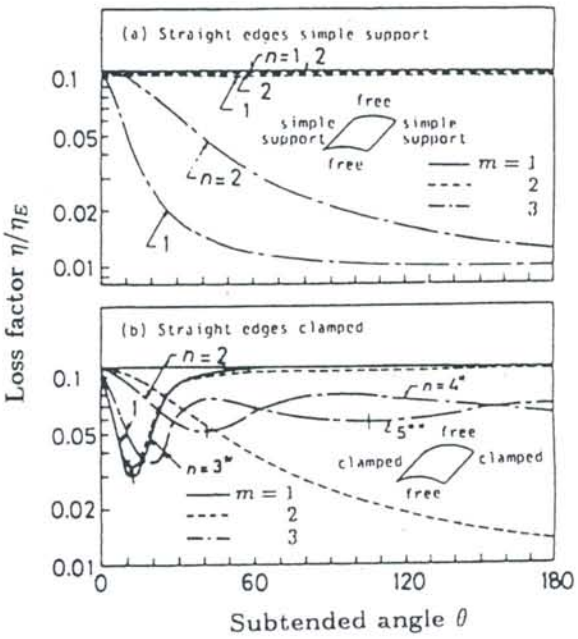

Fig.7 The variation of η/η_E with θ ($\xi = 1, \zeta = 0.01, h = 1, e = 0.01$). (a) a SFSF plate; (b) a CFCF plate.

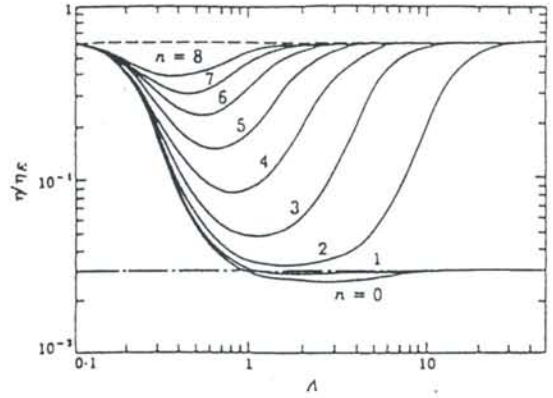

Fig.9 The variation of η/η_E with Λ.
($\zeta = H_1/a_1 = 0.01, h = H_2/H_1 = 3, e = E_2\left(1-\nu_1^2\right)/E_1\left(1-\nu_2^2\right) = 0.01$).
- - - - -,Extensional vibration of two-layered beams and plates; — - —, flexural vibration of two-layered beams and plates.

Coherent scattering effects in irregular structures

Douglas Photiadis
Naval Research Laboratory
Washington, DC 20375

Introduction

The scattering of elastic waves due to irregular variations in structural properties - variations in geometry or material parameters - produces a wide range of phenomena. In the limits of very large irregularity or very small irregularity, the effects of the scattering on the dynamic response of an elastic system lead to two competing physical pictures. In a way, this duality is similar to the wave-particle duality in quantum mechanics. In the small irregularity limit, the nature of the resonances of the system are nearly unchanged from those of an idealized 'uniform' system and consist of either traveling waves or global resonances built from traveling waves. In the large irregularity case, the scattering causes the modes of the system to localize and the response of the system consists of a superposition of these local, nearly uncoupled oscillators. It is in this latter case in which the coherent scattering effects due to irregularity are manifestly important. The question we wish to address here is: In what kind of 'real world' systems is this really important, and how should the investigator or engineer proceed in this case?

The physical basis for localization

Any spatial deviations in the properties of an elastic system will scatter elastic waves and, provided such deviations are spread throughout the system, will produce multiple scattering phenomena. In many situations however, coherence effects arising from this scattering will be negligible, and the scattering will produce just a diffuse random background field. Indeed, prior to Anderson's seminal work in 1958, this was assumed to be always the case: Irregularity would simply tend to evenly spread out the energy in a system and bring it to equilibrium, with each mode having an equal share of the energy. Such an assumption is at the heart of the Statistical Energy Analysis(SEA). In the context of the wave picture, localization arises from destructive interference and is a bit hard to understand. But in the context of coupled standing modes, Anderson localization is quite natural.

Consider then a prototype system, consisting of a string with attached masses. Let us suppose the masses to be rather heavy relative to the density of the string and fairly evenly spaced. In a modal picture, we consider the system to consist of a set of coupled string segments, and work out the normal modes of each segment with fixed ends. In this normal mode expansion, each segment is replaced by a set of oscillators. Near a particular frequency, we may as an approximation retain only the nearest resonance (the single band approximation) or perhaps the two nearest modes (the 2-band approximation). Our system hence is equivalent to a set of coupled simple harmonic oscillators and obeys,

$$-m_i\omega^2 x_i = -k(2x_i - x_{i+1} - x_{i-1}) - k_i x_i \ .$$

The individual oscillators have mass m_i and stiffness k_i, while the springs coupling the oscillators to one another are taken to have the uniform stiffness value k. One quickly finds

$$(\omega_i^2 - \omega^2)x_i = \frac{\Delta\omega^2}{4}(x_{i+1} - x_{i-1})$$

where we have written the coupling of the adjacent oscillators k in terms of the frequency bandwidth $\Delta\omega^2 = 4k/m$.

Each oscillator is a normal mode of a section of the string between two masses, and the oscillators have different frequencies because of the different spacings. In the case of a string with uniformly spaced masses, all the ω_i are equal and the traveling wave solutions $\exp(ikx)$ form a single band with a width $\Delta\omega^2$. To leading order, in an average sense, an irregular single degree of freedom coupled oscillator chain is characterized only by the bandwidth $\Delta\omega^2$ and the spread of the ω_i about the mean value ω_0,

$$W = \delta\omega^2 \ .$$

What is the nature of the resonant states on the string? In the limit of large irregularity, $\delta\omega^2 >> \Delta\omega^2$, each local resonance frequency is quite different from its neighbor's and energy is very weakly coupled down

the chain. One is not surprised that the normal modes of this system consist of spatially localized states with an exponentially localized wave packet arising from a more or less constant suppression factor $(\Delta\omega^2/\delta\omega^2)$ incurred a number of times as we march from site to site. This phenomena is localization due to irregularity. In the opposite limit, weak irregularity, we expect strong coupling due to the close match of resonance frequencies relative to the coupling, and hence extended modes. To some extent this is the case, although at sufficiently large distances in this 1-dimensional example, exponential localization again sets in.

This is of course only a toy example, but it does serve to illustrate the main physics which underlies localization phenomena. The key idea is that is energy is transmitted by well tuned neighboring oscillators and that detuning is measured relative to the coupling of the oscillators to one another - or to the inverse of the time it takes to transmit energy from one oscillator or portion of the string to the next.

System properties

The most important properties of the system which determine whether coherent scattering phenomena will occur are system dimensionality, scattering strength/irregularity, and damping.

Dimensionality

System dimensionality plays a dominant role in determining the importance of irregularity. The reason for this is primarily that each oscillator is coupled strongly only to its neighbors. In one dimension, there are only 2 neighbors which may be well matched to any given oscillator. In two dimensions, even assuming each oscillator must be the nearest neighbor, i.e. not related via a diagonal path (imagine a plate with oscillators attached in a sort of lattice), the number of neighboring oscillators is 4, while in three dimensions, the number of neighboring oscillators is 6. Should one be more realistic, and include diagonals, the numbers of neighboring oscillators in this cubic array are 8(2-D) and 26(3-D) respectively. Clearly, for a given degree of randomness producing a fixed variation of local resonance frequencies, our odds of encountering a nearby resonance frequency are much greater as the dimension increases. This is indeed the case, and the localization lengths increase dramatically as the system dimensionality increases.

In a linear chain system or an effectively 1-D wave system, one should suspect that localization phenomena will be prevalent. Great efforts must taken to avoid small irregularities which will produce localized modes - should global traveling modes be desired. In a 2-D system, localization phenomena will be much weaker unless the scattering strengths and irregularity of the system are both large. In this scenario, the prime suspects would be anisotropic systems in which wave behavior can become pseudo 1-D. In 3-D, it turns out that it is quite difficult to achieve localized modes in realistic elastic systems, and most likely, only in highly anisotropic systems are coherent scattering effects due to irregularity important.

Scattering strength/irregularity

The above simple example makes clear that coherent scattering phenomena are greatly enhanced by increased scattering strength, that is, decreased coupling, and increased irregularity. If our system is indeed a coupled chain, or transparently equivilent to a coupled chain as is the string with masses, it is relatively easy to determine the relevant ratio of frequencies, and hence to determine the importance of the irregularity.

In elastic wave systems, this is quite often not the case; the complexity of the system can make it difficult to determine even what the appropriate oscillators would be. In this case, it is most straightforward to measure or theoretically estimate the frequency bandwidths of the system and use this quantity as a measure of the coupling of the undetermined oscillators. The variation of resonance frequencies arising from the irregularity however may not be easy to either measure or estimate. This is an outstanding problem in this area.

The role of damping

Damping is of course a mechanism which tends to destroy any coherence effects. Typically, the system must be fairly lightly damped in order that localization phenomena due to irregularity is important. Interestingly enough, damping increases as the coupling of the elements of the system decreases, just as is the case for coherent scattering phenomena. The role of damping may be evaluated by estimating the damping length, $L_d = c_g\tau$, and comparing this quantity to the localization length L_c.

What tools should we use?

The standard tools

Numerical simulations have proven to be a very powerful and useful tool in the past. Any effectively 1-D system for which detailed predictions are desired should be analyzed in this way. Even reasonably large systems of this sort will yield to modern computer power. In 2-D and 3-D, this capability is still beyond our

grasp except at low frequencies, frequencies for which the phenomena we have been discussing is not relevant in any case. But further advances in computer speed or algorithms may allow direct numerical approaches to be quite useful.

The statistical energy analysis(SEA), as it stands, is not useful in this context. SEA assumes at the start that the various modes of the system within a particular bandwidth come to equilibrium. This is precisely what *does not* occur in a system for which coherent scattering is important.

Highly idealized modeling

Highly idealized modeling, replacing one's system by a set of coupled oscillators for example, can be a useful guide in qualitatively understanding the phenomena which will take place, and in addition, in identifying the critical parameters. In this area, because of the intense research in condensed matter physics over the past 30-40 years, a number of useful results have been obtained which can be directly applied to problems of this nature. It is not however, completely straightforward to exploit these results, and thus far, only a few of these results have been exploited.

Multiple scattering theories

The multiple scattering theories employed in a number of fields were built to solve the problem we have addressed here. Nevertheless, these theories still pose significant mathematical difficulties. For relatively weak scattering/weak irregularity, the multiple scattering theories will seamlessly provide mean field theories, corrections to these theories, and predictions of anomolous frequencies. In the case of strong scattering/ strong irregularity the multiple scattering theories are not so effective. The reason for this is clear: At a basic level, these theories assume one's system is a perturbed uniform elastic medium, at least locally. When this is not true, one may expect trouble from this approach. Nevertheless, much can be expected from these models before they break down.

Future directions..

There have been a number of new tools proposed to handle this problem. Here, I will mention just a couple. Recently, Bucaro et. al. proposed a model based on the local nature of the response of the system. This model basically assumes a point reacting impedance for the case of a ribbed shell with many internal oscillators. The model moreover assumes very little phase correlation even in the case of a spatially coherent external source. Good agreement with experiment was obtained. This result holds out the possibility that models of this sort, i.e. models in which each component of the structure are handled separately, can be successful.

Another recent advance was made by Woodhouse, Power, et. al. In this work, SEA was modified to take account of the knowledge of the mode shapes resulting from irregularity. This work too has produced some good results, and holds promise for the future.

This work was supported by the Office of Naval Research.

THEORY AND VIBRATION OF LAMINATED BARREL SHELLS

by

Mohamad S. Qatu
Department of Mechanical Engineering
Lake Superior State University
Sault Ste. Marie, MI 49783

INTRODUCTION

This paper deals with analysis of laminated composite barrel shells. Barrel shells are essentially cylindrical shells for which the longitudinal direction of the shell has some initial curvature. The curvature may be due to imperfection in manufacturing, or is a part of the design as is the case in barrel shells. The equations are developed for the general dynamic analysis of laminated barrel shells and can be reduced to the static analysis and the free vibration analysis. Natural frequencies are obtained for open and closed, isotropic and laminated barrels shells having shear diaphragm boundary conditions. For composite shells, the effects of curvature, thickness and orthotropy ratios as well as the lamination sequence on the nondimensional natural frequency parameters are studied.

A considerable amount of information on the free and forced vibration of cylindrical shells can be found in the books of Leissa (1973) and Soedel (1993). Recent surveys are found for the analysis of laminated shells (e.g., Noor et. al., 1996). A treatment is introduced by Soedel, 1993 to deal with barrel shells and simplified equations were derived. Barrel shells are treated as a special case of shells of revolution in which the angle that the radius of curvature along the shell direction makes with the center of revolution axis is close to 90 degrees. This simplified the equations and introduced constant lame parameters. This approach to the treatment of barrel shells is adopted here.

EQUATIONS FOR BARREL SHELLS

Consider a shell of revolution as shown in Fig. 1. The fundamental form can be written as (Soedel, 1993):

$$(ds)^2 = (d\alpha)^2 + sin^2(\phi)(d\beta)^2, \qquad where \qquad d\alpha = R_\alpha d\phi, \qquad d\beta = R_\beta d\theta \tag{1}$$

The Lame parameters are:

$$A = 1, \quad B = \sin(\phi) \tag{2}$$

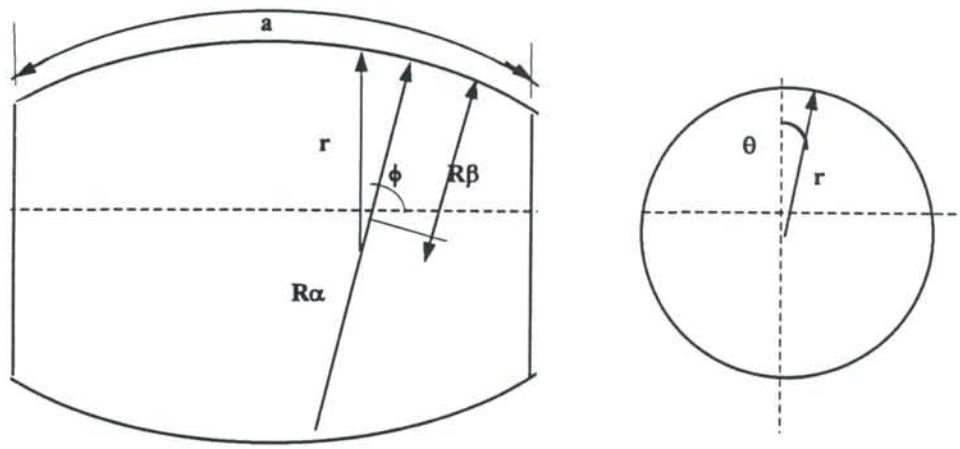

Fig. 1. Parameters used in barrel shell equations

For barrel shells of revolution, the angle ϕ varies between 75° and 105°. Thus, the following approximation is made:

$$\sin(\phi) \approx 1. \tag{3}$$

The fundamental form can the be approximated as :

$$(ds)^2 \approx (d\alpha)^2 + (d\beta)^2 \tag{4}$$

and the Lame parameters can be written as

$$A = 1, \qquad B \approx 1 \tag{5}$$

Furthermore, we will assume the radius of the barrel R_β to be constant. Based on these assumptions, we will only be able to consider barrel shells that have $|a/R_\alpha| \le 0.5$, and $|R_\alpha(1-\cos(a/2\,R_\alpha))| > R_\beta$.

Closed cylindrical shells can be treated by replacing the coordinate β with θ, and letting $b = \pi R_\beta$ (Leissa, 1973). It is also worth noting that the edge shear diaphragm boundaries repeat them selves at the nodal lines in the circumferential direction. The present formulation accounts for the case when $b > 2\pi R_\beta$.

Kinematic Relations

Midsurface strains and curvature changes are :

$$\begin{aligned}
\varepsilon_\alpha^\circ &= \frac{\partial u_\circ}{\partial \alpha} + \frac{w_\circ}{R_\alpha} & k_\alpha &= \frac{\partial}{\partial \alpha}\left(\frac{u_\circ}{R_\alpha} + \frac{v_\circ}{R_{\alpha\beta}} - \frac{\partial w_\circ}{\partial \alpha}\right) \\
\varepsilon_\beta^\circ &= \frac{\partial v_\circ}{\partial \beta} + \frac{w_\circ}{R_\beta} & k_\beta &= \frac{\partial}{\partial \beta}\left(\frac{u_\circ}{R_{\alpha\beta}} + \frac{v_\circ}{R_\beta} - \frac{\partial w_\circ}{\partial \beta}\right) \\
\gamma_{\alpha\beta}^\circ &= \frac{\partial v_\circ}{\partial \alpha} + \frac{\partial u_\circ}{\partial \beta} + \frac{2w_\circ}{R_{\alpha\beta}} & \tau &= \frac{\partial}{\partial \alpha}\left(\frac{u_\circ}{R_{\alpha\beta}} + \frac{v_\circ}{R_\beta} - \frac{\partial w_\circ}{\partial \beta}\right) + \frac{\partial}{\partial \beta}\left(\frac{v_\circ}{R_{\alpha\beta}} + \frac{u_\circ}{R_\alpha} - \frac{\partial w_\circ}{\partial \alpha}\right)
\end{aligned} \tag{6}$$

Stress Resultants

The stress resultants are related to middle surface strains and curvature changes through:

$$\begin{bmatrix} N_\alpha \\ N_\beta \\ N_{\alpha\beta} \\ -- \\ M_\alpha \\ M_\beta \\ M_{\alpha\beta} \end{bmatrix} = \begin{bmatrix} A_{11} & A_{12} & A_{16} & B_{11} & B_{12} & B_{16} \\ A_{12} & A_{22} & A_{26} & B_{12} & B_{22} & B_{26} \\ A_{16} & A_{26} & A_{66} & B_{16} & B_{26} & B_{66} \\ -- & -- & -- & -- & -- & -- \\ B_{11} & B_{12} & B_{16} & D_{11} & D_{12} & D_{16} \\ B_{12} & B_{22} & B_{26} & D_{12} & D_{22} & D_{26} \\ B_{16} & B_{26} & B_{66} & D_{16} & D_{26} & D_{66} \end{bmatrix} \begin{bmatrix} \varepsilon_\alpha^\circ \\ \varepsilon_\beta^\circ \\ \gamma_{\alpha\beta}^\circ \\ -- \\ k_\alpha \\ k_\beta \\ \tau \end{bmatrix} \tag{7}$$

where the A_{ij} , B_{ij} , and D_{ij} are the stiffness coefficients arising from the piecewise integration

Equations of Motion:

Deleting the body couples, the reduced equations of motion become (for constant Lame parameters A and B):

$$\begin{aligned}
&B\frac{\partial N_\alpha}{\partial \alpha} + A\frac{\partial N_{\alpha\beta}}{\partial \beta} + \frac{1}{R_\alpha}\left[B\frac{\partial M_\alpha}{\partial \alpha} + A\frac{\partial M_{\alpha\beta}}{\partial \beta}\right] + \frac{1}{R_{\alpha\beta}}\left[A\frac{\partial M_\beta}{\partial \beta} + B\frac{\partial M_{\alpha\beta}}{\partial \alpha}\right] + ABp_\alpha = -\rho\frac{\partial^2 u_\circ}{\partial t^2} \\
&A\frac{\partial N_\beta}{\partial \beta} + B\frac{\partial N_{\alpha\beta}}{\partial \alpha} + \frac{1}{R_{\alpha\beta}}\left[B\frac{\partial M_\alpha}{\partial \alpha} + A\frac{\partial M_{\alpha\beta}}{\partial \beta}\right] + \frac{1}{R_\beta}\left[A\frac{\partial M_\beta}{\partial \beta} + B\frac{\partial M_{\alpha\beta}}{\partial \alpha}\right] + ABp_\beta = -\rho\frac{\partial^2 v_\circ}{\partial t^2} \\
&-AB\left(\frac{2N_{\alpha\beta}}{R_{\alpha\beta}} + \frac{N_\alpha}{R_\alpha} + \frac{N_\beta}{R_\beta}\right) + B^2\frac{\partial^2 M_\alpha}{\partial \alpha^2} + 2AB\frac{\partial^2 M_{\alpha\beta}}{\partial \beta \partial \alpha} + A^2\frac{\partial^2 M_\beta}{\partial \beta^2} + AB(p_n) = -\rho\frac{\partial^2 w_\circ}{\partial t^2}
\end{aligned} \tag{8}$$

The above equations of equilibrium can be written in terms of displacements as

$$\begin{bmatrix} L_{11} & L_{12} & L_{13} \\ L_{21} & L_{22} & L_{23} \\ L_{31} & L_{32} & L_{33} \end{bmatrix} \begin{bmatrix} u_o \\ v_o \\ w_o \end{bmatrix} + \begin{bmatrix} -\rho & 0 & 0 \\ 0 & -\rho & 0 \\ 0 & 0 & \rho \end{bmatrix} \frac{\partial^2}{\partial t^2} \begin{bmatrix} u_o \\ v_o \\ w_o \end{bmatrix} = \begin{bmatrix} -p_x \\ -p_y \\ p_n \end{bmatrix} \tag{9}$$

Consider a barrel shell that is made of cross-ply laminates, thus

$$A_{16} = A_{26} = B_{16} = B_{26} = D_{16} = D_{26} = 0 \tag{10}$$

Assuming the radius of twist to be infinite. (i.e. $R_{\alpha\beta} = \infty$). Consider an open barrel shell, with shear diaphragm (S2) boundaries on all four edges. That is, the following boundary conditions apply:

$$\begin{aligned} &N_\alpha = w_o = v_o = M_\alpha = 0 \quad \text{for the edges} \quad \alpha = -a/2, +a/2 \\ &N_\beta = w_o = u_o = M_\beta = 0 \quad \text{for the edges} \quad \beta = -b/2, +b/2 \end{aligned} \tag{11}$$

The following solution satisfies the boundary conditions and the equations of motion exactly:

$$\begin{aligned} &u_o(\alpha,\beta,t) = \sum_{m=0}^{M} \sum_{n=0}^{N} U_{mn} \sin(\alpha_m \alpha)\cos(\beta_n \beta), \qquad v_o(\alpha,\beta,t) = \sum_{m=0}^{M} \sum_{n=0}^{N} V_{mn} \cos(\alpha_m \alpha)\sin(\beta_n \beta) \\ &w_o(\alpha,\beta,t) = \sum_{m=0}^{M} \sum_{n=0}^{N} W_{mn} \cos(\alpha_m \alpha)\cos(\beta_n \beta), \qquad \text{where} \quad \alpha_m = \frac{2m\pi}{a}, \beta_n = \frac{2n\pi}{b} \end{aligned} \tag{12}$$

VIBRATIONS OF BARREL SHELLS

Various curvature ratios in the longitudinal direction of the shell are treated including both negative and positive Gaussian curvature. The curvature ratio (a/R_α) along the longitudinal axis varies from -0.5 to 0.5. The ratio +0.5 (with $a/mR_\beta = 0.5$, and m =1) yields a spherical shells that is "chopped" from bottom and top. When a/R_α is taken as zero, a cylindrical shell occurs. The nondimensional frequency parameter $\Omega = \omega R_\beta \sqrt{\rho / E}$ is used. The material properties for graphite/epoxy are:

$E_1 = 20.02 \times 10^6$ psi, $E_2 = 1.3 \times 10^6$ psi, $G_{12} = 1.03 \times 10^6$ psi, $\nu_{12} = 0.3$

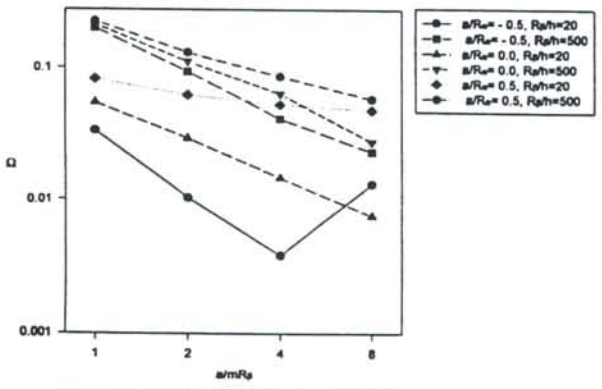

Thickness effects on the fundamental Ω for [0,90] graphite/epoxy closed barrel shells

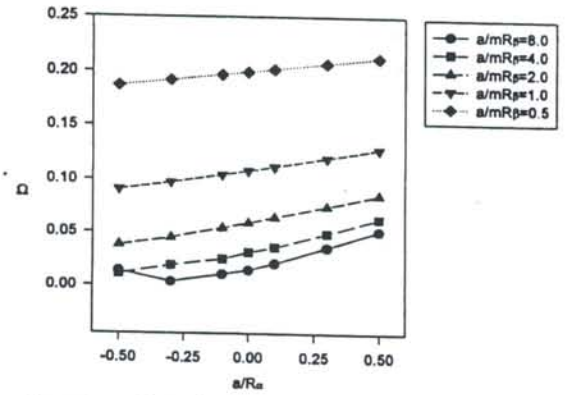

Curvature effects (a/R_α) on the fundamental Ω for [0,90] closed graphite/epoxy barrel shells, $R_\beta/h=100$.

References:

Leissa, A. W., (1973). Vibration of shells. NASA SP388, The government printing office, Washington, D.C.

Noor, A.K., Burton, W.S., and C.W. Bert, 1996. Computational Models for Sandwich Panels and Shells, Applied Mechanics Reviews, Vol. 49, pp. 155-199.

Soedel, W., 1993, Vibrations of Shells and Plates, 2nd Edition, Marcel Dekker.

DYNAMIC BEHAVIOUR OF PRETWISTED COMPOSITE PLATES - A FINITE ELEMENT ANALYSIS

P. K. Sinha and Amit Karmakar
Aerospace Engineering Department
Indian Institute of Technology
Kharagpur - 721 302, INDIA

INTRODUCTION

A cantilever pretwisted plate has significant applications in the turbomachinery, impeller and fan blades. In a weight sensitive application such as aircraft engine turbomachinery, composite materials are advantageous because of their low weight, high stiffness and strength. Structural properties of laminated composites could be tailored to realise high performance by controlling the lamination angle and stacking sequence of comprising layers. In realistic situations, these twisted plate structures have geometrical complexities arising due to their specific applications in various service environments. Certain dynamic parameters are also to be considered when these structural elements are in rotation, and the finite element method is an efficient tool to the designer for the dynamic anlaysis of such type of applications.

Chamis [1] tested HTS/K601 laminated composite [±40/±20/0] blades using holographic technique and compared the test data with the theoretical results obtained using NASTRAN. Qatu and Leissa [2] determined the natural frequencies and mode shapes of laminated cantilevered plates with pretwist using the laminated shallow shell theory in conjunction with the Ritz method. The effects of thickness ratio, pretwist and fibre angle on natural frequencies and mode shapes of three layer, graphite/epoxy and E-glass/epoxy angle ply plates were studied. McGee and Chu [3] carried out three - dimensional continuum vibration analysis for rotating, laminated composite blades using the Ritz method. Full geometric nonlinearity and the Coriolis acceleration term were included in the blade kinematics. Bhumbla and Kosmataka [4] developed the nonlinear finite element techniques using six noded triangular element to study the static deflection and free vibration behavior of spinning pretwisted composite plates.

The present investigation considers the combined effect of skew and precone angle on the vibration characteristics of the three basic laminate configurations viz. bending stiff: $[0_2/\pm30]_s$, quasi-isotropic: $[0/\pm45/90]_s$ and torsion stiff: $[\pm45/\mp45]_s$. The work involves the development of a nine noded 3-D degenerated composite shell element which is used in the finite element formulation for studying the dynamic behaviour of stationary and rotating laminated composite pretwisted cantilever plates because of the fact that this element can model complex geometrical plate behaviour accurately. While most of the studies available in the open literature are for uniform plates and linear pretwist, the cantilever plates with exponentially varying thickness and variable chordwise width have been considered in the present work and vibration characteristics of laminated composite plates are investigated for nonlinear pretwist. A trigonometric increment of pretwist angle along the plate length is considered and the cubic polynomial approximation is assumed for pretwist angle along each elemental length. The effects of shear deformation and rotary inertia are included. This work presents the concise study of the influence on the natural frequencies of parametres such as fibre orientation, aspect ratio, thickness ratio, angle of twist, skew and precone angle that is offset from the normal to the untwisted plate. The

non-dimensional fundamental frequencies furnished are the first known results of the type of analyses carried out here.

THEORETICAL BACKGROUND

The expression for thickness is assumed to be

$$h = h_0 e^{px+qy} \tag{1}$$

The change of variable is obtained from

$$\zeta = -1 + \frac{1}{t}[-h_k(1-\zeta_k) + 2\sum_{j=1}^{k} h_j] \ , \quad d\zeta = (\frac{h_k}{t})\, d\zeta_k \tag{2}$$

where h_k is the thickness of the k th layer.

The element elastic stiffness matrix is given by

$$[K]_e = \sum_{k=1}^{n} \int_{-1}^{1}\int_{-1}^{1}\int_{-1}^{1} [B]^T [D] [B] \det[J] (\frac{h_k}{t})\, d\xi\, d\eta\, d\zeta_k \tag{3}$$

where n is the total number of layers in the laminate.

The differential equation of the rotating plate is of the form

$$[M] \{ \ddot{\delta} \} + ([K] + [K_\sigma]) \{ \delta \} = F(\Omega^2) \tag{4}$$

where $F(\Omega^2)$ is the nodal equivalent centrifugal forces, and $[K_\sigma]$ is the geometric stiffness matrix due to rotation.

RESULTS AND DISCUSSION

The study on the free vibration characteristics of laminated composite non-linearly pretwisted cantilever plates with exponentially varying thickness and variable chordwise width is carried out and salient features are highlighted briefly. Non-linearity in angle of twist has positive effect on the frequency parameters (non-dimensional fundamental frequency per unit weight) apart from satisfying the functional requirement. For higher value of twist angle pronounced design improvement could be obtained. Exponentially varying thickness coupled with the variable chordwise width along spanwise direction leads to substantial increase in fundamental frequency and thereby the geometric configuration is established optimally. Composite plates with higher thickness ratio and lower thickness factor yield in general higher value of non-dimensional fundamental frequencies.

The study is next carried out to investigate the effects of precone angle, skew angle, pretwist, aspect ratio and thickness ratio on natural frequencies corresponding to three different laminate configurations viz. bending stiff: $[0_2/\pm30]_s$, quasi-isotropic: $[0/\pm45/90]_s$ and torsion stiff: $[\pm45/\mp45]_s$. The non-dimensional fundamental frequencies $[\bar{\omega}=\omega_n a^2(\rho/E_1 h_0^2)^{1/2}]$ for graphite/epoxy composite twisted rotating cantilevered plates corresponding to different aspect ratios, thickness ratios and twist angles are obtained. In general, frequency values exhibit a consistent trend with the increase of precone angle from 0^0 to 90^0 for all the laminates. It rises to a maximum value and then drops down to a minimum value at 90^0. The value at $\beta=90^0$ is the fundamental frequency at rest. But for the case of torsion stiff plate of aspect ratio unity and quasi-isotropic laminate of $a/b=3$, $b/h_0=5$ maximum value of non-dimensional frequency occurs corresponding to $\beta=0$ with $\psi=45^0$ and $\phi=45^0$. Lower values of the non-dimensional fundamental

frequencies are obtained due to the combined effect of precone angle and skew angle, for all the laminates analysed corresponding to a particular value of plate thickness. For the twisted plate, it is observed that higher value of skew angle has got pronounced effect on the bending stiff and quasi-isotropic laminates. Corresponding to higher value of the skew angle there is always a decrease in the frequency values with the increase of angle of twist for positive values of precone angle excepting $\beta=90^0$, for the bending stiff and quasi- isotropic laminates. For higher aspect ratio bending stiff and quasi-isotropic laminates provide higher frequency values, but for torsion stiff laminates this is valid only for positive values of precone angle excepting $\beta=90^0$. The influence on non-dimensional fundamental frequencies of thickness parameter (b/h_0) is manifested in higher value with decrease of plate thickness for bending stiff, quasi-isotropic and torsion stiff configurations. The results obtained are the first known non-dimensional frequencies of the different layups (bending stiff, quasi-isotropic and torsion stiff) considered and may serve as the reference solution for future investigations.

REFERENCES

1. Chamis, C. C. 1977. "Vibration Characteristics of Composite Fan Blades and Comparison with Measured Data," J. Aircraft, 14:644-647.
2. Qatu, M. S. and A. W. Leissa. 1991. "Vibration Studies for Laminated Composite Twisted Cantilever Plates," Int. J. Mech. Sc., 33(11):927-940.
3. McGee, O. G. and H. R. Chu. 1994. "Three-dimensional Vibration Analysis of Rotating Laminated Composite Blades," Journal of Engineering for Gas Turbines and Power, Trans. ASME, 116:663-671.
4. Bhumbla, R. and J. B. Kosmatka 1996. "Behavior of Spinning Pretwisted Composite Plates Using a Nonlinear Finite Element Approach," AIAA J., 34(8):1686-1695.

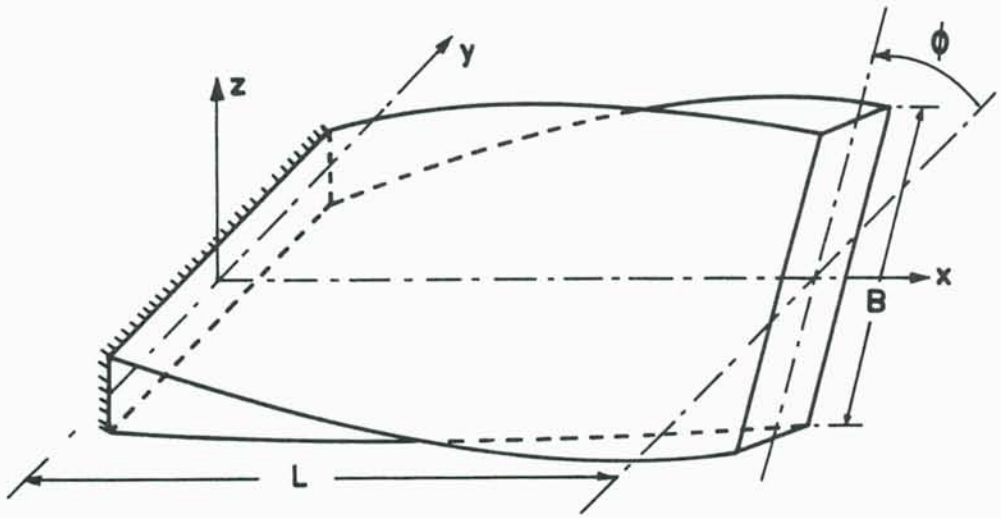

Fig. Twisted Plate.

Inconsistencies between the Vectorial and the Variational Formulation of Classical and Higher-order Shell Theories

Kostas P. Soldatos
Department of Theoretical Mechanics, University of Nottingham, Nottingham NG7 2RD, UK.

The well-known differential equations of motion (or equilibrium) of a classical plate theory (Kirchhoff, 1850; Reissner and Stavsky, 1961) can be obtained, in terms of the conventional force and moment resultants, by using either a variational approach (for instance, Hamilton's principle) or one of two alternative, equivalent, vectorial approaches. The first of these later approaches deals with a geometrical representation of the conventional force and moment resultants, acting on an element of the plate middle-plane, and a subsequent consideration of their balance (Donnell, 1976). In the alternative vectorial approach, considerations dealing with both the introduction and the balance of the conventional force and moment resultants are based on appropriate integration of the equations of motion (or equilibrium) of three-dimensional linear elasticity through the plate thickness. Using any of these approaches in connection with a classical plate theory that involves three unknown displacement functions (degrees of freedom), one obtains, in exactly the same form, three differential equations of motion (or equilibrium). Moreover, all three approaches are still equivalent in dealing with the formulation of the corresponding differential equations of a so-called first-order or uniform shear deformable plate theory (USDT) that involves five degrees of freedom (Reissner, 1945; Mindlin, 1951; Yang *et al*, 1966). Hence, any of these approaches yields, in exactly the same form, five differential equations that reflect the balance of conventional force and moment resultants.

This was found not to be the case for the class of the so-called parabolic shear deformable plate theories that still make use of five degrees of freedom and assume that transverse shear strains are parabolically distributed through the plate thickness (Reissner, 1975; Levinson, 1980; Bhimaraddi and Stevens, 1984; Reddy, 1984; Soldatos, 1988). For such a plate theory (PSDT), a discrepancy was observed between a vectorial and a variational derivation of equations of motion (or equilibrium). In more detail, the conventional vectorial approaches were based on the use of conventional force and moment resultants only. Contrary to this, a variational approach necessitated the introduction of certain additional, higher-order force and moment resultants, the physical meaning of which was not obvious. As a result, for the same or an equivalent displacement approximation, the conventional vectorial approach led to differential equations of motion or equilibrium that were considerably different from those obtained variationally.

A solution to that problem, caused by the discrepancy observed between the vectorial and variational formulations a higher-order plate theory, was given by the new vectorial approach proposed recently (Soldatos, 1993; 1995). In any particular case that deals with a classical or a first-order plate theory, this new, generalised, vectorial approach reduces into the corresponding conventional approach that is based on appropriate integrations of the equations of motion (or equilibrium) of three-dimensional linear elasticity through the plate thickness (Soldatos, 1993). Moreover, this new approach was found suitable for the vectorial formulation of the governing differential equations of all variationally consistent plate theories available in the literature, including the ones that further take transverse normal deformation effects into consideration (Soldatos, 1995).

A corresponding problem, dealing with a "shell-type" variational inconsistency of the conventional vectorial approach was recently addressed in (Soldatos, 1994). This was detected by performing conventional vectorial formulation on the most commonly used first-approximation classical cylindrical shell theories of Love (1927),

Sanders (1959) and Donnell (1933) and, subsequently, by comparing the outcome with the corresponding variational result. The discrepancies observed led to the following conclusions: *(i)* as far as shell-type structures are concerned, the afore-mentioned inconsistency is not connected with the formulation of higher-order, transverse shear deformable theories only but it occurs even in cases dealing with the formulation of classical shell theories; *(ii)* since classical shell theories are long known and widely used in the literature, this inconsistency shell problem is much older than the corresponding plate problem discussed and resolved in (Soldatos, 1993 1995); and *(iii)* in spite the existence of certain relevant vectorial formulations (Herrmann and Mirsky, 1956; Mirsky and Herrmann, 1957), the problem becomes even more complicated with second- or higher-approximation classical shell theories (Flügge, 1960) or in cases that transverse shear deformation effects are involved.

The purpose of this paper is *(i)* to re-address this "shell-type" variational inconsistency; and *(ii)* to extend the applicability of the new approach presented in (Soldatos, 1993; 1995) towards the vectorial formulation of the variationally consistent equations of motion (or equilibrium) of the afore-mentioned first-approximation classical shell theories of Love (1927), Sanders (1959) (also known as best first-approximation theory) and Donnell (1933) (also known as quasi-shallow shell theory). It is emphasised that, dealing with classical shell theories only, this extension lacks the generality of the corresponding flat plate approach presented in (Soldatos, 1993; 1995). It is hoped, however, that it will contribute towards a new constructive debate and, perhaps, towards the solution of the inconsistency problem described in (Soldatos, 1994). For convenience, and in a close connection with (Soldatos, 1994), the new formulation is presented for the relatively simple geometric configuration of a circular cylindrical shell.

The success of the new vectorial approach (Soldatos, 1993; 1995), with regard to this "shell-type" inconsistency problem, is based on the distinction of the independent actions of the middle-surface strains, changes of curvatures and twist, through appropriate rearrangements of the well-known kinematic relations employed in the afore-mentioned classical shell theories. It is further shown that the vectorial derivation attempted is completely successful only within the limits of Love's kinematic approximations. This is due to the fact that the strain-displacement relations employed in either a Donnell-type or a Sanders-type shell theory are obtained in a rather artificial manner, upon suitably altering the corresponding Love-type relations. The Love-type kinematic relations appear therefore to be the only strain-displacement relations that are obtained in a consistent manner on the basis of the displacement approximations employed for the development of a first-approximation classical shell theory.

REFERENCES

Bhimaraddi, A. and Stevens, L.K. (1984) A higher order theory for free vibration of orthotropic, homogeneous and laminated rectangular plates. *J. Appl. Mech.* **51**, 195-198.

Donnell, L. H. (1933) *Stability of Thin-walled Tubes under Torsion*. NACA Report 479.

Donnell, L.H. (1976) *Beams, Plates and Shells*. New York: McGraw-Hill.

Flügge, W. 1960 *Stresses in Shells*. Berlin: Springer.

Herrmann, G. and Mirsky, I. (1956) Three-dimensional and shell-theory analysis of axially symmetric motions of cylinders. *J. Appl. Mech.* **23**, 563-568.

Kirchhoff ,G. (1850) Über das Gleichgewicht und die Bewegung einer elastichen Scheibe. *J. Reine Ang. Math.* **40**, 51-88.

Levinson, M. (1980) An accurate simple theory of the statics and dynamics of elastic plates. *Mech. Res. Comm.* **7**, 343-350.

Love, A.E.H. (1927) *A Treatise on the Mathematical Theory of Elasticity*. 4th edn., Cambridge University Press.

Mindlin, R.D. (1951) Influence of rotatory inertia and shear on flexural vibrations of isotropic elastic plates. *J. Appl. Mech.* **18**, 31-38.

Mirsky, I. and Herrmann, G. (1957) Nonaxially symmetric motions of cylindrical shells. *J. Ac. Soc. Am.* **29**, 1116-1123.

Reddy, J.N. (1984) A simple higher-order theory for laminated composite plates. *J. Appl. Mech.* **51**, 745-752.

Reissner, E. (1945) The effect of transverse shear deformation on the bending of elastic plates. *J. Appl. Mech.* **12**, A69-A77.

Reissner, E. (1975) On transverse bending of plates including the effect of transverse shear deformation. *Int. J. Solids Struct* **11**, 569-573.

Reissner, E. And Stavsky, Y. (1961) Bending and stretching of certain types of heterogeneous aeolotropic elastic plates. *J. Appl. Mech.* **28**, 402-408.

Sanders, J.L. (1959) *An Improved First Approximation Theory for Thin Shells*. NASA Report R-24.

Soldatos, K.P. (1988) On certain refined theories for plate bending. *J. Appl. Mech.* **55**, 994-995.

Soldatos, K.P. (1993) Vectorial approach for the formulation of variationally consistent higher-order plate theories. *Comp. Engng* **3**, 3-17.

Soldatos, K.P. (1994) A question of consistency in the variational and vectorial formulation of dynamic shell theories. *J. Sound Vibr.* **175**, 711-714.

Soldatos, K.P. (1995) Generalisation of variationally consistent plate theories on the basis of a vectorial formulation, *J. Sound Vibr.* **183**, 819-839.

Yang, P.C., Norris, C. and Stavsky, Y. (1966) Elastic wave propagation in heterogeneous plates. *Int. J. Solids Struct.* **2**, 665-684.

Exact Solution for Vibrations of a Combined System Consisting of Multiple Curved and Straight Bars

K. Suzuki
Professor, Faculty of Engineering
Yamagata University
Yonezawa, 992 Japan

INTRODUCTION

The study on vibrations of a combined system consisting of multiple curved and straight bars is of great importance in wide variety of technical applications like earthquake proof design of piping systems of chemical plants, thermal power plants and atomic plants. There exist a number of investigations dealing with the vibrations of curved beams and their combined system (cf. the publication summarized in Chidamparam and Leissa [1]). Suzuki et al [2,3] presented an exact solution procedure for solving free vibrations for a combined system of plane curved bars and straight bars. They obtained the frequency equations by minimizing the Lagrangian of the combined system expressed in quadratic forms of unknown boundary values. But the Lagrangian approach has a fault that the order of determinant becomes higher as the number of joints increases.

In this paper, an exact solution procedure for solving the vibrations of the combined system is presented by making use of the transfer matrix method. The field and the point transfer matrices are formulated by using the exact solutions of each equation of motion for the curved and straight bars. As numerical examples, frequencies of U-bars are presented, and reliability and availavility of the present method are discussed.

ANALYSIS

EQUATIONS OF MOTION FOR IN-PLANE VIBRATION OF A PLANE CURVED BAR

Takahashi et al [4] obtained the equations of motion for in-plane vibrations of a plane curved bar by minimizing the Lagrangian of the system. Let us derive here the equations of motion by considering the equilibrium of the forces and the moments acting on an element of a plane curved bar.

Figure 1 denotes the directions of displacements, forces and moments on an element of a plane curved bar with the arc length ds and the central angle $d\theta$. Let us denote the displacement along tangent on the center line by $\bar{u}$ and that towards the center of curvature by $\bar{v}$. Then the bending moment $\overline{M}_b$, the shearing force $\overline{F}_s$ and the tangential force $\overline{F}_t$ are expressed from Love[5] as follows:

$$\begin{aligned} \overline{M_b} &= -EI\left\{\frac{\partial^2\bar{v}}{\partial s^2}+\frac{\partial}{\partial s}\left(\frac{\bar{u}}{\rho}\right)\right\} \\ \overline{F_s} &= \frac{\partial \overline{M_b}}{\partial s} \\ \overline{F_t} &= EA\left(\frac{\partial\bar{u}}{\partial s}-\frac{\bar{v}}{\rho}\right) \end{aligned} \qquad (1)$$

where EI, EA and $1/\rho$ are the bending rigidity, the longitudinal rigidity and the curvature of centerline, respectively. Consider now the equilibrium of the forces towards the center of curvature and along tangent on the center line and take the equilibrium of the moments with respect to the point m (or n) on the element in Fig.1. Assuming that $\sin(d\theta/2)\fallingdotseq d\theta/2$, $\cos(d\theta/2)\fallingdotseq 1$ and neglecting the small terms of second order, one obtains

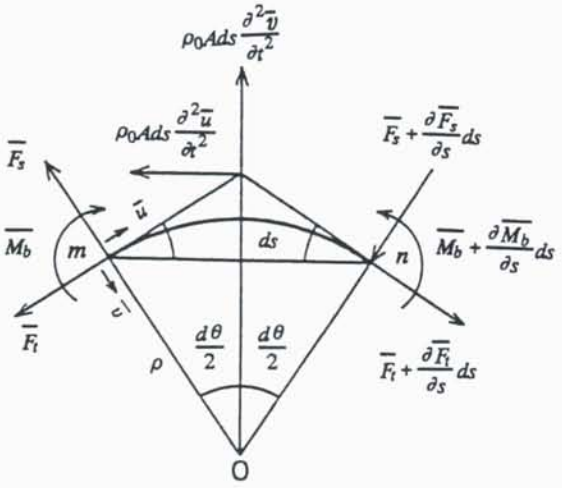

Fig.1 Directions of displacements, forces and moments on an element (In-plane vibration)

$$\rho_0 A\frac{\partial^2\bar{v}}{\partial t^2}-\frac{\partial\bar{F}_s}{\partial s}-\frac{1}{\rho}\bar{F}_t=0$$
$$\rho_0 A\frac{\partial^2\bar{u}}{\partial t^2}-\frac{\partial\bar{F}_t}{\partial s}+\frac{1}{\rho}\bar{F}_s=0 \qquad (2)$$
$$\frac{\partial\bar{M}_b}{\partial s}=\bar{F}_s$$

where ρ_0, A and t are the density, the cross -sectional area and the time, respectively. Equations (2) correspond with those obtained by Takahashi and others [4].

FIELD TRANSFER MATRIX OF A CURVED BAR

For the harmonic vibration, one may assume the solution to Eqs. (2) as:

$$\bar{u}=u(s)\sin(\omega t+\varepsilon)$$
$$\bar{v}=v(s)\sin(\omega t+\varepsilon) \qquad (3)$$

where ω is the circular frequency and ε is an arbitrary phase angle.

The transformation of variable

$$\frac{dx}{ds}=\frac{1}{\rho}=G\Phi(x) \qquad (4)$$

is now introduced, where x is a variable that shows an angle between the tangent at the origin of s and the one at any point on the center line, G is a constant determined by the shape of the curve and $\Phi(x)$ is a qunction of θ. The exact solution to Eqs.(2) can be obtained and the general solutions are expressed in the form [4]

$$u=\sum_{i=1}^{6}C_i\mu_i(x),\quad v=\sum_{i=1}^{6}C_i v_i(x) \qquad (5)$$

where C_1–C_6 are arbitrary constants and $|u_i(x), v_i(x)|_{i=1-6}$ are six independent solutions. By using Eqs.(5), one obtains the field transfer matrix T_{Fn} as follows:

$$Z_{n+1}{}^L=T_{Fn}Z_n{}^R \qquad (6)$$

where T_{Fn} is a matrix of order (6×6) and Z is a state vector, and

$$Z=[u\ \ v\ \ v'\ \ M_b\ \ T_F\ \ S_f\ ]^T$$
$$M_b=-EIG^2\Phi\frac{d}{dx}(\Phi U)$$
$$T_F=EIG^3\Phi\left[(\nu/G\ell)^2W+\Phi\frac{d}{dx}(\Phi U)\right]$$
$$S_f=-EIG\Phi\frac{d}{dx}\left(\Phi\frac{d}{dx}(\Phi U)\right),\quad \nu^2=\frac{A\ell^2}{I}$$
$$v'=G\Phi\frac{dv}{dx},\quad U=\frac{dv}{dx}+u,\quad W=\frac{du}{dx}-v \qquad (7)$$

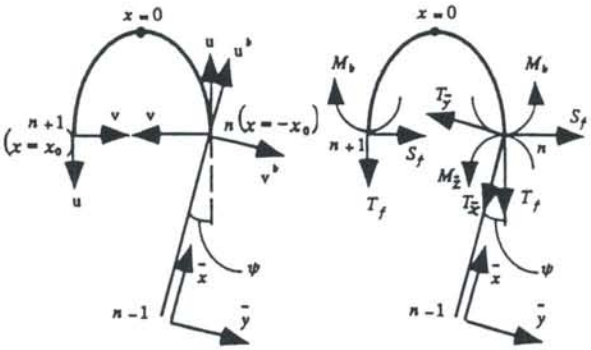

Fig.2 Conditions of Continuity at a connecting point (n) of curved and straight bars

POINT TRANSFER MATRIX

Figure 2 denotes the conditions of continuity at a connecting point (n) of curved and straight bars. Let us take the $\bar{x}$ and $\bar{y}$ axes for a straight bar as shown in Fig.2, and the $\bar{z}$ axis is taken perpendicular to the $\bar{x}$ $\bar{y}$ plane and positive downward. Denote the displacements and the forces in the $\bar{x}$ and $\bar{y}$ directions by (u^b, v^b) and ($T_{\bar{x}}$, $T_{\bar{y}}$), respectively and the rotation angle and the bending moment about the $\bar{z}$ axis by $\theta_{\bar{z}}$ and $M_{\bar{z}}$. Then one has

$$\theta_{\bar{z}}=\frac{dv^b}{dx},\quad M_{\bar{z}}=-EI_{\bar{z}}\frac{d^2v^b}{d\bar{x}^2}$$
$$T_{\bar{x}}=-EA\frac{du^b}{d\bar{x}},\quad T_{\bar{y}}=EI_{\bar{z}}\frac{d^3v^b}{d\bar{x}^3} \qquad (8)$$

The conditions of continuity at the point n are given by the following expression:

$$\begin{bmatrix} u\ (-x_0)\\ v\ (-x_0)\\ \frac{dv}{ds}(-x_0)\\ M_b(-x_0)\\ T_f(-x_0)\\ S_f(-x_0)\end{bmatrix}_R=\begin{bmatrix}\cos\psi & -\sin\psi & 0 & 0 & 0 & 0\\ -\sin\psi & -\cos\psi & 0 & 0 & 0 & 0\\ 0 & 0 & -1 & 0 & 0 & 0\\ 0 & 0 & 0 & 1 & 0 & 0\\ 0 & 0 & 0 & 0 & \cos\psi & -\sin\psi\\ 0 & 0 & 0 & 0 & -\sin\psi & -\cos\psi\end{bmatrix}_n\begin{bmatrix}u^b\\ v^b\\ \theta_{\bar{z}}\\ M_{\bar{z}}\\ T_{\bar{x}}\\ T_{\bar{y}}\end{bmatrix}_L \qquad (9)$$

or

$$Z_n{}^R=T_{pn}Z_n{}^L \qquad (10)$$

Matrix T_{pn} is called a point transfer matrix. From Eqs.(6) and (10), one finds

$$Z_{n+1}{}^L=T_{Fn}T_{pn}Z_n{}^L \qquad (11)$$

Table 1 Comparison among the frequencies α by linear divisions and those by exact solution (In-plane antisymmetric vibration of a semi elliptic arc bar with clamped ends, μ =0.2, ν = 100)

Division \ Mode	1 st	2nd	3rd
4	2.069	4.466	5.968
6	2.053	4.309	6.478
8	2.044	4.291	6.369
10	2.044	4.287	6.357
Exact solution	2.035	4.278	6.345

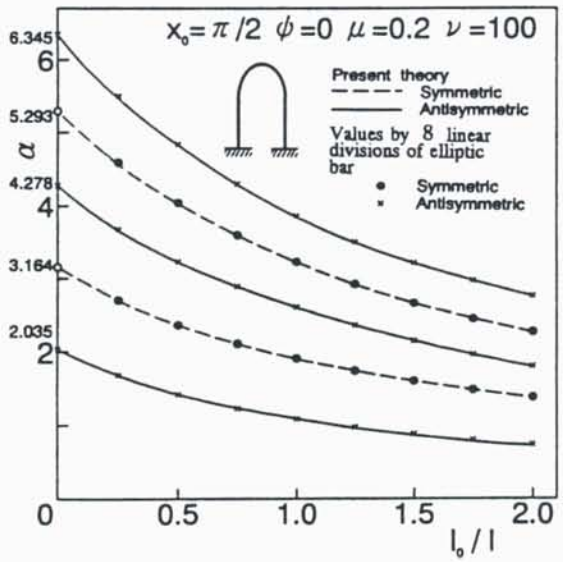

Fig.3 Frequency curves for U-bars of elliptic and straight bars

NUMERICAL EXAMPLES

Numerical studies are made for U-bars with clamped ends consisting of elliptic arc bars and straight bars. All elliptic and curved bars are taken to have equal cross-section and material constant. To show the characteristics of the vibration, the nondimensional frequency parameter α , length ratio l_0/l, ellipticity of curve μ and slenderness ratio ν are used:

$$\alpha^4 = \rho_0 A\omega^2 \ell^4 / EI, \quad \ell = \sqrt{(a^2+b^2)/2}$$
$$\mu = (a^2-b^2)/(a^2+b^2) \qquad (12)$$

where 2*a* and 2b are the major and the minor axes of ellipse, l is the representative radius and l_0 is the length of straight bar.

Table 1 shows the comparison among the frequencies obtained by linear divisions and those by the present method (exact solution) for in-plane antisymmetric vibrations of a semi-elliptic

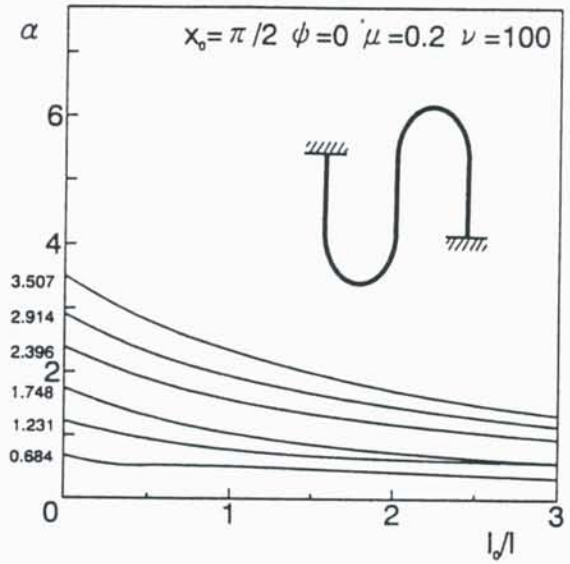

Fig.4 Frequency curves for U-bars of elliptic and straight bars

arc bar with clamped ends.

Figures 3 and 4 show the frequency curves for in-plane vibrations of U-bars consisting of elliptic and straight bars.

REFERENCES

[1] Chidamparam,P. and Leissa,A.W., (1993) Vibrations of planar curved beams, rings and arches, App Mech Rev 43(9), p467-483

[2] Suzuki,K, Asakura,A and Takahashi, S (1979) Vibrations of a connecting system of curved bars (in-plane), Bull JSME 22 (172), p1439-1447

[3] Suzuki,K and Takahashi,S (1979) Vibrations of a connecting system of curved bar (out-of -plane), Bull JSME 22 (172), p1448-1455

[4] Takahashi, S, Suzuki, K, Fukazawa, K and Nakamachi, K (1977) In-plane vibration of elliptic arc bar and sinus curve bar, Bull JSME 20(148), p1236-1243

[5] Love, A. E. H. (1927) A Treatise on the Mathematical Theory of Elasticity, 4th ed., Cambridge Univ. Press, London

Nonlinear Normal Modes in Vibration Theory?

Alexander F. Vakakis, Associate Professor
Department of Mechanical & Industrial Engineering
University of Illinois at Urbana - Champaign
1206 W. Green Street, Urbana, IL 61801

The title of this presentation might seem self-contradictory: Engineers and physicists traditionally associate the concept of 'normal mode' with linear vibration theory and regard it as closely related to the principle of linear superposition. Indeed, in classical linear theory the modes of vibration of continuous system can be used to decouple the equations of motion, and to express arbitrary free or forced oscillations as superpositions of modal responses. The linear modes are computed by solving linear boundary value problems, and obey well-defined orthogonality conditions. Moreover, any forced resonances of a system under external harmonic forces always occur in neighborhoods of normal modes. It is a well known result that the principle of linear superposition generally does not apply in nonlinear systems. Thus, it is obvious to pose the following questions: Can the concept of 'normal mode' be generalized to nonlinear theory, and, if it can, what is its utility since there is no nonlinear principle of superposition?

An obvious definition of a *nonlinear* normal mode (NNM) is an extension of the definition of the normal mode of classical vibration theory. In that context, one defines a NNM of an undamped discrete or continuous system as a synchronous periodic oscillation where all material points of the system reach their extreme values or pass through zero simultaneously. Alternative definitions of NNMs can be found in (Vakakis et al., 1996). It turns out that nonlinear systems can possess more normal modes than their linearized counterparts. This is due to NNM bifurcations which do not exist in linear theory, and which complicate the nonlinear dynamics. Hence, extending linear concepts such as modal analysis to nonlinear systems must be performed with care. In the following we discuss in detail two main applications of NNMs, namely, *their influence on forced resonances* and *nonlinear localization and motion confinement*. Later we summarize new potential areas of applications of NNMs to vibration analysis.

An important property of NNMs relates to forced resonances. *In analogy to linear theory, forced resonances in nonlinear systems occur in neighborhoods of NNMs* (Vakakis et al., 1996). Hence, knowledge of the structure of the normal modes of a nonlinear oscillator can provide valuable insight on the structure of its resonances, a feature of considerable engineering importance. Moreover, since the normal modes of a nonlinear continuous system may exceed in number the modes of its linearized counterpart, certain nonlinear forced resonances may be essentially nonlinear and have no analogs in linear theory; in such cases a 'linearization' of the system either might not be possible, or might not provide all the possible resonances that can be realized.

As an example, we consider the cyclic flexible assembly depicted in Figure 1, consisting of N identical uniform cantilever beams, coupled by means of linear stiffnesses. Assuming beam inextensionality and finite-amplitude oscillations, nonlinear inertia and curvature terms give rise to geometric nonlinearities which, as shown, can affect significantly the dynamic response (King and Vakakis, 1995). The governing equations of motion are of the following form:

$$v_{itt} + v_{ixxxx} + \varepsilon c_i v_{it} + \varepsilon \Big\{ v_{ix}[v_{ix}\, v_{ixx}]_x + \frac{1}{2}\int_l^x \Big[\int_0^s v_{i\xi}^2(\xi,t)\, d\xi \Big]_{tt}\, ds \Big\}_x =$$

$$= -\varepsilon \frac{KL^4}{EI} \{2v_i(l/L) - v_{i-1}(l/L) - v_{i+1}(l/L)\}\, \delta(x-l/L) + \frac{P_i(x,t)}{\varepsilon^{1/2}}\ , \quad i=1,\ldots,N \qquad (1)$$

where K is the nonlinear coupling stiffness, c_i is the coefficient of distributed viscous damping for the i-th beam, $\delta(\bullet)$ is Dirac's function, $P_i(x,t)$ is the distributed excitation applied to the i-th beam,

and $v_0 \equiv v_N$, $v_{N+1} \equiv v_1$ due to cyclicity. It is assumed that the coupling linear stiffnesses and the viscous damping coefficients are small, $O(\varepsilon)$ quantities (with $|\varepsilon|<<1$), and that the beam deflections are of $O(\varepsilon^{1/2})$. It is additionally assumed that the distributed excitations $P_i(x,t)$ possess harmonic time dependence of frequency $(\omega_1 + \varepsilon\sigma)$ and identical spatial distribution to the first linearized cantilever mode of each beam:

$$P_i(x,t) = \Phi_1(x) \cos(\omega_1 + \varepsilon\sigma)t\,, \quad 0 < x < 1, \quad i = 1,...,N \tag{2}$$

In (2), $\Phi_1(x)$ is the spatial distribution and ω_1 the natural frequency of the first linearized cantilever mode of each beam. We consider fundamental resonances, and approximate the steady state responses of the beams as follows (King and Vakakis, 1995):

$$v_i(x,t) = \Phi_1(x)\, a_i \cos[(\omega+\varepsilon\sigma)t+\beta_i] + O(\varepsilon), \quad i = 1,...,N \tag{3}$$

In Figure 2 we depict the fundamental resonance branches of the system with N = 4 beams, and harmonic excitation applied to only beam 1. The coupling stiffness is assigned a value which guarantees the existence of additional NNMs with no counterparts in linear theory. The complicated structure of the resonance curves is caused by NNM bifurcations taking place in the unforced, undamped system, which increase in complexity as the number of beams increases. As many as twelve stable co-existing fundamental resonances can be observed; linear theory would predict the existence of, at most, four resonances.

One of the most interesting applications of NNMs in vibration analysis is *nonlinear mode localization*. By this term we mean the property of a subclass of NNMs to be spatially confined, i.e., to localize to certain areas of a structure. Considering the resonance plots of Figure 2 for the cyclic assembly, we note that the branch 1 of fundamental resonances is *strongly localized* since it corresponds to a response that is mainly confined to the directly forced beam 1. This strongly localized solution occurs in the neighborhood of a localized NNM of the undamped unforced system and has no counterpart in linear theory. There also exist *weakly localized* resonance branches during which the forced beam and adjacent beams oscillate with comparable amplitudes, whereas all other beams undergo much smaller vibrations (branches 7 and 8 in Fig.2). Hence, a basic property of a subclass of NNMs is that they spatially confine vibrational energy, a feature which can find application in vibration and shock isolation designs of mechanical oscillators. The concept of NNM provides a valuable tool for understanding mode localization and motion confinement in nonlinear vibrating systems. In that context, nonlinear mode localization is defined as the spatial confinement of the vibrational energy of a subset of NNMs.

NNMs can find applications in additional areas of vibration theory, including modal analysis and system identification (MA-SI), where traditional techniques for analyzing nonlinear structures are based on the assumptions of weak nonlinearities and of a modal structure similar to that of an underlying linearized system. As shown above, nonlinear systems can have complicated resonances, and in performing nonlinear MA-SI one must consider the possibility that certain of the sought modes are essentially nonlinear, with no counterparts in linear theory. In this context, the concept of NNM can provide a valuable tool for understanding the effects of structural nonlinearities on the dynamics, and for developing a new class of nonlinear MA-SI methodologies that can be used for analyzing practical structures with essential nonlinearities such as, clearances or dry friction.

Additionally, the NNM localization phenomenon can be implemented in novel active or passive vibration isolation designs, where a disturbance generated by external forces is first spatially confined to a predetermined part of a structure, and, then, passively/actively eliminated. Inducing localized NNMs in a flexible structure enhances its controllability, since in designing for active control one needs to consider only a small substructure (where the disturbance is confined) instead of controlling the entire structure; of course, issues of control spill-over and excitation of unwanted modes should also be addressed.

King, M.E., and Vakakis, A.F. (1995). A very complicated structure of resonances in a nonlinear system with cyclic symmetry, *Nonl. Dyn.*, **7**, 85-104.
Vakakis, A.F., Manevitch, L.I., Mikhlin, Yu.V., Pilipchuck, V.N., and Zevin, A.A. (1996). *Normal Modes and Localization in Nonlinear Systems*, J. Wiley & Sons, New York.

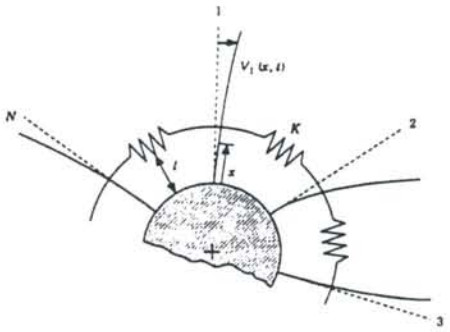

Figure 1. The cyclic assembly of N geometrically nonlinear beams.

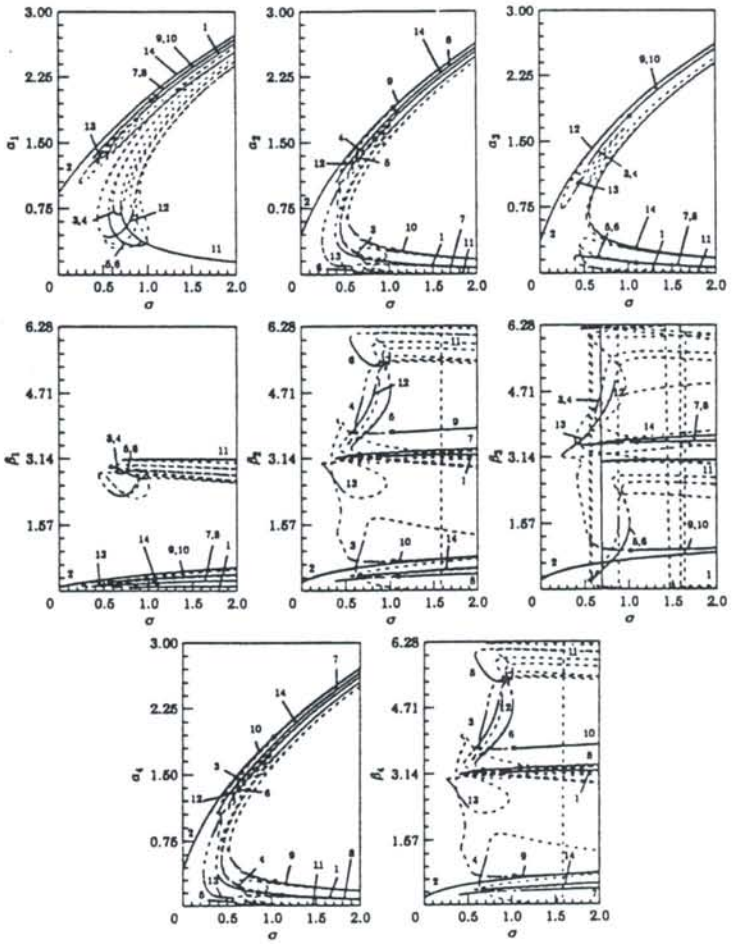

Figure 2. Fundamental resonances for N = 4 beams: —— Stable, ------ Unstable steady states.

Spatially Modulated Vibration Modes in Rotationally Periodic Continuous Systems

M. Kim, J. Moon, and J. A. Wickert
Department of Mechanical Engineering
Carnegie Mellon University
Pittsburgh, PA 15213-3890

Background

Structures that are nearly axisymmetric play important roles in diverse engineering applications, including disk and drum brakes, computer disk drives, gas turbine assemblies, gyroscopes, automotive tires, and power transmission. A rich literature describing the vibration of those particular systems, and of axisymmetric or nearly-axisymmetric models of them, is available and dates at least to early studies by Rayleigh addressing the acoustics of church bells.

To fix ideas, each vibration mode of a solid axisymmetric circular disk is classified (NC, ND) according to the numbers of nodal circles and diameters. Defined by the condition ND = 0, the singlet (or distinct) modes have eigenvalues that are isolated roots of a characteristic equation, and these modes are independent of the angular coordinate. All doublet (or degenerate) modes with ND > 0, on the other hand, occur in pairs with two-fold repeated natural frequencies. Each member of such a pair has either sinusoidal S or cosinusoidal C angular dependence at wavenumber ND, and the mode shape is void of all other harmonics.

Alternatively, if the disk deviates from axisymmetry in that one or more model features varies with angular position, significant changes can occur to the frequency and mode structure, particularly so for the doublets. Of technical interest are configurations in which N features are equally distributed around the disk. While rotationally periodic features do affect the singlet modes, more notable changes occur to the doublets. Frequency splitting has been investigated within the context of various physical systems including bladed disk assemblies, cooling towers, circular rings, automotive tires, slotted sawblades, domain asymmetry, and bolted connections. For some doublets, the natural frequencies split into distinct values when the features are introduced, and criteria are available to predict which modes retain repeated frequencies and which split. In short, when N is an even number, each doublet having ND = m*N/2 for m = 1, 2, 3, ... splits, but when N is odd, the criterion becomes ND = m*N instead. All other doublets persist with repeated frequency.

Mode Shape Modulation

In the light of these changes to the split doublets, the behavior of the repeated ones can appear at first glance to be of secondary concern, or at the very least, less interesting. However, the repeated doublets are susceptible to significant mode modulation which occurs through the superposition of the shape's harmonic at the base wavenumber ND with contaminant harmonics at certain wavenumbers k, which are uniquely determined from ND and N.

In Fig. 1, collocated point transfer functions were measured with two fixtures–axisymmetric clamping, and six evenly-spaced displacement constraints–up to 850 Hz. With six such stiffness features present, doublet modes having one, two, four, or five nodal diameters retained repeated frequencies, but as expected, the three and six nodal diameter doublets split in frequency into their sine and cosine components. Figure 2 shows the measured section taken along a line of constant radius around the disk for the mode that maps asymptotically to (0,4), and which has repeated frequency 335 Hz in Fig. 1. In this case, the maxima and minima are notably modulated, and the mode shape is no longer described by a trigonometric function evaluated at a single wavenumber. When the shape is represented by a classical Fourier expansion, harmonics in addition to the base wavenumber ND = 4 become evident. This "four nodal diameter" mode is noticeably contaminated by the second harmonic, and to lesser degrees by the eighth and tenth.

Modulation Criterion

Vibration of a nominally axisymmetric continuous structure is considered, in which its rotationally periodic character is established through discrete stiffness features. The modulation criterion is developed by perturbation of the structure's eigenvalue problem, wherein the stiffness features are treated as evenly-spaced perturbations to the stiffness operator. The analysis is conducted for both the singlet and doublet modes, with emphasis being on the latter for which modulation is most acute. The treatment of base modes with ND $\neq$ 0 is classical, but it requires that the absolute phases of the doublet's members be chosen relative to the feature pattern such that as the perturbation parameter grows, the eigenfunctions transition smoothly.

Singlet Modes. Each axisymmetric mode becomes distorted by other singlet modes, and by cosine-oriented doublet members having nodal diameters equal to the number of stiffness features, twice it, thrice it, and so forth. The family of sine-oriented modes, and all other cosine modes, do not contaminate the singlets at the first level of approximation.

Doublet Modes. Either because of symmetry or normalization requirements, the base S and C members do not contribute to their own, or to each other's, first-order correction. That is, prospective contamination occurs at k $\neq$ ND. Recognizing that (i) the discrete features are equally-spaced with certain symmetries relative to the sine and cosine mode components, (ii) the unperturbed mode shape is harmonic at wavenumber ND, and (iii) the mode shape distortion is also harmonic but at different wavenumbers, evaluation of the requisite inner products in the calculation lead to the following guideline for predicting spatial modulation: *If any of the equalities* $| ND \pm k | = N, 2N, 3N, \ldots$ *is satisfied, the harmonic S and C base modes will become contaminated by the doublet member having wavenumber k and like symmetry.* In Fig. 3, for instance, the "five nodal diameter mode" of the disk with six constraints has modulation at k = 1 and 7.

Depending on the values taken by the natural frequencies, and the projections of the base modes onto the stiffness operator, particular k will contaminate the base mode to a greater extent than others. Of course, numerical values for the contamination coefficients can be calculated for a specified structural model and feature distribution, but for the purposes of predicting and interpreting measured spatial modulation, this criterion is useful to identify which distorting harmonics are expected to be present.

With N = 6, therefore, the criterion predicts that the doublet which is asymptotic to (0,4) in the axisymmetric limit becomes contaminated by wavenumbers 2, 8, 10, ... Figure 4 graphically represents the wavenumbers that contribute to each doublet's distorted shape. For a specified number of nodal diameters in the base mode, the wavenumbers depicted as shaded blocks contribute to the perturbed modes as the features are gradually introduced to the structure. Such checkerboard diagrams are constructed from diagonals of unity slope which emanate from points N, 2N, 3N, ... on both axes. Also shown is the main diagonal which indicates the Fourier content of the base modes.

Conclusion

It is expected that spatial modulation has implications for the engineering of rotating machine components. In some turbomachinery applications, structures are excited in vibration by a hydro- or aerodynamic load that has spatial distribution established by the periodic geometry of stationary components. The distribution of such loads can be spatially periodic with wavelength dependent on, for instance, the number of stator vanes in a compressor stage. To the degree that the load's corresponding Fourier decomposition comprises multiple harmonics, it will have non-vanishing projection onto any mode with one or more like wavenumbers. All other vibration modes remain orthogonal and, in principle, quiescent in response. With a view towards identifying resonant operating conditions, a spatially modulated mode can be driven by loads with Fourier content at ND, as well as at other contaminating k.

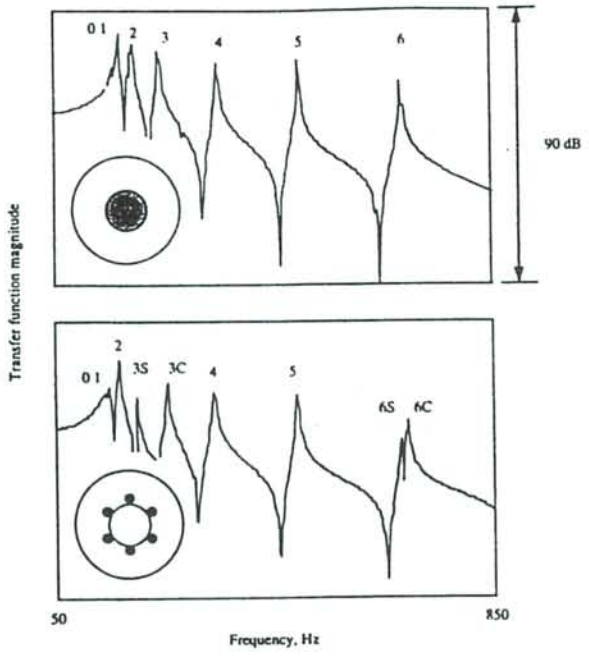

Figure 1: Measured collocated transfer functions of the disk with nominally clamped-free boundary conditions (upper), and with six equally-spaced displacement and slope constraints around the inner edge (lower). Values of ND, and the sine or cosine orientation of the split modes, are indicated.

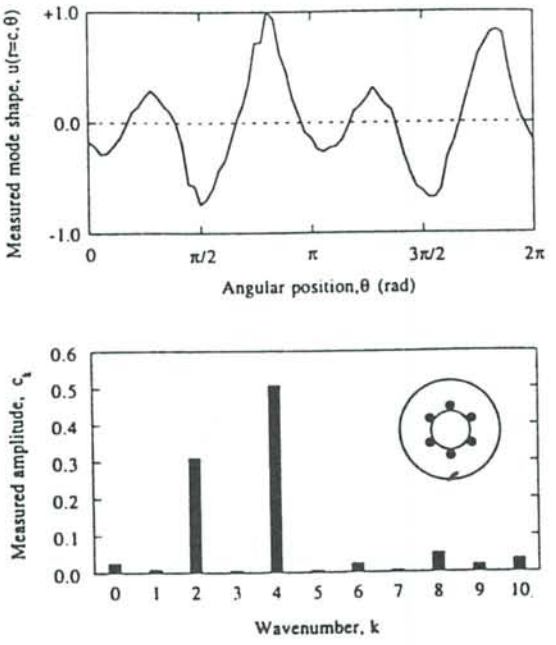

Figure 2: Measured mode shape of the disk which illustrates spatial modulation; N = 6 stiffness features. This mode has repeated natural frequency, and is asymptotic to (0,4) as the displacement and slope constraints are removed. As indicated by the Fourier decomposition, significant contamination occurs at k = 2.

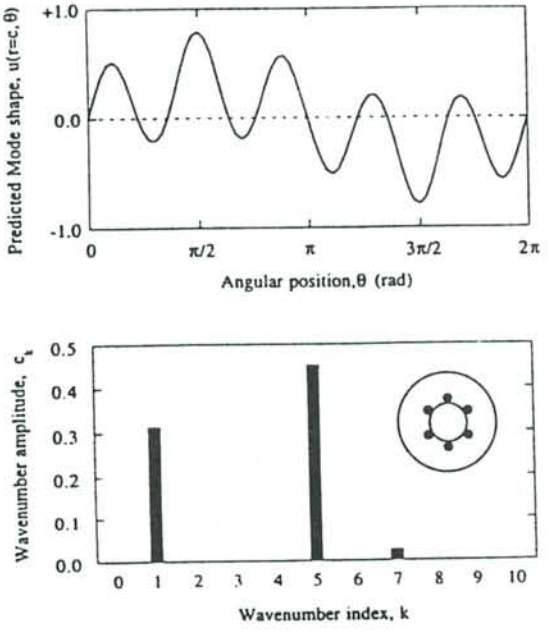

Figure 3: Predicted antisymmetric mode shape which is asymptotic to (0,5)S; N = 6 stiffness features. The symmetric companion has repeated frequency, but it is not shown here for clarity. Contamination occurs at k = 1, and to a lesser degree at k = 7.

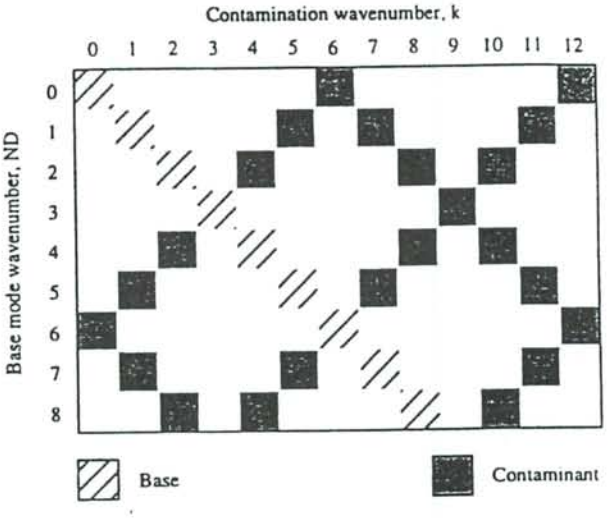

Figure 4: Checkerboard diagram depicting the contamination wavenumbers for each base mode in the presence of six features.

Applications of an efficient free vibration root counting algorithm for dynamic stiffness matrix methods

F W Williams
School of Engineering, University of Wales Cardiff, Cardiff CF2 3TB, U.K.

Because of the nature of this paper it considers only the author's own use of the algorithm of eqn (1), of which he was co-originator [1,2], and which counts J, the number of natural frequencies below any trial frequency, without finding them.

$$J=J_0+ s\{\mathbf{K}\} \qquad (1)$$

Here: **K** = dynamic stiffness matrix; s{**K**}= number of negative leading diagonal elements after Gauss elimination has been applied to **K**; and J_0= value J would have if all freedoms of **D**, the displacement vector to which **K** corresponds (so **KD=0** for free vibrations) were to be clamped.

The algorithm can be used to: converge iteratively on natural frequencies [1], to obtain modal densities [3], or to re-design to move inconveniently situated natural frequencies [4]. A good mode finding method able to separate coincident modes was also developed [5] and refined [6].

Multi-level substructuring extensions and applications of the algorithm have been a continuous thread of work [7, 8, 9]. The algorithm has also been extended to : proper use of symmetry [10]; rotationally periodic structures and substructures [9], including stayed columns [11]; to problems for which Lagrangian multipliers are used [12, 13]; and to spinning structures [14].

Applications have included plane frames [1, 15], optionally with Timoshenko effects [15, 16], taper [17], elastic foundations [18] and flexural-torsional coupling [19]. Listings have been published [20, 15]. This work has also been extended to space frames, for which the large program BUNVIS-RG exists [21, 22].

Prismatic assemblies of plates (e.g. aircraft wing panels) were included from the beginning [2, 23] and optionally include laminated materials [8], through thickness shear deformation[24] and wave propagation [25]. The 50K line software VICONOPT has resulted [26].

Faster solutions have been obtained by : improving the Gauss elimination [27]; improving the iterative convergence method used to choose the values of frequency at which J is computed [28, 29]; using linear [30] or quadratic matrix pencils locally [31] during convergence; and using parallel computers [32, 33].

References

1. Williams, F.W. & Wittrick, W.H., "An automatic computational procedure for calculating natural frequencies of skeletal structures", *Int. J. Mech. Sci.*, 12, 1970, p 781.
2. Wittrick, W.H. & Williams, F.W., "Natural vibrations of thin, prismatic, flat-walled structures", IUTAM Symposium, Liège, Aug., 1970, p 563.
3. Williams, F.W. & Banerjee, J.R., "Accurately computed modal densities for panels and cylinders, including corrugations and stiffeners", *J. Sound Vib.*, 93, 1984, p 481.
4. Williams, F.W., "Rapid analysis of the effects of structural modifications on inconveniently situated eigenvalues", *Comp. & Struc.*, 3, 1973, p 1465.
5. Hopper, C.T. & Williams, F.W., "Mode finding in non-linear structural eigenvalue calculations", *J. Struc. Mech.*, 5, 1977, p 255.
6. Ronagh, H.R., Lawther, R. & Williams, F.W., "Calculation of eigenvectors with uniform accuracy", *J. Eng. Mech., ASCE*, 121, 1995, p 948.
7. Williams, F.W., "Natural frequencies of repetitive structures", *Q. J. Mech. Appl. Math.*, 24, 1971, p 285.
8. Wittrick, W.H. & Williams, F.W., "Buckling and vibration of anisotropic or isotropic plate assemblies under combined loadings", *Int. J. Mech. Sci.*, 16, 1974, p 209.
9. Williams, F.W., "Exact eigenvalue calculations for structures with rotationally periodic substructures", *Int. J. Num. Meth. Eng.*, 23, 1986, p 695.
10. Williams, F.W., "A warning on the use of symmetry in classical eigenvalue analyses", *Int. J. Num. Meth. Eng.*, 12, 1978, p 379.
11. Banerjee, J.R. & Williams, F.W., "Evaluation of efficiently computed exact vibration characteristics of space platforms assembled from stayed columns", *J. Sound Vib.*, 95, 1984, p 405.
12. Williams, F.W. & Anderson, M.S., "Incorporation of Lagrangian multipliers into an algorithm for finding exact natural frequencies or critical buckling loads", *Int. J. Mech. Sci.*, 25, 1983, p 579.
13. Powell, S.M., Kennedy, D. & Williams, F.W., "Efficient multi-level substructuring with constraints for buckling and vibration analysis of prismatic plate assemblies", *Int. J. Mech. Sci.*, 39, 1997, p 795.
14. Wittrick, W.H. & Williams, F.W. "On the free vibration analysis of spinning structures by using discrete or distributed mass models", *J. Sound Vib.*, 82, 1982, p 1.
15. Howson, W.P., Banerjee, J.R. & Williams, F.W., "Concise equations and program for exact eigensolutions of plane frames including member shear", *Adv. Eng. Software*, 5, 1983, p 137.
16. Howson, W.P. & Williams, F.W., "Natural frequencies of frames with axially loaded Timoshenko members", *J. Sound Vib*, 26, 1973, p 503.
17. Banerjee, J.R. & Williams, F.W., "Exact Bernoulli-Euler dynamic stiffness matrix for a range of tapered beams", *Int. J. Num. Meth. Eng.*, 21, 1985, p 2289.
18. Capron, M.D. & Williams, F.W., "Exact dynamic stiffnesses for an axially loaded uniform Timoshenko member embedded in an elastic medium", *J. Sound Vib*, 124, 1988, p 453.
19. Banerjee, J.R. & Williams, F.W., "Coupled bending-torsional dynamic stiffness matrix for Timoshenko beam elements", *Comp. & Struc.*, 42, 1992, p 301.
20. Williams, F.W. & Howson, W.P., "Compact computation of natural frequencies and buckling loads for plane frames", *Int. J. Num. Meth. Eng.*, 11, 1977, p 1067.

21. Anderson, M.S. & Williams, F.W., "Natural vibration and buckling of general periodic lattice structures", *AIAA J.*, 24, 1986, p 163.
22. Anderson, M.S. & Williams, F.W., "BUNVIS-RG: Exact frame buckling and vibration program, with repetitive geometry and substructuring", *J. Spacecraft and Rockets*, 24, 1987, p 353.
23. Williams, F.W., "Computation of natural frequencies and initial buckling stresses of prismatic plate assemblies", *J. Sound Vib.*, 21, 1972, p 87.
24. Williams, P.W.L., Williams, F.W. & Kennedy, D., "Inclusion of transverse shear deformation in optimum design of aircraft wing panels", *AIAA J.*, 34, 1996, p 2456.
25. Williams, F.W., Ouyang, H.J., Kennedy, D. & York, C.B., "Wave propagation along longitudinally periodically supported or stiffened prismatic plate assemblies", *J. Sound Vib.*, 186, 1995, p 197.
26. Kennedy, D., Williams, F.W. & Anderson, M.S., "Buckling and vibration analysis of laminated panels using VICONOPT", *J. Aerospace Eng. ASCE,* 7, 1994, p 245.
27. Williams, F.W. & Kennedy, D., "Fast Gauss-Doolittle matrix triangulation", *Comp. & Struc.*, 28, 1988, p 143.
28. Kennedy, D. & Williams, F.W., "More efficient use of determinants to solve transcendental structural eigenvalue problems reliably", *Comp. & Struc.*, 41, 1991, p 973.
29. Williams, F.W. & Kennedy, D., "Accelerated solutions for transcendental stiffness matrix eigenproblems", *Shock and Vib*, 3, 1996, p 287.
30. Hopper, C.T., Simpson, A. & Williams, F.W., "A study of the bounds on eigenvalues of a transcendental dynamic stiffness matrix provided by a simply derived linear matrix pencil", *J. Struc. Mech.,* 8, 1980, p 365.
31. Ye, J. & Williams, F.W., "A successive bounding method to find the exact eigenvalues of transcendental stiffness matrix formulations", *Int. J. Num. Meth. Eng.,* 38, 1995, p 1057.
32. Kennedy, D., Watkins, W.J. & Williams, F.W., "Hybrid parallel computation of transcendental structural eigenvalues", *AIAA J.*, 33, 1995, p 2194.
33. Watkins, W.J., Kennedy, D. & Williams, F.W., "On estimating machine dependency of fine- and coarse-grain parallel structural computations", *Microcomp. in Civ. Eng.*, 12, 1997, p 119.

FREE VIBRATION OF SPINNING ANGLE-PLY LAMINATED CIRCULAR CYLINDRICAL SHELLS

Gen YAMADA, Yukinori KOBAYASHI and Takashi YAMAGUCHI
Division of Mechanical Science, Hokkaido University, Sapporo, 060, Japan

INTRODUCTION

An analysis is presented for free vibrations of spinning angle-ply laminated circular cylindrical shells having any combination of boundary conditions. The governing equations and the boundary conditions of the shell are derived by applying Hamilton's principle to the strain and kinetic energies of the shell in consideration of the second order terms of strains. The equations of motion are separated into the quasi-static components and dynamic ones. The deformed state under the steady rotation is determined numerically from the quasi-static equation, and the dynamic equations of the vibration are solved by using the modified Galerkin's method. In numerical examples, the natural frequencies of the spinning angle-ply circular cylindrical shells are calculated, and effects of lamination parameters and boundary conditions on the free vibration are studied.

ANALYSIS

Figure 1 shows a circular cylindrical shell of the axial length L, thickness H and constant spinning speed Ω, and the radius from the center axis to the middle surface is denoted by R. The coordinates $(x,\ \theta,\ z)$ and the displacements $u,\ v,\ w$ in the middle surface of the shell are taken as shown in the figure.

The strain energy of the spinning shell is derived by considering nonlinear terms due to large deformation, in the normal and shear strains. And the kinetic energy T of it is expressed as

$$T = \frac{R}{2}\int_x\int_\theta \rho H\left[\left(\frac{\partial u}{\partial t}\right)^2 + \left\{\frac{\partial v}{\partial t} + (R+w)\Omega\right\}^2 + \left(\frac{\partial w}{\partial t} - v\Omega\right)^2\right] d\theta dx \tag{1}$$

where ρ is the density of the shell.

The displacements can be written as the sum of the quasi-static components which are independent of time and the dynamic ones. The quantities marked with $\overline{\ }$ are the dimensionless quasi-static variables and those with $\sim$ are dimensionless dynamic ones.

$$\frac{u}{R} = \overline{u} + \tilde{u}\ ,\quad \frac{v}{R} = \overline{v}\ ,\quad \frac{w}{R} = \overline{w} + \tilde{w} \tag{2}$$

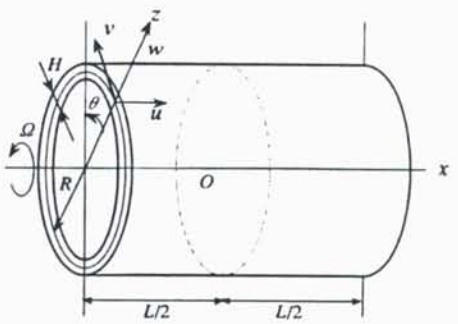

Fig.1 Spinning cylindrical shell and its coordinate systems

In this paper, the nondimensional displacements are approximated by the following functions

$$\begin{aligned}
&\overline{u}(\xi) = \sum_{i=1}^{I} \overline{U}_i X_{1i}(\xi), \quad \overline{w}(\xi) = \sum_{i=1}^{I} \overline{W}_i X_{3i}(\xi) \\
&\widetilde{u}(\xi,\theta,t) = \sum_{i=1}^{I}\sum_{j=1}^{J} \widetilde{U}_{ij} X_{1i}(\xi) Y_j(\theta) e^{i\lambda t}, \quad \widetilde{v}(\xi,\theta,t) = \sum_{i=1}^{I}\sum_{j=1}^{J} \widetilde{V}_{ij} X_{2i}(\xi) Y_j(\theta) e^{i\lambda t} \\
&\widetilde{w}(\xi,\theta,t) = \sum_{i=1}^{I}\sum_{j=1}^{J} \widetilde{W}_{ij} X_{3i}(\xi) Y_j(\theta) e^{i\lambda t}
\end{aligned} \tag{3}$$

where

$$X_{mi}(\xi) = \xi^{i-1}(1+\xi)^{\alpha_m}(1-\xi)^{\beta_m}, \quad Y_j(\theta) = \begin{cases} \cos n\theta & (j=1) \\ \sin n\theta & (j=2) \end{cases} \tag{4}$$

and n is the circumferential wave number. The quantities $\overline{U}_i$, $\overline{W}_i$, $\widetilde{U}_{ij}$, $\widetilde{V}_{ij}$, $\widetilde{W}_{ij}$ are unknown coefficients. And the exponents α_m, β_m in the admissible functions $X_{mi}(\xi)$ are boundary indicies introduced such that the displacement functions (3) automatically satisfy given boundary conditions. For the simplicity of the analysis, the following parameters are also introduced.

$$\xi = \frac{x}{(L/2)}, \quad \eta = \frac{z}{R}, \quad (l, h) = \frac{1}{R}(L, H), \quad \Omega^{*2} = \frac{\rho R^2 \Omega^2}{E_2}, \quad \lambda^2 = \frac{\rho R^2 \omega^2}{E_2} \tag{5}$$

Here, ω is the angular frequency of the system.

By substituting Eqs.(3) into the strain energy equation and Eq.(1), and applying Hamilton's principle to the Lagrange functional L, the governing equations and boundary conditions of the spinning shell are derived. The equations of motion and the boundary conditions for the steady state spinning shell are obtained by neglecting all the dynamic components, and those for the free vibration of the shell are also introduced by neglecting only the quasi-static components. Here, only the first order terms of strain are considerd. By applying the modified Galerkin's method to the equations of motion for quasi-static state, simultaneous equations are obtained for detemining the quasi-static state. The quasi-static displacements $\overline{u}$, $\overline{w}$ are determined by solving these equations.

The equations of free vibration of shells are also derived by using the similar procedure.

$$\overline{N}_x \frac{\partial^2 \widetilde{u}}{\partial \xi^2} + \frac{\partial \widetilde{N}_x}{\partial \xi} + \overline{N}_\theta \frac{\partial^2 \widetilde{u}}{\partial \theta^2} + 2\overline{N}_{x\theta} \frac{\partial^2 \widetilde{u}}{\partial \xi \partial \theta} + \frac{\partial \widetilde{N}_{x\theta}}{\partial \theta} + h\lambda^2 \widetilde{u} = 0 \tag{6}$$

$$\begin{aligned}
&\overline{N}_x \frac{\partial^2 \widetilde{v}}{\partial \xi^2} + \overline{N}_\theta \left(\frac{\partial^2 \widetilde{v}}{\partial \theta^2} + 2\frac{\partial \widetilde{w}}{\partial \theta} - \widetilde{v} \right) + \frac{\partial \widetilde{N}_\theta}{\partial \theta} + 2\overline{N}_{x\theta} \left(\frac{\partial^2 \widetilde{v}}{\partial \xi \partial \theta} + \frac{\partial \widetilde{w}}{\partial \xi} \right) \\
&+ \frac{\partial \widetilde{N}_{x\theta}}{\partial \xi} + \frac{\partial \widetilde{M}_\theta}{\partial \theta} + \frac{\partial \widetilde{M}_{x\theta}}{\partial \xi} + h\left(\lambda^2 \widetilde{v} - 2\Omega^* \lambda i \widetilde{w} + \Omega^{*2} \widetilde{v} \right) = 0
\end{aligned} \tag{7}$$

$$\begin{aligned}
&\overline{N}_x \frac{\partial^2 \widetilde{w}}{\partial \xi^2} - \widetilde{N}_\theta + \overline{N}_\theta \left(\frac{\partial^2 \widetilde{w}}{\partial \theta^2} - 2\frac{\partial \widetilde{v}}{\partial \theta} - \widetilde{w} \right) + 2\overline{N}_{x\theta} \left(\frac{\partial^2 \widetilde{w}}{\partial \xi \partial \theta} - \frac{\partial \widetilde{v}}{\partial \xi} \right) \\
&+ \frac{\partial^2 \widetilde{M}_x}{\partial \xi^2} + \frac{\partial^2 \widetilde{M}_\theta}{\partial \theta^2} + +2\frac{\partial^2 \widetilde{M}_{\xi\theta}}{\partial \xi \partial \theta} + h\left(\lambda^2 \widetilde{w} + 2\Omega_* \lambda i \widetilde{v} + \Omega^{*2} \widetilde{w} \right\} = 0
\end{aligned} \tag{8}$$

Here, the derivatives of force and moment resultants $\overline{N}_x$,$\overline{N}_\theta$, $\overline{N}_{x\theta}$,$\overline{M}_x$,$\overline{M}_\theta$, $\overline{M}_{x\theta}$ are neglected due

to the small quantities. The products of the quasi-static terms, which are the second order terms of strains, and the dynaminc terms are also neglected.

By applying the modified Galerkin's method to the equations of motion (6)~(8) for the free vibration of the shell and the boundary conditions, the frequency equation can be derived. And the natural frequencies of spinning angle-ply laminated circular cylindrical shells are determined by solving the frequency equation.

NUMERICAL RESULTS AND DISCUSSIONS

By using the scheme described before, a numerical calculation is carried out for angle-ply laminated circular cylindrical shells having small thickness ratio (h=0.02). A graphite/epoxy, which is a highly orthotropic fiber-reinforced material, is selected, the material properties used here are E_1 =138GPa, E_2 =8.96GPa, G_{12} =7.10GPa, ν_{12} =0.3 (subscript 1 denotes the major material-symmetry direction, subscript 2 denotes the in-plane transverse direction). The layer sequence is described, for example, as (α, - α) from inner to outer lamina of the shell.

Table 1 shows the convergence characteristics of eigenvalues of vibration λ of the simply-supported, double layered ($45°/-45°$) circular cylindrical shell. The letters (f) and (b) correspond to forward and backward waves, respectively. As shown in Table 1, the parameters converge within 4 significant digits by taking I=12 terms, therefore the following calculations are made by using 12 terms.

Figure 2 presents the eigenvalues of vibration λ versus the dimensionless spinning angular velocity Ω for a simply-supported, double layered shell ($45°/-45°$). The eigencurves show the lowest eigenvalues of each circumferential wave number n (attached to curves) for the backward and forward waves by solid and dotted lines, respectively. The eigenvalues of vibration for the backward wave increase with an increase of the spinning velocity of the shell.

Table 1 Convergence characteristics of frequency parameters of a simply-supported, angle-ply laminated cylindrical shell
($45°$ / $-45°$) , $l = 2$, $h = 0.02$, $n = 2$

Ω^*	I			
	8	10	12	13
0.0	0.8693	0.8691	0.8690	0.8690
0.1 (f)	0.7948	0.7945	0.7945	0.7945
0.1 (b)	0.9581	0.9578	0.9578	0.9578
0.2 (f)	0.7342	0.7339	0.7339	0.7339
0.2 (b)	1.061	1.061	1.061	1.061

(f) : forward (b) : backward

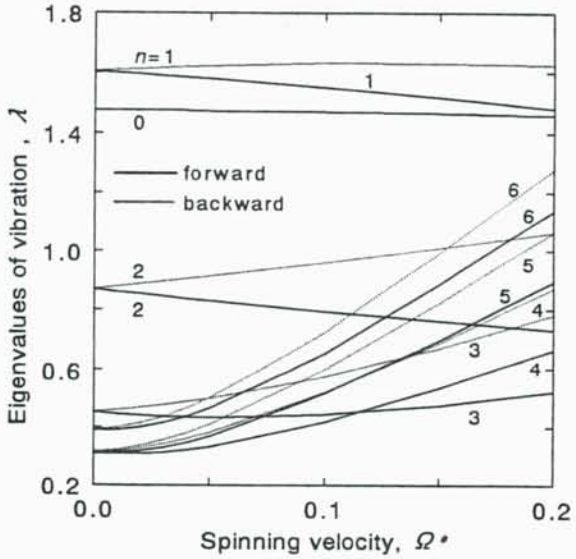

Fig.2 Eigenvalues of vibration for a spinning shell simply-supported at both ends, ($45°$ / $-45°$), h=0.02, l=2.0

STABILITY OF FLUTTERED BEAMS SUBJECTED TO CIRCULATORY RANDOM FORCES

By
T. H. Young, Professor
and
C. C. Jen, Graduate Student
Department of Mechanical Engineering
National Taiwan Institute of Technology
Taipei, Taiwan, R.O.C.

1. INTRODUCTION

Engineering structures are often subjected to circulatory forces. Such forces may be generated by air flows, jet propulsion and thermal stresses, etc.. Numerous research works deal with this kind of problems [1–4]. When the magnitude of the static circulatory force is below a certain value, all the natural frequencies of the structure remain positive and distinct, and the system is stable. As the magnitude of the force reaches a critical value, one of the natural frequencies drops to zero or two of the natural frequencies close up and coalesce, and the system becomes unstable at this instant. The former is said to be buckling instability, while the latter is said to be flutter instability.

When a structure subjected to static circulatory forces is fluttered, additional force perturbation may stabilize the structure. Fu and Nemat–Nasser [5] first found that a beam subjected to critical follower and harmonic forces may remain stable. Recently Young and Chen [6] also showed that a panel subjected to super– critical aerodynamic and in–plane harmonic forces can be stable in certain situations. Therefore, this work will study the stability of a fluttered beam subjected to a follower random force. The force is assumed as a zero–mean, low–intensity white noise.

2. THEORETICAL ANALYSIS

A cantilever beam of length l is subjected to a follower static and random force, as shown in Figure 1. The random force $P_1(t)$ is assumed as a zero–mean, low–intensity Gaussian white noise. By the classical beam theory, the equation of motion and the corresponding boundary conditions can be derived. To satisfy all the geometric boundary conditions, the displacement w is assumed as

$$w(x,\ t)= \Sigma_{n=1}^{N}\ q_n(t)\left(\frac{x}{l}\right)^{n+1} \tag{1}$$

where q_n are generalized coordinates in time t. By applying the extended Galerkin method and carrying out the integrations exactly yields a set of ordinary differential equations in time, This set of equations can be rewritten into a set of the first–order differential equations as

$$[M^*]\dot{x} + [K^*]x = -P_1(t)[F_1^*]x, \tag{2}$$

where $$[M^*]= \begin{bmatrix}[M] & [0]\\ [0] & [I]\end{bmatrix}, \qquad [K^*]= \begin{bmatrix}[C] & ([K] + P_0[F_0])\\ -[I] & [0]\end{bmatrix},$$

$$[F_1^*]=\begin{bmatrix}[0] & [F_1]\\ [0] & [0]\end{bmatrix}, \qquad \text{and } \mathbf{x}=\begin{bmatrix}\dot{\mathbf{q}}\\ \mathbf{q}\end{bmatrix},$$

in which [I] is an identity matrix, [M], [C] and [K] are the mass, damping and stiffness matrices, respectively, and [F] is the force matrix, which is asymmetirc because the static force P_o is nonconservative.

Assume that, without the random excitation, this is a circulatory system, that is, the system will first yield to flutter instability as the static follower force reaches a critical value P_{cr}. It is observed that at the onset of fluttering, i.e., $P_o = P_{cr}$, one of the damping ratios is equal to zero, and this mode is refered to as the critical mode. Therefore, introduce a linear transform

$$\begin{bmatrix}\dot{\mathbf{q}}\\ \mathbf{q}\end{bmatrix} = [\mathbf{b}_1, \mathbf{c}_1, \ldots, \mathbf{b}_N, \mathbf{c}_N]\mathbf{u} \tag{3}$$

where $\mathbf{u}$ is a $2N\times 1$ column matrix, and $\mathbf{b}_n$ and $\mathbf{c}_n$ are the real and imaginary parts of the right eigenvectors $\mathbf{x}_n$, respectively. Substituting equation (3) into equation (2), using the critical configuration as the reference, premultiplying the matrix $[\mathbf{d}_1, \mathbf{e}_1, \ldots, \mathbf{d}_N, \mathbf{e}_N]^T$, where $\mathbf{d}_n$ and $\mathbf{e}_n$ are the real and imaginary parts of the left eigenvectors $\mathbf{y}_n$, respectively, and utilizing the biorthogonality of the right and left eigenvectors yields a set of pairwisely uncoupled equations. The solutions of this set of equations are assumed as

$$u_{2n-1} = a_n e^{-\zeta_n \omega_n t}\cos(\omega_n t + \phi_n), \qquad u_{2n} = -a_n e^{-\zeta_n \omega_n t}\sin(\omega_n t + \phi_n)$$
$$n = 1, 2, \ldots, N \tag{4}$$

If the damping rations ζ_n and the load ratio $\eta = (P_o - P_{cr})/P_{cr}$ are small, and if the random excitation $P_1(t)/P_{cr}$ is a white noise of intensity K, the stochastic avergaing procedure may be used, and (a_1, ϕ_1) can be uniformly approximated in the weakly sense by a Markov difusion process. The Lyapunov exponent of the critical mode defined as

$$\lambda = \lim_{T\to\infty} \frac{1}{T}\ln a_1, \tag{5}$$

which can be obtained from the Ito equation for a_1. If the Liapunov exponent is negative, the critical mode is always bounded. Therefore, the criterion for the asymptotic sample stability of the system is that this Liapunov exponent is negative.

3. NUMERICAL EXAMPLE

The asymptotic sample stability boundary of a fluttered cantilever beam subjected to a follower random force are illustrated in Figure 2. The figure shows that with the presence of the random follower excitation, the beam may remain stable even when the static follower force has exceeded its critical value. Moreover, the effect of the viscous damping makes the stability boundary to shift to the right and makes it steeper.

4. CONCLUDING REMARKS

An analysis of the stability of fluttered beams subjected to follower random forces has been presented in this work. The random force is characterized as a small–intensity white noise. Numerical results show that due to this random follower excitation, the beam may remain stable even if the static follower force has exceeded

its critical value.

REFERENCES

[1] Bolotin, V. V., 1963, *Nonconservative Problems of the Theory of Elastic Stability*, Pergamon Press Ltd., Oxford.

[2] Ziegler, H., 1977, *Principles of Structural Stability*, Birkhauser Verlag Basel, Stuttgart.

[3] Leipholz, H., 1980, *Stability of Elastic Systems*, Sijthoff & Noordhoff International Publishers BV, Alphen aan den Rijn, The Netherlands.

[4] Dowell, E. H., 1975, *Aeroelasticity of Plates and Shell*, Noordhoff International Publishing, Leyden, The Netherlands.

[5] Fu, F. C. L. and Nemat–Nasser, S., 1975, "Response and Stability of Linear Dynamic Systems with Many Degrees of Freedom Subjected to Nonconservative and Harmonic Forces," *Journal of Applied Mechanics*, Vol. 42, pp. 458–463.

[6] Young, T. H. and Chen, F. Y., 1994, "Stability of Fluttered Panels Subjected to In–Plane Harmonic Forces," *AIAA Journal*, Vol. 31, pp. 1667–1673.

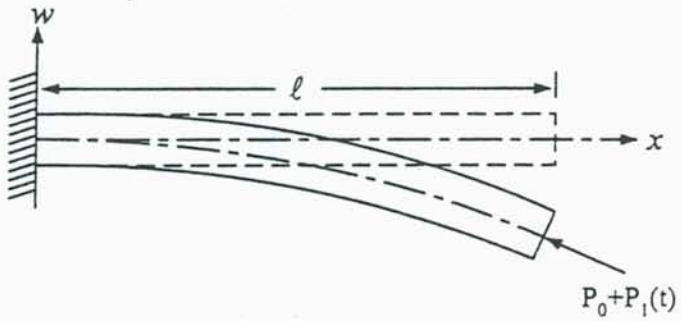

Figure 1. Configuration of a cantilever beam subjected to follower static and random force.

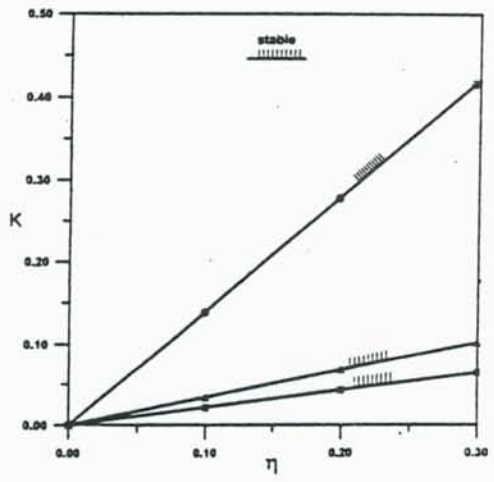

Figure 2. Asymptotic sample stability boundary of a fluttered cantilever beam subjected to a follower random excitation.

Transition Point Solutions For Thin Shell Vibration

R.J. Zhang

(Department of Engineering Mechanics, Tongji University, Shanghai 200092, China)

On the vibrational shell of revolution, there is transition point when the frequency locates in a special interval. Through the transition point, a circumference divides the shell into three parts: the vicinity of the transition circumference and both sides far from the circumference. Different behaviors of any displacement mode of free vibration in the three parts make it difficult to find a uniform expression, valid in whole shell, for the mode. Many investigators devote themselves to the finding. In 1966, Ross obtained matching asymptotic solutions in the simple case of the axisymmetric vibration. In 1979, Gol'denvizer et al. published a monograph in Russian. From the monograph we can see that the authors obtained uniformly valid expressions for all the solutions except a singular membrane one. The complicated nature of shell vibration with transition point was discussed by Steele in 1976.

In 1991 the author presented all eight asymptotic solutions for the non-axisymmetric vibration and all six ones for the axisymmetric vibration. They are uniformly valid in the whole shell and satisfy the accuracy of the theory of thin shells. The achievement of the complete success depends on three families of comparison function, z_h (h=1,2,3,4), R and J being defined, in terms of which the singular membrane solution and four bending solutions can be expanded, respectively.

REFERENCES

Zhang, R.J. and Zhang, W., Turning Point Solutions For Thin Shell Vibrations, Int. J. Solids & Structures, Vol 27, No.10 (1991) 1311-1326

Homogenization Model of Beam Bundle in Fluid

R.J. Zhang

(Department of Engineering Mechanics, Tongji University, Shanghai 200092, China)

So called beam bundle is composed of a great number of (tubular) beams with periodic structure, which are immersed in an acoustic fluid. It is important to evaluate its natural frequency, added fluid mass and equivalent sound speed.

In the present paper the beam bundle is regarded as a fibber-reinforced composite materials: beam is like reinforced fibber and fluid matrix, and then uses the asymptotic homogenization method to develop a simple and enough rigorous mathematical model. The model consists of the following three equations:

$$|X|\left(\frac{\lambda}{c_f^2}+\frac{1-\lambda}{c_s^2}\right)\ddot{p}-\nabla_\alpha\left(A_{\alpha\beta}\nabla_\beta p\right)-|X_f|\nabla_3\nabla_3 p+\overline{\rho}_f\nabla_\alpha\left(B_{\alpha\beta}\ddot{w}_\beta\right)=0 \tag{1}$$

$$M_{\alpha\beta}\ddot{w}_\beta+B_{\alpha\beta}\nabla_\beta p+\nabla_3\nabla_3\left(EI\nabla_3\nabla_3 w_\alpha\right)=0\,. \tag{2}$$

where the pressure of fluid p and the transversal displacement of beam w_α are three unknown functions to be determined. $|X|$ is the area of the unit cell; $|X_f|$ is the area of fluid in the cell; $\lambda=|X_f|/|X|$ is the porosity of the beam bundle; $\overline{\rho}_f$ is the mean density of fluid; c_f and c_s are the respective sound speed in fluid and beam; EI is the flexural rigidity of the beam; Greek subscripts assume the value 1 and 2 and

$$A_{\alpha\beta}=|X_f|\delta_{\alpha\beta}-D_{\alpha\beta}, \tag{3}$$

$$B_{\alpha\beta}=|X_s|\delta_{\alpha\beta}+D_{\alpha\beta}, \tag{4}$$

$$M_{\alpha\beta}=\overline{\rho}_s|X_s|\delta_{\alpha\beta}+\overline{\rho}_f D_{\alpha\beta}\,. \tag{5}$$

where $\delta_{\alpha\beta}$ is the Knonecker delta; $|X_s|$ is the cross sectional area of beam; $\overline{\rho}_s$ is the mean density of beam and $D_{\alpha\beta}$ can be expressed in terms of the local function χ_α as follows:

$$D_{\alpha\beta}=\frac{|X|}{|Y|}\int_{Y_f}\chi_{\beta,\alpha}dy\,. \tag{6}$$

χ_α satisfies the following local problem

$$\begin{cases} \chi_{\alpha,\beta\beta} = 0 \\ \chi_{\alpha,\beta} n_\beta = n_\alpha \\ \chi_\alpha \ \ is \ \ periodic \ \ function \ \ of \ \ local \ \ coordinates \ \ y \\ \dfrac{1}{|Y|}\int_{Y_f} \chi_\alpha dy = 0 \end{cases} \tag{7}$$

As can be seen from definition of $M_{\alpha\beta}$ in (5) that the significance of $\overline{\rho}_f D_{\alpha\beta}$ is an added fluid mass per unit length of beam. Hence, $D_{\alpha\beta}$ indicates the cross sectional area of the fluid attached on the beam. Then we can see from (4) that $B_{\alpha\beta}$ denotes the effective cross sectional area of the beam, which is the total cross sectional area of the beam and the added fluid. Moreover, (3) indicates that $A_{\alpha\beta}$ expresses the area of fluid in the unit cell which is not added on the beam.

It is interesting to indicate the fact that the earlier results, given by Schumann and Benner in 1981 and Brochard and Hammami in 1991, respectively, are the 2-D application of the present 3-D theory.

In the one-dimensional case the natural frequency of the beam bundle can be easily formulated as follows:

$$\frac{\varpi_a}{\varpi_f} = \sqrt{1 + \frac{2-\lambda}{\kappa\lambda}}, \tag{8}$$

where ϖ_a and ϖ_f are circular frequencies in air and in fluid, respectively; $\kappa = \overline{\rho}_s / \overline{\rho}_f$ is the density ratio of beam to fluid. In (8) we have used the asymptotic expression of $D_{\alpha\beta}$ as follows:

$$D_{\alpha\beta} = \frac{\lambda(1-\lambda)}{2-\lambda}|X|\delta_{\alpha\beta} \qquad \text{for} \quad 1-\lambda << 1 \tag{9}$$

A set of experimental data provided by H.-J. Wehling et al. is

$$\lambda = 0.552, \quad \kappa = 10.67, \quad \text{and} \quad \frac{\varpi_a}{\varpi_f} = 1.124. \tag{10}$$

Substituting the first two into the expression (8) we obtain the approximate theoretical value of the frequency:

$$\frac{\varpi_a}{\varpi_f} = 1.116. \tag{11}$$

This value differs from the experimental result by only 0.7%.